AD-A051 428 LOWELL UNIV RESEARCH FOUNDATION MASS F/G 4/1
DIGITAL IONOSPHERIC SOUNDING IN THE ARCTIC.(U)
JUL 77 K BIBL, B W REINISCH, S SMITH F19628-76-C-0012
UNCLASSIFIED ULRF-387/CAR AFGL-TR-77-0152 NL

1 OF 2
AD A051 428

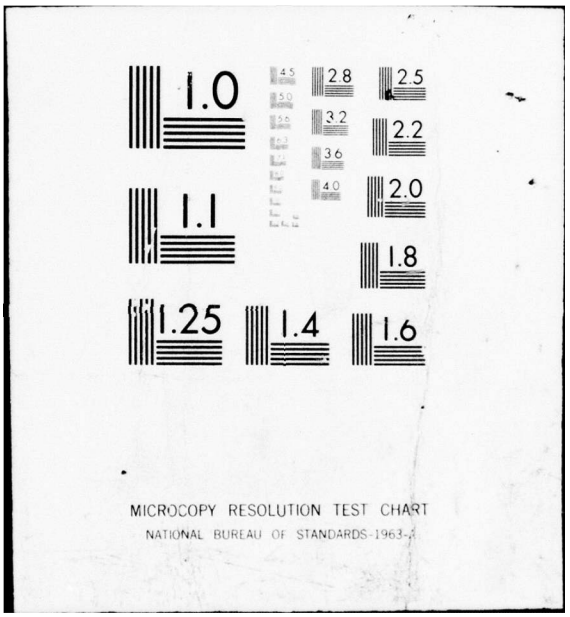
1.0
1.1
1.25
1.4
1.6
1.8
2.0
2.2
2.5
2.8
3.2
3.6
4.0
4.5
5.0
5.6
6.3
7.1
MICROCOPY RESOLUTION TEST CHART
NATIONAL BUREAU OF STANDARDS-1963-A

AFGL-TR-77-0152

DIGITAL IONOSPHERIC SOUNDING IN THE ARCTIC

Klaus Bibl
Bodo W. Reinisch
Sheryl Smith

University of Lowell
Center for Atmospheric Research
450 Aiken Street
Lowell, Massachusetts

July 1977

Final Report for Period 1 July 1975 - 30 April 1977

Approved for public release; distribution unlimited.

AIR FORCE GEOPHYSICS LABORATORY
AIR FORCE SYSTEMS COMMAND
UNITED STATES AIR FORCE
HANSCOM AFB, MASSACHUSETTS 01731

SECURITY CLASSIFICATION OF THIS PAGE (When Data Entered)

REPORT DOCUMENTATION PAGE

READ INSTRUCTIONS BEFORE COMPLETING FORM

1. REPORT NUMBER: AFGL-TR-77-0152	2. GOVT ACCESSION NO.
3. RECIPIENT'S CATALOG NUMBER	
4. TITLE (and Subtitle): DIGITAL IONOSPHERIC SOUNDING IN THE ARCTIC.	5. TYPE OF REPORT & PERIOD COVERED: Scientific - Final rept. 1 Jul 75 - 30 Apr 77
6. PERFORMING ORG. REPORT NUMBER: ULRF-387/CAR	
7. AUTHOR(s): Klaus Bibl, Bodo W. Reinisch, Sheryl Smith	8. CONTRACT OR GRANT NUMBER(s): F19628-76-C-0012
9. PERFORMING ORGANIZATION NAME AND ADDRESS: University of Lowell, Center for Atmospheric Research, 450 Aiken Street, Lowell, Massachusetts 01854	10. PROGRAM ELEMENT, PROJECT, TASK AREA & WORK UNIT NUMBERS: 62101F; 7663-09-AD
11. CONTROLLING OFFICE NAME AND ADDRESS: Air Force Geophysics Laboratory, Hanscom AFB, Massachusetts 01731, Contract Monitor: Jurgen Buchau, PHI	12. REPORT DATE: Jul 1977; 13. NUMBER OF PAGES: 110
14. MONITORING AGENCY NAME & ADDRESS (if different from Controlling Office)	15. SECURITY CLASS. (of this report)
	15a. DECLASSIFICATION/DOWNGRADING SCHEDULE

16. DISTRIBUTION STATEMENT (of this Report)

Approved for public release; distribution unlimited.

17. DISTRIBUTION STATEMENT (of the abstract entered in Block 20, if different from Report)

18. SUPPLEMENTARY NOTES

19. KEY WORDS (Continue on reverse side if necessary and identify by block number)

Digital Sounding
Arctic Ionosphere
Discrete Fourier Transform

20. ABSTRACT (Continue on reverse side if necessary and identify by block number)

Digital techniques applied to ionospheric sounding measure new parameters of the reflected radio signals, like Doppler shift wave polarization, and incidence angles. The Digisonde on-board AFGL's Airborne Ionospheric Observatory was modified to incorporate a discrete Fourier transform for each frequency-range bin. Goose Bay vertical ionograms were scaled in terms of 23 parameters. The monthly median curves of the most important →

DD FORM 1 JAN 73 1473 EDITION OF 1 NOV 65 IS OBSOLETE

UNCLASSIFIED
SECURITY CLASSIFICATION OF THIS PAGE (When Data Entered)

ionospheric parameters for the period March 1975 to February 1976 are presented in the report.

TABLE OF CONTENTS

1.0 INTRODUCTION

Digital techniques have opened new alleys in the field of ionospheric sounding. System reliability and data accuracy have improved; new parameters are measured: amplitude, phase, incidence angle, polarization and Doppler shifts; data storage on digital magnetic tape makes computer processing easy.

Air Force Geophysics Laboratory's Ionospheric Dynamics Branch operates two Digisondes, one in Goose Bay, Labrador and the second on-board a KC-135 aircraft. We have modified the aircraft Digisonde by introducing the technique of spectral integration. Phase coherent integration is a powerful technique that significantly increases the system sensitivity as compared to power integration. The new Processing Controller that was integrated in the aircraft Digisonde makes a Discrete Fourier Transform (DFT) in each frequency-range bin thus carrying out phase coherent integration for each Doppler shifted spectral line. The Doppler shifts, of course, are introduced by the moving ionosphere and/or the moving aircraft.

To make the Goose Bay observations available to the scientific community, we have scaled the hourly vertical ionograms according to URSI specifications. The quarter-hourly ionograms, both vertical and oblique backscatter, are available on magnetic tape and paper printout.

2.0 DIGISONDE SYSTEMS

2.1 Goose Bay System

Because of the large dynamic variations in signal field strengths a digital automatic gain control was incorporated in the Digisonde in addition to the already existing time dependent gain control. The latter changes the receiver gain in steps of 10 dB in the evening and in the morning to compensate for the diurnal variation in D region absorption. The new automatic gain control takes for each transmitted frequency the range bin with the largest amplitude as decision maker. If in the initial phase of the integration time the amplitude is smaller than 90% of the end value the receiver gain is changed by one or two 10 dB steps. The modified receiver gain is stored in the preface (position 23) of the output data.

The two Granger wide band RF amplifiers were made compatible by introducing new wide-band transformers. One of the plate circuit delay lines was replaced. Tests and calibrations were performed to demonstrate proper operation of the amplifiers.

2.2 Aircraft System

The phase coherent integration in the original Digisonde could not be applied if a significant Doppler shift was imposed on the signal. The Doppler frequency is given by

$$d = \frac{1}{\pi} \underline{k} \cdot (\underline{V}_A - \underline{V}_I) ,$$

where $\underline{k}$ is the wave vector, specifying the looking angle, $\underline{V}_A$ is the aircraft velocity and $\underline{V}_I$ is the velocity vector of the ionosphere.

The new Processing Controller that is now incorporated in the aircraft Digisonde is not merely overcoming this problem by using spectral integration, but by measuring the Doppler frequencies it makes available a new parameter in ionosonde observations. The features of the Processing Controller are described in Appendix A.

2.3 Data Replay System

The Digicoder of AFGL's data replay system was modified so as to allow for greater formatting flexibility. The printout can use three different fonts now: the original Digicoder font with the 6 by 4 matrix, a double sized Digicoder font with a 12 by 8 font and 64 level BCD font with a 12 by 8 font (Figure 1).

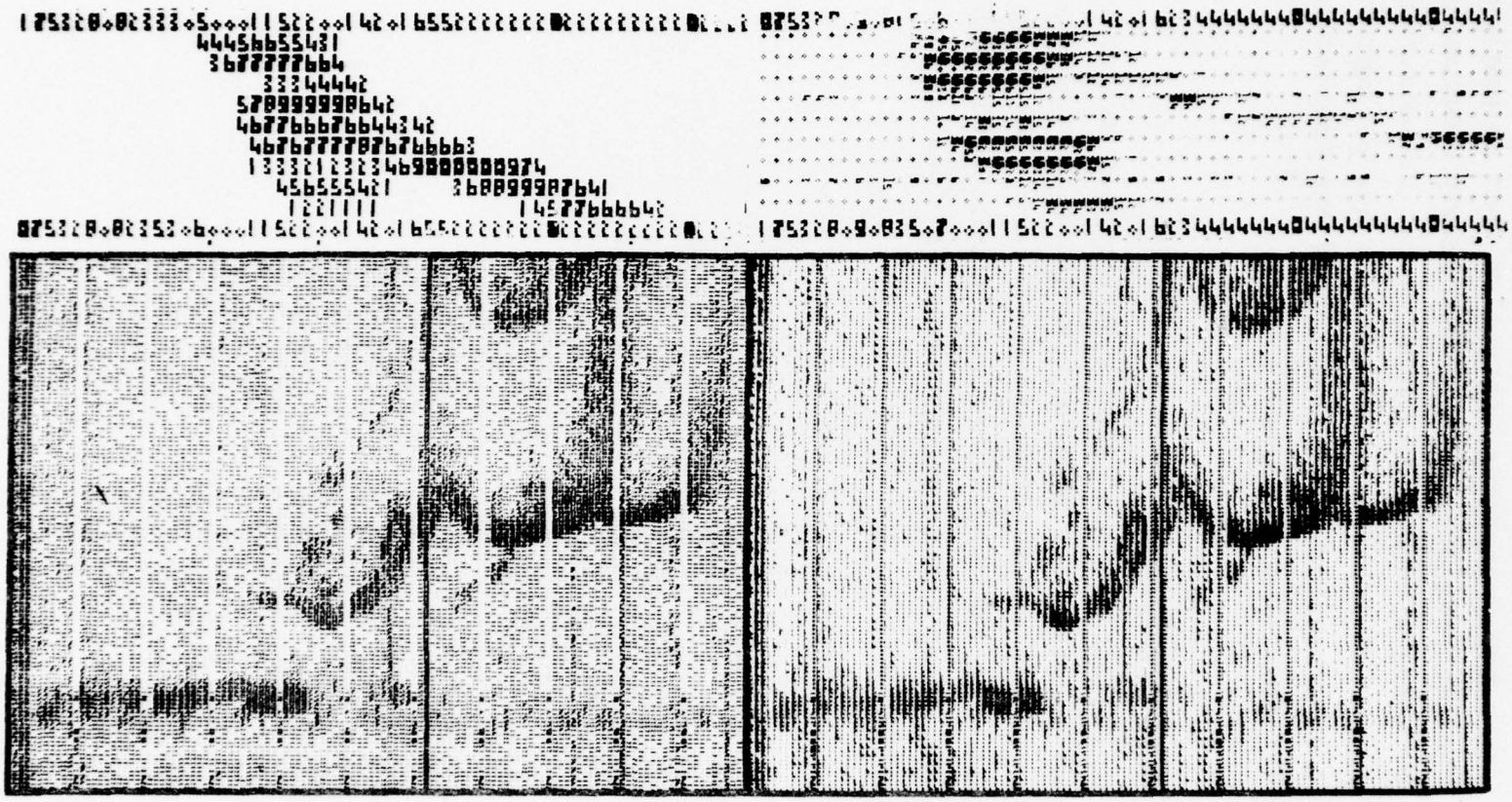

OPTI-FONT
VERTICAL IONOGRAM
4dB RESOLUTION

64 LEVEL FONT
VERTICAL IONOGRAM
1dB RESOLUTION

IONOGRAM AND PREFACE

FIGURE 1

3.0 DATA PROCESSING

3.1 Ionogram Evaluation

To obtain a good survey of the diurnal and seasonal variations of the arctic ionosphere at Goose Bay, the hourly vertical ionograms from March 1975 to February 1976 were scaled according to URSI definition. In addition, we scaled the top frequencies and virtual heights of oblique Es and F echoes, generally assumed to indicate the location of the northern edge of the ionospheric trough. The following 23 parameters were scaled: foE, foF1, foF2, foF0B*, foEs, foEs2*, frEs, fbEs, fminF0B*, foI, foT, h'E, h'Es, h'Es2*, h'F, h'F2, h'F0B*, kpF2, MUF(3000)F2, MUF(3000)F1, Type Es and Type Es2 (* = oblique echoes).

In Appendix B we show the diurnal variations of the monthly median values of h'E, h'Es, h'F, h'F2 and foE, foEs, foF1, foF2. As an indicator of the sporadic E activity Appendix B also presents the foEs distribution curves. It should be noted that the night E, a relatively thick layer at E region altitude, that frequently forms in the arctic ionosphere due to particle ionization, has been included in these foEs distribution curves.

The individual hourly values are kept on file and are available on request.

3.2 Seminar in Ionogram Reduction

A comprehensive course in scaling of digital ionograms was taught at the University of Lowell to personnel from AFGL. The course used as text the "URSI Handbook of Ionogram Interpretation" by Piggot and Rawer. As a complementary aid we had prepared the "Succinct Guide to the Reduction of Digital Ionograms" which is tailored to the Digisonde ionograms

and emphasizes the special conditions occurring in the arctic ionosphere. This little guide, attached as Appendix C to this report, is very helpful for new personnel trained on ionogram scaling, although it is not in any way a complete ionogram scaling manual.

APPENDIX A

THE UNIVERSAL DIGITAL IONOSONDE

UNIVERSITY OF LOWELL
COLLEGE OF PURE AND APPLIED SCIENCE
CENTER FOR ATMOSPHERIC RESEARCH
Lowell, Massachusetts

THE UNIVERSAL DIGITAL IONOSONDE

by

Klaus Bibl

Bodo W. Reinisch

Dedicated to the Memory of Dr. Wolfgang Pfister (1906-1976)

Submitted to Radio Science

May 1977

THE UNIVERSAL DIGITAL IONOSONDE

Klaus Bibl and Bodo W. Reinisch

University of Lowell Center for Atmospheric Research,
450 Aiken Street, Lowell, Massachusetts 01854

Dedicated to the Memory of Dr. Wolfgang Pfister (1906-1976)

ABSTRACT

The digital ionospheric sounding system "Digisonde 128PS" explores ionospheric structure and dynamics by exploiting all observables of the reflected electromagnetic wave: range, amplitude, phase, Doppler, incidence angle and wave polarization. The Digisonde operates in two complementary modes of observations: the Ionogram Mode with full range and frequency display but limited resolution in Doppler and incidence angle, and the Doppler-Drift Mode operating with a limited number of frequency-range bins but full resolution in Doppler and incidence angle. This technique reduces the volume of magnetically recorded output data to a manageable size. Special digital-analog hybrid techniques are used for the presentation of the multi-parameter ionograms and the sky maps.

INTRODUCTION

Remote sensing of the atmosphere is a continuous requirement for the understanding of our environment and for the warning of natural and man-made events that affect man's life.

The Wide Band Satellite program conducted by the U.S. Defense Nuclear Agency for the investigation of the aurora and equatorial ionosphere required ground based equipment for continuous monitoring of the ionosphere with regard to vertical and horizontal electron density distributions and to the motions of ionospheric irregularities. The explanation of scintillation and spread F phenomena are prime goals of this program. The tasks of an ionosonde are to study and monitor the ionosphere by radio means. The research objectives of the ionosonde demand special capabilities and adequate flexibility from the instrument, requirements which, in general, are expensive. In contrast, the most important requirement for a monitoring ionosonde is low cost, since only a dense network of sounders can produce a global picture of the ionosphere. It appears, therefore, that two sets of ionosondes are needed, one for research and one for monitoring purposes. Such a diversification, however, would be very unsatisfactory unless the "monitoring ionosonde" (M.I.) can easily be expanded to a "research ionosonde" (R.I.), and, also important, the R.I. can fulfill the operational requirements of an M.I.

Our answer to the existing need was the development of the Digisonde (Bibl et al, 1970; Phillips, 1974) an advanced digital ionosonde. Since 1969 Digisondes were used for both ionospheric monitoring (AFCRL's "Geophysics and Space Data Bulletin"; Ionosphären-Institut Breisach "Ionosphären-Daten"; Institut Royal Meteorologique de Belgique "Observations Ionospheriques") and for research (Bibl et al, 1975; Reinisch, 1973; Philbrick et al, 1973 and 1974; MacLeod et al, 1973; Reinisch and MacLeod, 1973). The

initial difficulty of the digital sounder was the high cost of the components and of the peripheral recording equipment. In the last three years very versatile digital integrated circuits came on the market at low prices, especially the so-called read-only-memories (ROM's) and the microprocessors. This allowed us to build the new Digisonde 128PS at moderate costs with all the capabilities of an R.I.

OBSERVABLES FOR IONOSPHERICALLY REFLECTED RADIO SIGNALS

The ideal ionosonde must be able to measure all parameters that characterize the reflected radio wave. Some new ionosondes were recently described in the literature emphasizing either one wave parameter, for instance the phase (Hammer and Bourne, 1976) for accurate virtual height determination or, low costs (Morgan and Pratt, 1975). It appears that only digital techniques can succeed in determining all the wave parameters.

Fortunately, the list of parameters is not too long: group travel time or h' (1), amplitude (2), phase (3), precise frequency, i.e. Doppler offset (4) from transmitted frequency, incidence angle (5), and wave polarization (6), i.e. ordinary or extraordinary echo. The curvature (7) of the wave front may be of interest for certain experiments. To obtain a complete picture of the structure and of the motions in the ionosphere, it is desirable to measure parameters 2 through 7 as functions of the virtual height h' and the transmitted frequency f over large

ranges of h' and f, and with good resolution, i.e. small increments in range and frequency. But the amount of data would become excessive unless digital preprocessing and multiplexed output formatting reduce the volume of output data to manageable size. The argument could be made, that rather than outputting the measured data one could immediately extract the physical information which is of interest in the very moment, and not store the measured data. This approach may lead to erroneous results without the possibility of data reverification and reinterpretation. The solution to the apparent dilemma is to preprocess the data, reduce the redundancies, and flag each data point with a parameter identification. The appropriate identification techniques will be explained in the next sections.

The simultaneous monitoring of the entire five-dimensional complex amplitude space (range, frequency, Doppler, azimuth and zenith angle) is neither feasible nor advisable. Instead, the Digisonde 128PS operates in two complementary modes, the ionogram and the drift mode. By complementary we mean that a combination of the two data sets generated in the two modes, contains all relevant information of the five-dimensional space. In the ionogram mode, 128 or 256 range bins (virtual heights) are sampled in a selected band of transmitted frequencies, with full amplitude resolution (1/2 or 1 dB), but limited information about the incidence angles and Doppler frequencies. The wave polarization is identified for all frequency-range bins (FRB). In the drift mode, only a limited number of FRB's are selected and, of course,

these will be FRB's with echo signals. A priori assumptions about the pulse shape of the echoes and about the selection of specific frequencies during the ionogram (Wright, 1975) are avoided in order not to bias the two basic data sets. Table 1 lists the wave parameters that the Digisonde observes and the techniques that are used to measure these parameters.

SYSTEM CONFIGURATION

The Digisonde is housed in two standard 19" racks (Figure 1), one holding the actual ionosonde, the other the 10 kW wide-band pulse transmitter. Figure 2 shows the block diagram of the sounding system. Besides the 10 kW TRANSMITTER there are only four chassis: the PROCESSING CONTROLLER, the TRANSCEIVER, the ANTENNA SWITCH, and the MICROCOMPUTER. The digital output data are recorded on one 7-track magnetic tape drive, for both ionogram and drift measurements. The ionograms are displayed in real time on a high intensity plasma display and simultaneously recorded on an electrostatic printer. A digital-analog hybrid method is applied for the data presentation (Patenaude et al, 1973), as illustrated in Figure 3. The small optically weighted number font gives the data printout the appearance of an intensity modulated analog picture while it retains the digital information. In Figure 3, the amplitude values are given in 4 dB increments. After ten data lines a preface line is inserted containing date, time (hour, minutes, seconds) and all program parameters (pulse repetition rate, receiver gain, etc.).

The PROCESSING CONTROLLER is the brain of the Digisonde system. All control functions branch out from here to the rest of the system, and the entire digital data preprocessing is performed here, including the discrete Fourier transform. A small keyboard, mounted on the front panel, enables selection of the operational parameters. Data may also be entered on a teletype terminal which is preferable when a typed record of the entry is desired.

The TRANSCEIVER is the analog signal processor which is controlled by digital signals from the PROCESSING CONTROLLER. The digitally synthesized transmitter frequency is fed through a two stage active filter with 400 kHz bandwidth that is kept constant over the entire frequency range from .5 to 40 MHz. The same bandpass filters are alternately used as tuned input stages for signal reception, protecting the first mixer from high level off-frequency interferers that would otherwise cause undesirable cross-modulations, and as tuned output stages. The 1. local oscillator is kept 2 MHz off the transmitter frequency resulting in a 2 MHz first intermediate frequency (IF) which is then converted to the final IF of 255 kHz. The IF bandpass filter is composed of ten uncoupled LC circuits with individual bandwidths of 70 kHz, resulting in an overall bandwidth of 15 kHz.

The real-time post-processing is performed in the MICROCOMPUTER. Its main task is the calculation of the sky maps which give an immediate picture of the horizontal structure of the ionosphere. Cross-correlation of the complex spectra obtained

for the different antennas determines the incidence angle for each spectral component. A true height algorithm converts the virtual heights of the echo traces in the ionogram into a vertical electron density profile which is plotted onto the ionogram on the Plasma Display. The MICROCOMPUTER can also be used off-line for the processing of ionogram and drift tapes.

MULTI-PARAMETER IONOGRAMS

Operational Programs. Three different ionogram programs are stored in the Digisonde, two of which can be programmed by the keyboard or the computer, and the third is maintained in a non-volatile FROM (field-programmable read-only-memory). The ionogram rate can be selected out of a set of 12 ionogram sequences, extending from 1 to 120 ionograms per hour (Table 2). Ionograms can, of course, also be started by manual or computer commands. The most important programmable operational parameters are listed in Table 3. Most entries in the Table are self-explanatory, but some items need to be discussed. Item #3, for instance, lists either equidistant frequency increments or a dual step size, for example 10 and 90 kHz. The dual mode, selected for phase measurements, increases the group height resolution:

$$h' = (c/4\pi)\ \Delta\phi/\Delta f\ ,$$

(c = speed of light, $\Delta\phi/\Delta f$ = change of phase with frequency). The large frequency steps provide for high resolution, and the small steps resolve the 2π ambiguity. For the 10 and 90 kHz

mode, the resolution in virtual height is

$$\delta h' = (c/4\pi)\,\delta(\Delta\phi)/\Delta f = (c/4\pi)\,2\pi/16 \cdot 9 \cdot 10^4 \approx 100 \text{ m}$$

and the 2π ambiguity range is

$$\Delta h' = (c/4\pi)\,2\pi/10^4 \text{ Hz} = 15 \text{ km},$$

which is easily resolved by the amplitude-range measurement. If, and only if any of the dual frequency increment modes are selected, will the phase be recorded.

The range increments (item #4) can be varied over a large set of possibilities from 0.5 to 10.5 km. The Digisonde samples two times 128 ranges and the two range groups can form one large range window, or two non-abutting windows. To obtain a better group height resolution in the E-region than in the F-region a bi-linear scale can be selected. For instance, the E-region can be sampled with 1.5 km increments and the F-region with 3.0 km. The phase coding of the transmitted radio waves makes it possible to identify echoes in a later pulse period. The phase code sequence is a quasi-random series of 180° phase shifts applied to the HF of consecutive pulses. This "keys" the individual transmitter pulses and permits the use of high pulse repetition rates. The coding also helps to suppress quasi-coherent interferers in the course of the spectral integration process.

Doppler and Incidence Angle. Spectral analysis is performed separately for each FRB. Since it would be impossible to record a complete spectrum of say 128 lines for each bin, the spectrum is limited to 16 lines, arranged symmetrically around

zero Doppler shift. The Doppler frequencies together with the incidence angle measurements help to interpret the ionograms in terms of the structure and the motions in the ionosphere, and we expect that our measurements will provide new inputs to the phenomenon of spread F. Phase coherent integration without spectral resolution, i.e. assuming zero Doppler frequency, would render the system insensitive to moving reflectors like the auroral ionosphere or chemical releases. Without phase coherent integration, on the other hand, the ionosonde would be useless in all densely populated areas with high prevailing radio interference levels. An escape to ever higher transmitter power is not the answer in such circumstances, since that would turn the ionosonde into an unacceptable source of interference for other radio services.

The azimuthal component of the incidence angle is measured for each FRB with a resolution of 30°. For this measurement, ten of the antennas of the receiving array are summed via switched delay lines. The delays are determined in such a way that the zenith angle is kept equal to 15° while the azimuth angle is scanned. Different zenith angles can be chosen by replacing the set of delay lines. For each of the selected azimuth angles the signals are phase coherently integrated for each FRB, respectively. These measurements are virtually simultaneous since the typical scanning time is 30 msec. After all the samples of a given transmitter frequency are taken, the azimuthal incidence in each height bin is determined by a differential

technique. The six amplitudes (in case of 60° resolution), obtained for the six azimuthal directions are compared and the maximum amplitude together with the corresponding azimuthal identifier are retained in the output. Other combinations of incidence angles can be selected, as vertical-north-north/east, or vertical-south-south/west, etc. The differential method is very sensitive even when the beam width formed by the antenna array is not small. As a matter of fact, the beam width should be big enough to avoid deadspots on the sky. For this reason we selected the inner ten antennas of the receiving array for the ionogram observation.

The same differential technique is applied for all the other ionogram parameters. After the set of spectral lines is calculated the maximum line together with the line number is determined for output storage. Each of the ten inner antennas separates the ordinary and the extraordinary modes by using crossed-loop antennas. At latitudes for which the quasi-longitudinal approximation holds, the two loops are added and subtracted via a $\pm\pi/2$ phase shifter; at the magnetic equator the two perpendicular loops are used independently. Again, for each FRB both antenna outputs are compared (after integration); the larger amplitude is stored and decides whether the FRB receives an O or an X flag.

COMBINATION OF IONOGRAM PARAMETERS AND THE IONOGRAM OUTPUT FORMAT

Not all the wave parameters are recorded with maximum resolution in each ionogram. The combination of parameters depends on the type of observational program that is carried out. On the other hand it would be unwise to change the data output format each time the measuring program is changed. Based on the experience we had during the past ten years with the older Digisonde systems we opted for a standard format for the recording on magnetic tape. The format is indeed the same as the format of the earlier Digisondes. For each transmitted frequency 128 nine-bit data points are recorded together with an identifying preface. The nine data bits comprise six amplitude bits and three status bits that describe the selected wave parameters. In some cases the amplitude resolution is decreased to five bits in order to increase the status word to four bits. An unambiguous identification of the amplitude and status bits is always contained in the preface. Seven-track digital tape drives were chosen for recording, since only a minority of computer facilities can handle nine-track tapes.

It was stated earlier that the Digisonde collects either 128 or 256 range samples. In the latter case the total range is divided into two range windows. Before storing the data in the 128 output array, the differential method is applied again, selecting for each FRB the larger amplitude from the two

range windows; the respective window number is stored in the status word. The probability of two echoes residing in the same bin number in windows 1 and 2 is generally less than 5%, unless severe range spread conditions prevail, in which case the operator can reduce the repetition rate.

The maximum number of data integration channels for each FRB is 24, limited by the memory capacity in the PROCESSING CONTROLLER and the speed of the microcircuits. Hence not all the parameters can simultaneously be measured with maximum resolution. A total of 32 parameter combinations (Table 4) can be selected by varying the number of spectral lines (1 to 16), range windows (1 or 2), polarizations (1 or 2) and incidence angles (1 to 6). The pulse repetition rate and the number of time samples used in the calculation of the Fourier series determine the spectral frequencies. The operator must merely select which frequencies he wants to retain for recording by using a table. This is a decision between good Doppler resolution or wide Doppler range. One must recognize that the sampling period doubles when two antenna configurations are sampled in alternation, and increases proportionately for more configurations. In turn, the frequencies of the selected spectral lines reduce proportionally.

Ionogram Display. Real-time display and printout of the digital ionograms is a necessity for an R.I. and at least desirable for an M.I. A special technique, originally developed for the Digisonde, uses optically weighted fonts for the printout

of the ionograms (Figure 3). The parameterization of the ionograms as expressed by the 4 or 3-bit status word actually produces 16 (or 8) ionograms within each set of ionogram data. Printing the amplitudes without regard to the status word creates a conventional ionogram. The electrostatic printer of the Digisonde allows to print two ionograms side-by-side with 128 range bins each. A set of 80 dual ionogram combinations can be selected for printout. Some interesting examples are:

Positive Doppler	- Negative Doppler
Low Doppler	- High Doppler
Ordinary	- Extraordinary
Range Window 1	- Range Window 2
East Echoes	- West Echoes
Vertical Echoes	- Non-Vertical Echoes
All Echoes	- North Echoes

If the selected two parameters are exclusive, like positive and negative Doppler, the amplitude data will be distributed amongst the ionogram frames according to the sign of the Doppler frequency; blanks will appear at the empty FRB's. A special combination is the folded ionogram (status disregarded) together with the status ionograms, showing the status values rather than the amplitudes. An example is shown in Figure 4 where the folded amplitude ionogram (bottom) is printed together with the incidence/polarization status ionogram (top), the darker numbers indicate the O-component.

For experiments requiring fast response by the operator we prefer the plasma display over the printer. Even though the

electrostatic printer is very fast (a line with 256 numbers is printed in about 60 msec), the ionogram does not become visible until after the paper has moved out of the printer. The plasma display, on the other hand, immediately shows the data for each transmitted frequency. The plasma display and the hard copy printout have cursors inserted indicating the FRB's used in the previous drift measurement.

For M.I.'s it is more important to present ionospheric characteristics (Nakata et al, 1953) showing absorption (echo amplitudes), top E and top F frequencies and virtual heights as function of time. Analog ionosondes have recorded these characteristics on-line for many years (Bibl, 1960). Some Digisonde stations (U.S. Army in Fort Monmouth, New Jersey and Air Force Geophysics Laboratory in Goose Bay, Labrador) print digital characteristics in real time (Reinisch and Smith, 1977). This feature will be implemented in the new Digisonde described here.

DOPPLER-DRIFT MODE

The rhombic transmitter antenna illuminates a relatively large area in the ionosphere, with a diameter of several hundred kilometers. Echoes return to the receiver site from all surfaces of adequate electron density that fulfill the perpendicularity condition. A Doppler shift will be imposed on the reflected radio waves (Pfister, 1970) when the ionospheric plasma moves, which is almost always the case. The Doppler shift d is

determined by the velocity $\underline{v}$ of the reflector and the radio wave vector $\underline{k}$:

$$d = (1/\pi)\ \underline{k}\cdot\underline{v}\ .$$

Hence, the spectral analysis separates different reflection areas and it resolves the angular spread in each area (Pfister et al, 1968-1975). There will be cases where the same Doppler frequency will be generated in different reflection points; by using four or more spaced receiving antennas these cases can generally be resolved.

Figure 5 relates the angular deflection to the associated spectral variation. Two neighboring sources (reflection points) differ in their Doppler frequency by

$$\delta d = (1/\pi)\ k\ v\ \delta(\cos\psi)$$

where ψ is the angle between $\underline{v}$ and $\underline{k}$. Using the angles of Figure 5, where $\underline{v}$ was assumed to be horizontal, we write:

$$\cos\psi = \sin\theta\ \cos(\phi-\phi')$$

and

$$\delta\ \cos\psi = \cos\theta\ \cos(\phi-\phi')\ \delta\theta - \sin\theta\ \sin(\phi-\phi')\ \delta\phi.$$

When looking in the direction of the velocity vector, i.e. $\phi = \phi'$ the variation in Doppler becomes:

$$\delta d = (1/\pi)\ k\ v\ \cos\theta\ \delta\theta\ .$$

For a given spectral resolution δd the angular resolution is therefore:

$$\delta\theta = \pi\ \delta d/(k\ v\ \cos\theta) = \lambda\ \delta d/(2\ v\ \cos\theta).$$

By substituting some typical values $\delta d = 0.03$ Hz, $\lambda = 50$ m (6 MHz) and $v = 100$ m/s one obtains for small angles θ

$$\delta\theta = 7.5 \cdot 10^{-3}$$

corresponding to a source separation of 1.5 km in 200 km altitude. By storing the energy from such closely spaced sources in different spectral channels we can determine their location even in the presence of other strong sources with different Dopplers. When looking in the direction of $\underline{v}$, sources with $\delta\theta = 0$ separated by a small angle $\delta\phi$ have the same Doppler and can only be resolved by a sufficiently large antenna aperture.

The drift mode provides the complementary data to the ionograms. Up to six FRB's are selected for accurate Doppler and incidence angle measurements. A total of 24 signal channels are simultaneously processed. Subsets of 4, 6, 8, 12 or 24 receiving antennas can be selected permitting 6, 4, 3, 2 or 1 FRB's, respectively.

Receiving Antenna Array. Figure 6 shows the antenna array that was developed for DNA's wideband satellite experiments at Kwajalein (3° magn. north) in which satellite, rocket and sounding observations are combined for the investigation of the equatorial ionosphere. The aperture of this 25-antenna array is about 400 m and the minimum spacing is 50 m. The scale size of the individual antennas is 2 m, i.e. small compared to the antenna separation. This is important in order to avoid coupling. The individual loop antennas are carefully terminated, and wideband preamplifiers in each loop feed the 50 Ω coaxial cables that carry the signals to the ANTENNA SWITCH. While the antennas are being scanned the cables of all unused antennas are terminated by

50 Ω in the ANTENNA SWITCH; this, again, is done to eliminate coupling by reradiation. Even though the drift mode never scans more than 24 antennas a 25th antenna was added at the center of the array for the formation of smaller symmetric sub-arrays consisting of only 4, 7, or 10 antennas (Table 5). The ten inner antennas actually consist of crossed-loops as described earlier. All 35 antenna elements (25 antennas, ten of which have double polarization) are connected to the central ANTENNA SWITCH which either scans the array in the drift mode, or selects groups of antennas in the ionogram mode. Different groups of antennas are selected by simple keyboard instructions.

Drift Programs. Observational programs that are combined with rocket or satellite measurements, or that are carried out in the rapidly changing auroral ionosphere require fast decisions by the operator with regard to selection of the "best" FRB's, antenna aperture, spectral resolution and range and the sequence of measurements. Table 5 lists the values of the operational parameters available for the Doppler-Drift mode. These parameters can be selected via the front panel keyboard on the PROCESSING CONTROLLER, or they can initially be stored in the MICROCOMPUTER for use at the appropriate time.

The maximum number of data channels is again 24, as in the ionogram mode. Only there we have 128 ranges and the channels are used for selected Doppler lines, polarizations, etc. In the drift mode there are, in general, 128 spectral lines and the data channels are divided between antennas and FRB's. If the

full 24 antenna array is scanned, only one FRB is monitored, for four antennas six FRB's, etc. Previous drift measurements with older Digisondes that were repeated every five minutes showed even in mid-latitudes discontinuities between consecutive time windows which made it difficult to interpret the data. The new Digisonde allows for a minimum window spacing of three sec, resulting, of course, in a limited spectral resolution of 1/2 Hz (Table 5).

Discrete Fourier Transform. The receiver output, IF = 225 kHz, is first logarithmically compressed and then digitized in a quadrature method. The quadrature samples X and Y are used directly to calculate the complex Fourier series for each channel j:

$$F_{j\ell} = (1/T) \sum_n [X_j(n\Delta t) + iY_j(n\Delta t)] \exp -i(2\pi \ell\, n\Delta t/T)$$

$$= (1/T) \sum_n [X_{jn} \cos\beta_{\ell n} + Y_{jn} \sin\beta_{\ell n}]$$

$$+ (i/T) \sum_n [-X_{jn} \sin\beta_{\ell n} + Y_{jn} \cos\beta_{\ell n}]$$

where ℓ is the Doppler line, T is the length of the time window and $\beta_{\ell n} = 2\pi \ell\, n\Delta t/T$. While the initial multiplication of the time samples with the trigonometric functions is carried out in the logarithmic domain, the final summation is, of course, performed in the linear domain. Hanning weighting is applied in the frequency domain by averaging three adjacent spectral lines with weights of 1-2-1. The result of the 24 channel Fourier analysis are 24 number arrays of the form

$$F_{j\ell} = \{M_{j\ell}, \phi_{j\ell}\} \qquad \begin{matrix} j = 1, \ldots, 24 \\ -64 \leq \ell \leq 63 \end{matrix}$$

where $M_{j\ell}$ are the logarithmic spectral amplitudes (64 dB range in 1 dB increments, or 32 dB with 1/2 dB) and $\phi_{j\ell}$ are the corresponding phases with a resolution of $2\pi/256$. It was necessary to develop a method of calculation that requires no extra time beyond the last time sample, since the time between windows is less than one second, used for recording of the spectra on magnetic tape for later computer processing. Directly following digitization the quadrature pair is multiplied by all 128 time-adjusted values of $\cos\beta_{\ell n}$ and $\sin\beta_{\ell n}$, respectively, and the 256 spectral samples thus obtained are added to the previous 256 samples. After the last time sample the final four sums $\sum_n X_{jn} \cos\beta_{\ell n}$, $\sum_n X_{jn} \sin\beta_{\ell n}$, $\sum_n Y_{jn} \cos\beta_{\ell n}$ and $\sum_n Y_{jn} \sin\beta_{\ell n}$ are suitably combined for each j-channel to form the real and imaginary parts of the spectra.

Incidence Angles. The Doppler-drift mode generates a sequence of momentary pictures of the ionosphere's structure and motions. As a first step, we create for each time window a sky map that shows the position of all the simultaneous reflection points existing during the measurement, together with their intensity and their Doppler frequency. An example of a sky map is shown in Figure 7. We manually connected the reflection points by an arrowed line that points in the direction of increasing Doppler frequency. Of course, each FRB requires its own sky map. For the on-line sky maps the Digisonde selects one FRB, the other

FRB's can be processed off-line in a computer using the tape recorded data.

To produce the angular spectra, the frequency-wave-number-power density is calculated (Sales et al, 1975)

$$P_{\ell k} = \sum_{j} \sum_{j'} W_{jj'} F_{j\ell} F^{*}_{j'\ell} e^{-i\underline{k}\cdot(\underline{a}_j - \underline{a}_{j'})}$$

where $F_{j\ell}$ is the spectrum for antenna j, $\underline{k}$ is the wave vector and specifies the looking angle, and $\underline{a}_j$ is the antenna distance vector; $W_{jj'}$ is a weighting factor (Varad and McComish, 1975) which optimizes the array performance. For the on-line generation of the sky maps in the Digisonde, the calculations use four antennas, and since in that case antenna weighting does not offer any advantage, we set $W_{jj'} \equiv 1$. The power density can then be rewritten as

$$P_{\ell k} = |\sum A_{j\ell} \exp i\,(\phi_{j\ell} - \underline{k}\cdot\underline{a}_j)|^2$$

where we substituted $F_{j\ell} = A_{j\ell} \exp i\phi_{j\ell}$. For each looking angle, specified by $\underline{k}$, the spectrum $P_{\ell k}$ must be calculated. The sky map is composed of 40 × 40 points, which means that 1600 spectra must be calculated in a few seconds. Even a large computer would be hard pressed to master this task. We developed special microcomputer controlled hardware that calculates the 1600 power spectra $P_{\ell k}$ in about three seconds. It is practically impossible to print out the complete spectrum for each individual $\underline{k}$. Instead, we determine for each Doppler component its position in the sky (indicated by maximum power). If more than one Doppler component occupies the same point, the one with the largest amplitude is

selected. Both the power and the number of the Doppler line are presented.

Ionospheric Modelling. Once the ionospheric reflection points are found one can proceed to fit ionospheric models to these points. The mathematics and the computer software for this problem are presently being developed on the basis of assuming a two dimensional ionospheric density structure described by two wave vectors $\underline{\Omega}_1$ and $\underline{\Omega}_2$ that lie in a tilted plane:

$$z = z_0 + ax + by + A_1\cos[\underline{\Omega}_1\cdot(\underline{r}-\underline{r}_1)] + A_2\cos[\underline{\Omega}_2\cdot(\underline{r}-\underline{r}_2)]$$

The constraint in the fitting procedure is the condition of perpendicularity at the observed reflection points. Preliminary results for the location of the reflection points by a one-dimensional structure were derived earlier (Bibl, 1974), but our observations seem to suggest isodensity surfaces that are modulated in two dimensions.

The method of calculating the three-dimensional drift vector from the distribution of Doppler frequencies $d = d(\underline{k})$ was described in an earlier paper (Bibl et al, 1975). The calculated drift vectors together with the sequence of sky maps will reveal the small and large scale motions.

CONCLUSION

The Digisonde 128PS represents a systematic approach to the measurement of the ionosphere with radio waves. All wave signatures are exploited to retrieve information on the structure

and the dynamics of the reflecting medium. The large variety of observational programs is conveniently organized in a set of subroutines that make fast program changes possible. Selection of individual operational parameters is internally controlled and a default algorithm corrects the selection if an illegal parameter combination was requested. The phase-coherent spectral integration provides good signal-to-noise ratio even in environments with high interference, or in cases where a small transmitting antenna or limited power is required. An automatic frequency selection scheme tests, in the ionogram mode, three closely spaced frequencies around the nominal frequency for the lowest interference before the start of integration. Digital automatic gain control further improves the appearance of the ionograms. A time dependent gain control, programmed for the entire year, adjusts the receiver gain for day, twilight and night conditions in 6 dB increments.

We believe that this instrument will create new knowledge for the physical explanation of spread F conditions, travelling ionospheric disturbances, the high latitude trough, scintillations, as well as radio communication problems involving the ionosphere.

ACKNOWLEDGEMENT

This work was in part supported by the DNA Contract No. DNA001-76-C-0268 and the AF Contract No. F19628-77-C-0024. The Digisonde observations in Goose Bay, Labrador, directed by Jurgen Buchau, AFGL, induced many ideas that were implemented in the new system. We want to thank Mr. Buchau for the many valuable suggestions he contributed during the development phase of the instrument.

REFERENCES

Bibl, K. (1960), Dynamic characteristics of the ionosphere and their coherency with the local and planetary magnetic index, J. Geophys. Res., 65, 2333-2342.

Bibl, K. (1974), Velocity of the reflection points reveals structure and motions in the ionosphere, COSPAR, Methods of Measurements and Results of Lower Ionosphere Structure, edited by K. Rawer, Akademie-Verlag, Berlin, 369-375.

Bibl, K., J. A. Patenaude and B. W. Reinisch (1970), Digital integrating goniometric ionospheric sounder - Digisonde 128, Final Report, AFCRL-71-0002, Air Force Geophysics Laboratory, Hanscom Air Force Base, Bedford, Massachusetts 01731.

Bibl, K., W. Pfister, B. W. Reinisch and G. S. Sales (1975), Velocities of small and medium scale ionospheric irregularities deduced from doppler and arrival angle measurements, in COSPAR, Space Research XV, edited by M. J. Rycroft, Akademie-Verlag, Berlin, 405-411.

Hammer, P. R. and I. A. Bourne (1976), A high resolution ionosonde - 1. technique and analysis methods, JATP, 38, 935-943.

Hammer, P. R. and I. A. Bourne (1976), A high resolution ionosonde - 2. equipment and preliminary results, JATP, 38, 945-956.

MacLeod, M. A., T. J. Keneshea and B. W. Reinisch (1973), The Aladdin II ionosphere: a comparison of theoretical calculations with Digisonde observations, EOS Transactions, Am. Geophys. Union, 54, 381.

Morgan, M. G. and B. Pratt (1975), Reliable ionosonde for continuous automatic operation, Radio Sci., 10, 859-866.

Nakata, Y., M. Kan and H. Uyeda (1953), Rept. Ionosphere Research Japan, 7, 129-135.

Patenaude, J., K. Bibl and B. W. Reinisch (1973), Direct digital graphics - the display of large data fields, American Laboratory, 15, 95-101.

Pfister, W. (1971), The wave-like nature of inhomogeneities in the E-region, JATP, 33, 999-1025.

Pfister, W., et al, Pulse sounding with closely spaced receivers as a tool for measuring atmospheric motions and fine structure in the ionosphere

Vol. I, Environmental Research Paper No. 295, 1968
Vol. II, Environmental Research Paper No. 295, 1968
Vol. III, Environmental Research Paper No. 317, 1970
Vol. IV, Environmental Research Paper No. 329, 1970
Vol. V, Environmental Research Paper No. 469, 1974
Vol. VI, Environmental Research Paper No. 470, 1974
Vol. VII, Environmental Research Paper No. 506, 1975
Vol. VIII, Environmental Research Paper No. 507, 1975
Air Force Geophysics Laboratory, Hanscom Air Force Base, Bedford, Massachusetts 01731.

Philbrick, C. R., R. S. Narcisi, R. E. Good, H. S. Hoffman, T. J. Keneshea, M. A. MacLeod, S. P. Zimmerman and B. W. Reinisch (1973), The Aladdin experiment - part II, composition, COSPAR, Space Research XIII, edited by M. J. Rycroft and S. K. Runcorn, Akademie-Verlag, Berlin, 441-449.

Philbrick, C. R., D. Golomb, S. P. Zimmerman, T. J. Keneshea, M. A. MacLeod, R. E. Good, B. S. Dandekar and B. W. Reinisch (1974), The Aladdin II experiment - part II, composition (preliminary results), COSPAR, Space Research XIV, 89-95.

Phillips, M. L. (1974), Ground-based vertical-incidence ionograms, IEEE Trans. on Antennas and Propagation AP-22, 785-792.

Reinisch, B. W. (1973), Burnt-out rocket punches hole into ionosphere, COSPAR, Space Research XIII, edited by M. J. Rycroft and S. K. Runcorn, Akademie-Verlag, Berlin, 503-506.

Reinisch, B. W. and M. A. MacLeod (1973), Chemical releases at sunset trigger sporadic E, EOS Transactions, Am. Geophys. Union, 54, 379.

Reinisch, B. W. and S. Smith (1976), Geomonitor - digital real time processor for geophysical data, Final Report, AFGL-TR-76-0292, Air Force Geophysics Laboratory, Hanscom Air Force Base, Bedford, Massachusetts 01731.

Sales, G. S., J. I. Videberg and R. Varad (1975), DAASM project - high latitude aircraft HF propagation experiment, Scientific Report, AFCRL-TR-75-0290, Environmental Research Paper No. 516, Air Force Geophysics Laboratory, Hanscom Air Force Base, Bedford, Massachusetts 01731.

Varad, R. and W. C. McComish (1975), The maximum likelihood method, application to DAASM studies, Final Report, AFCRL-TR-75-0551, Air Force Geophysics Laboratory, Hanscom Air Force Base, Bedford, Massachusetts 01731.

Wright, J. W. (1975), Development of systems for remote sensing of ionospheric structure and dynamics, NOAA, ERL/SEL, Preprint 206, NOAA, Boulder, Colorado 80302.

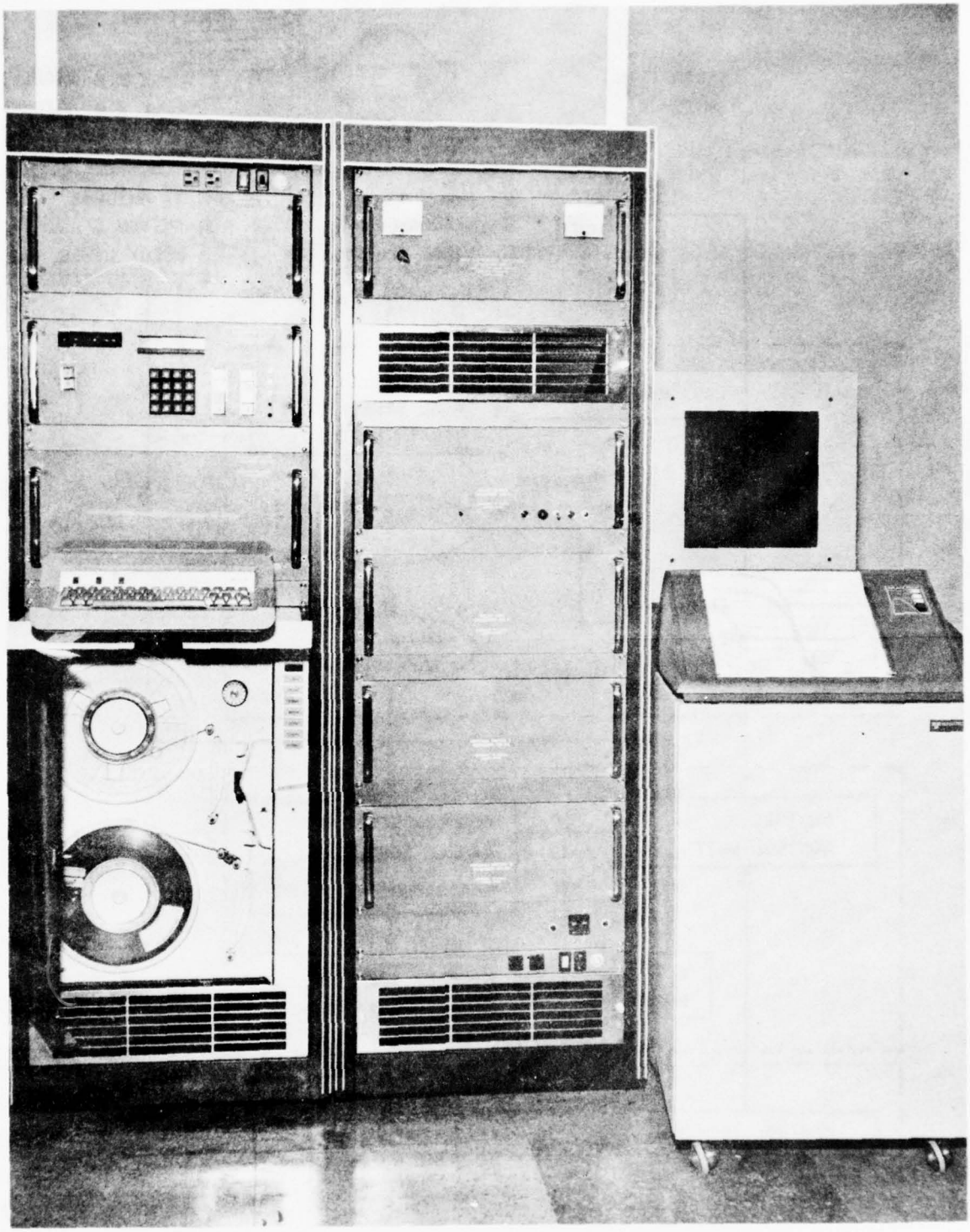

DIGISONDE 128PS

FIGURE 1

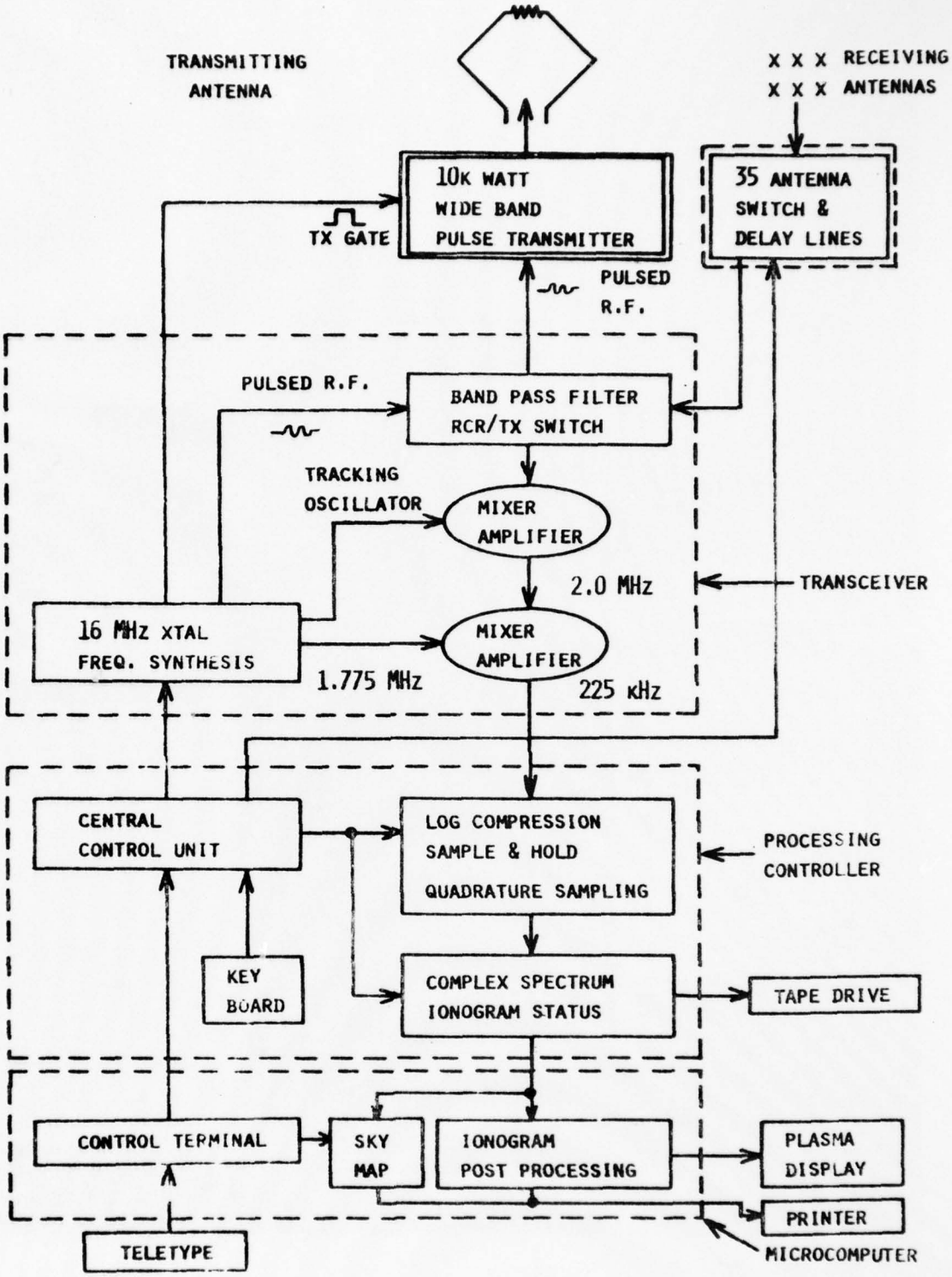

SYSTEM DIAGRAM

FIGURE 2

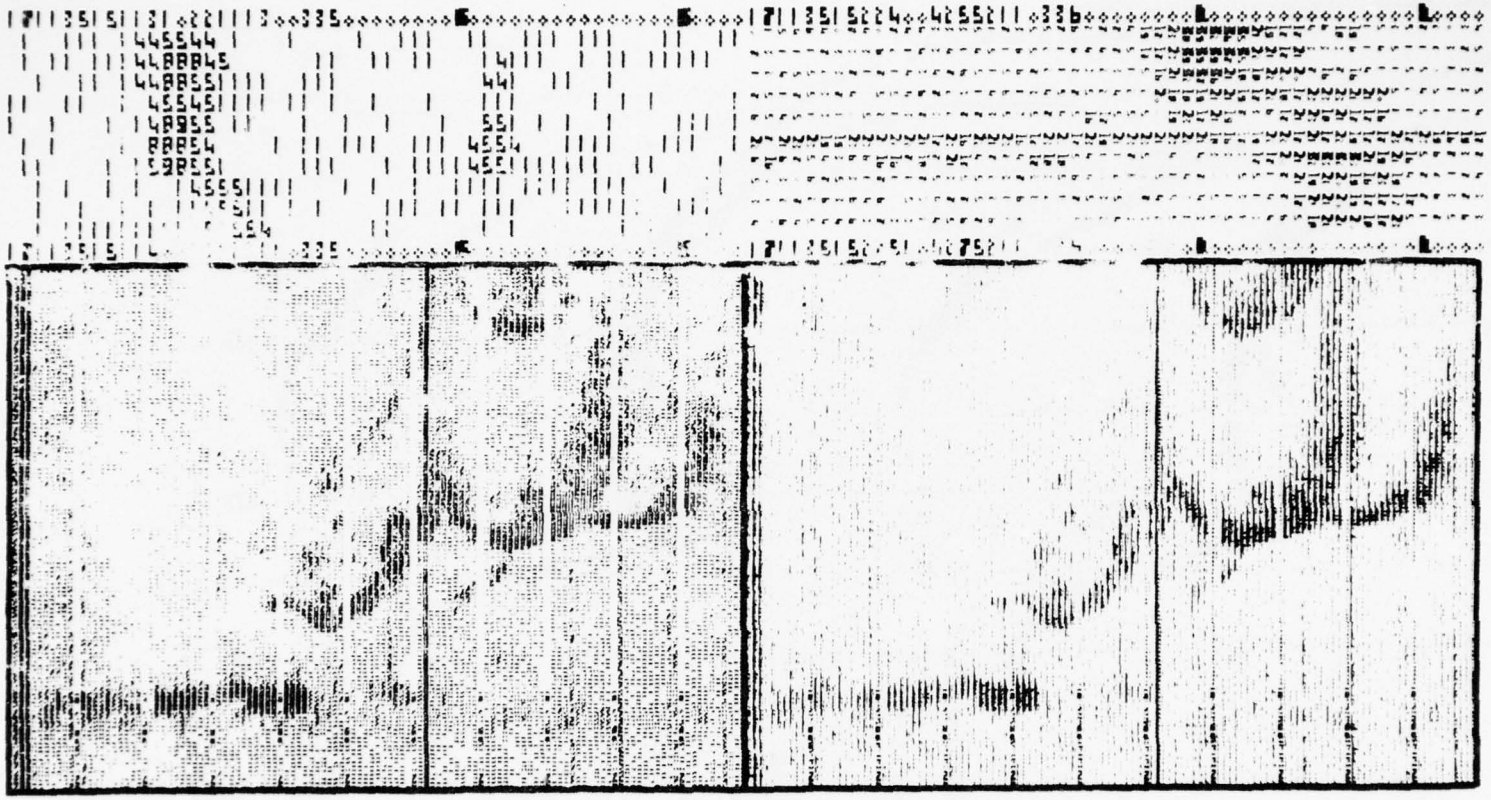

DIGICODER FONTS

OPTI-FONT ®
VERTICAL IONOGRAM
4dB RESOLUTION

64 LEVEL FONT
VERTICAL IONOGRAM
1dB RESOLUTION

IONOGRAM AND PREFACE

FIGURE 3

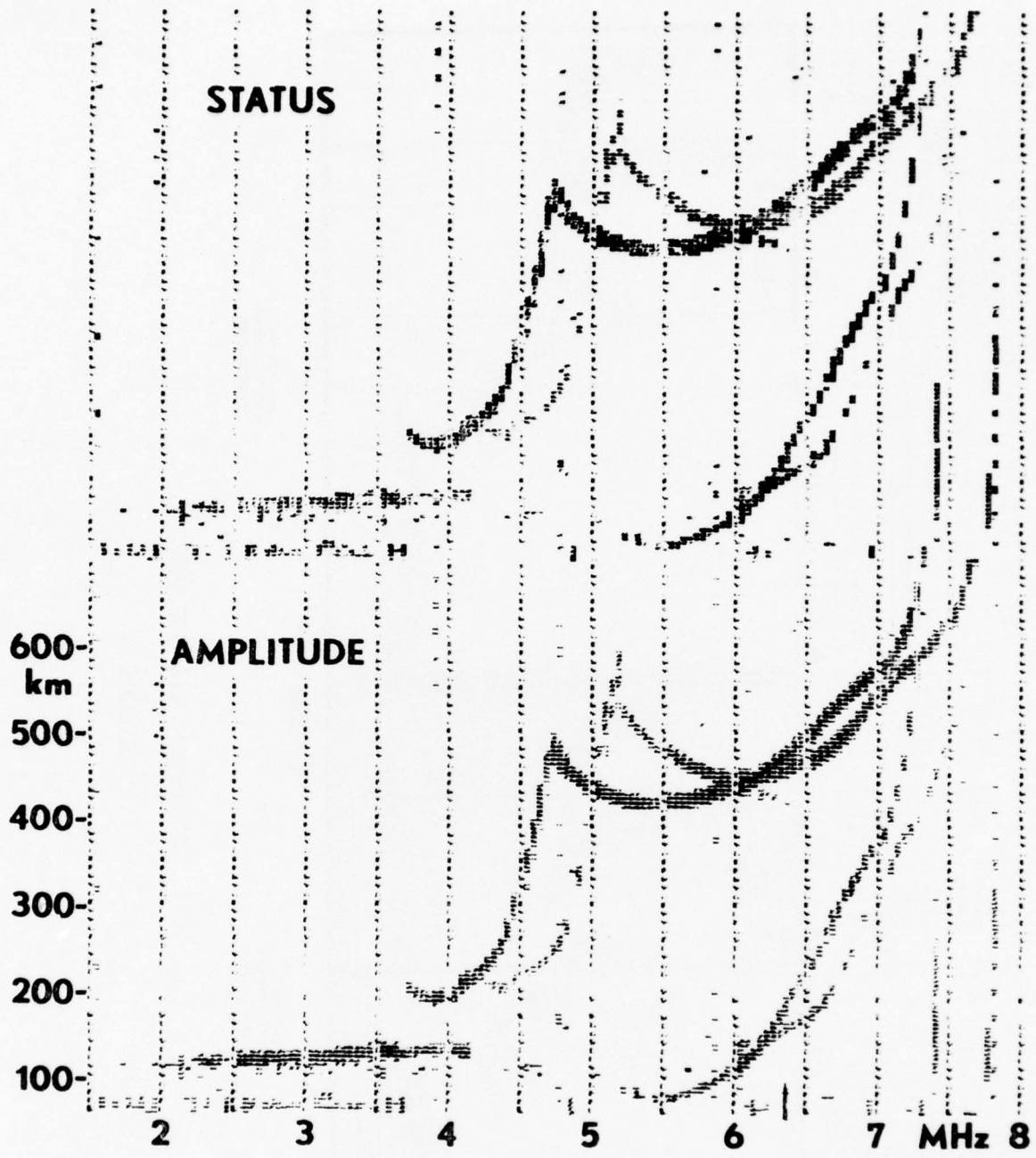

DUAL IONOGRAM

FIGURE 4

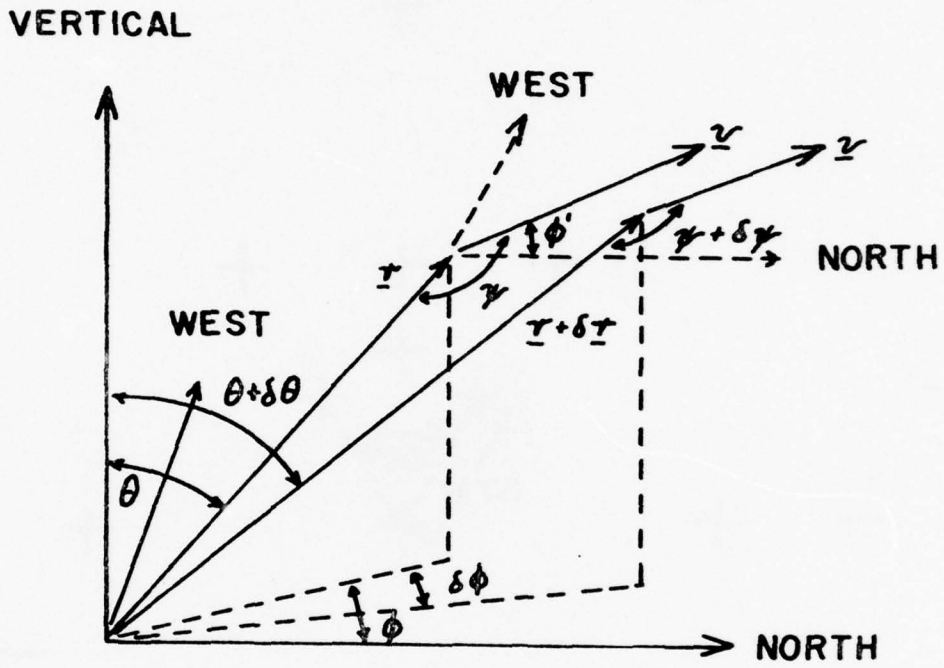

DOPPLER GEOMETRY

FIGURE 5

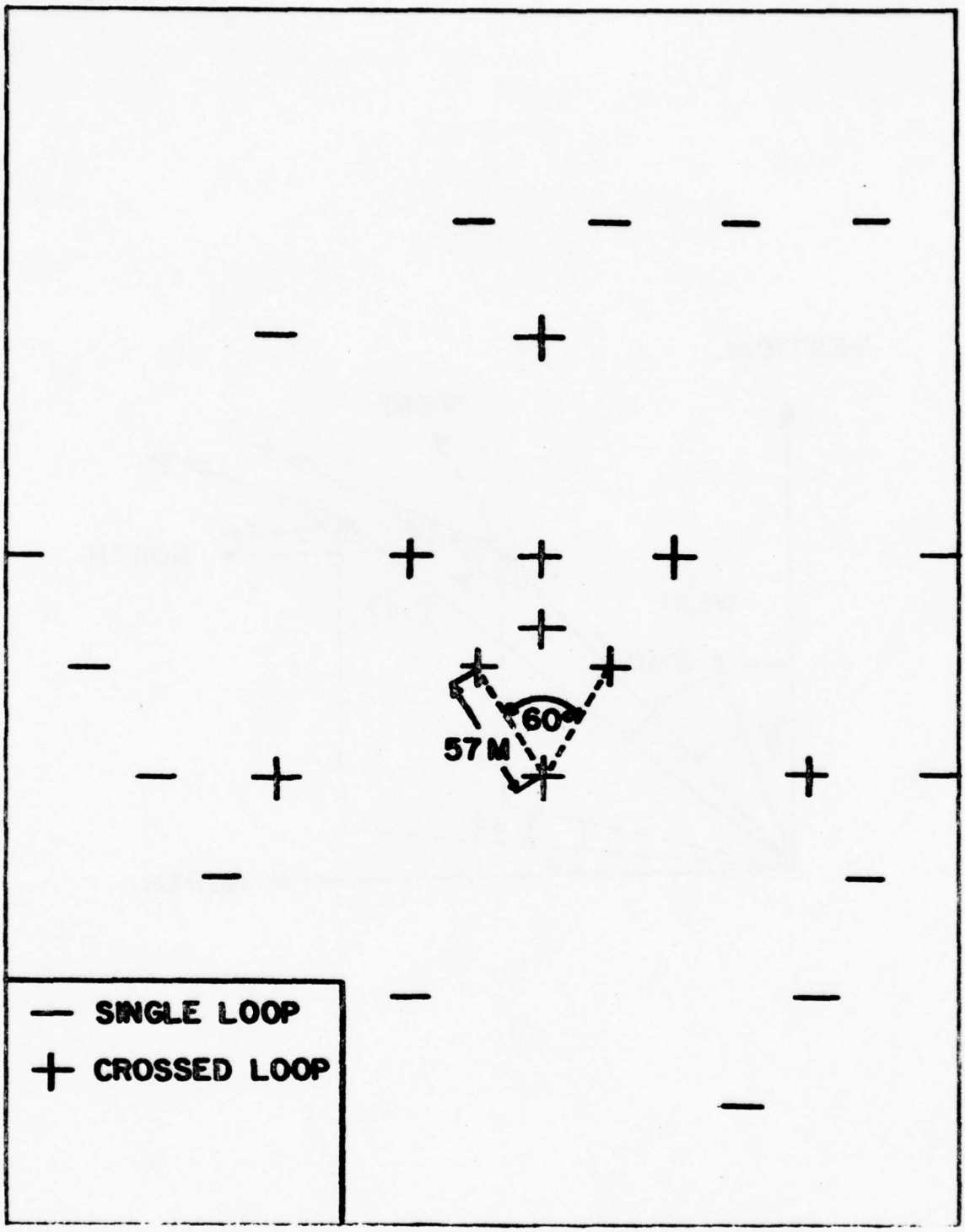

25 ANTENNA RECEIVING ARRAY

FIGURE 6

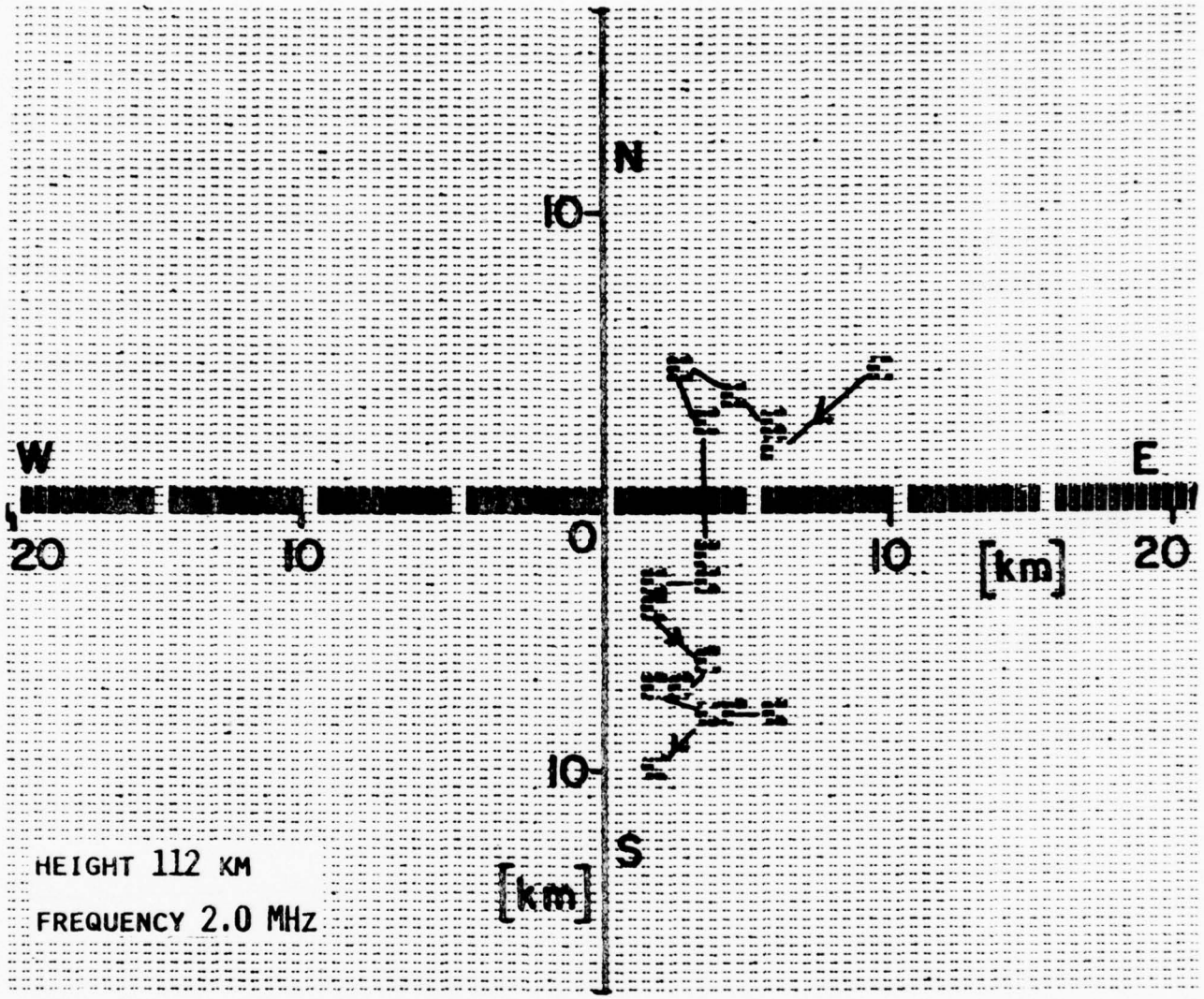

SKY MAP

FIGURE 7

WAVE PARAMETER	MEASURING TECHNIQUE
Amplitude	Digitization of Log-Compressed Signal in 1/2 dB Steps; Coherent Integration Over Between 16 and 256 Quadrature Samples.
Phase	Ratio of Integrated Quadrature Samples, Synchronization of IF and Sampling Time.
Range	Synchronization of Transmitter Pulse and Sampling Time.
Incidence Angles	Receiving Antenna Array and Antenna Switch.
Doppler	Discrete Complex Fourier Transform.
Wave Polarization	Polarized Receiving Antennas and Antenna Switch.

MEASURING TECHNIQUES

TABLE 1

o-Switch	PERIOD [min]	STARTING TIMES		
		A-Ionogram	B-Ionogram	C-Ionogram
0	∞			
2	1	30"		
3	5	X1'30", X6'30"		
4	10	X9'00" (X≠5)		59'00"
5	15	14', 29', 44'00"		59'00"
6	30	29'00"		59'00"
7	60			59'00"
10	0.5	30"	00"	
11	2.5	X1'30", X6'30"	X4'00", X9'00"	
12	5	X9'00" (X≠5)	X4'00"	59'00"
13		14', 29', 44'00"	09', 24', 39', 54'00"	59'00"
14		29'00"	09', 39'00"	59'00"
15			09'00"	59'00"

AUTOMATIC IONOGRAM SEQUENCES

TABLE 2

*	FUNCTION	DIMENSION	VALUE
1	Begin Frequency	[MHz]	0, 1, 2, ..., 39
2	End Frequency	[MHz]	1, 2, ..., 40
3	Frequency Increments	[kHz]	5, 10, 25, 50, 100, 200 5 & 20, 10 & 40, 10 & 90, 20 & 180
4	Range Increments	[km]	0.5, 1.0, 1.5, 2.0, 3.0, 4.5, 5.0, 6.0, 10.5
5	Range Samples		128, 256
6	Doppler Resolution	[Hz]	0.2, 0.4, 0.8, 1.6, 3.2, 6.3, 12.5, 25.0*
7	Number of Doppler Lines		1, 2, 4, 8, 16
8	Amplitude Resolution	[dB]	0.5, 1.0
9	Phase	[°]	22.5
10	Pulse Repetition Rate	[Hz]	50, 100, 200, 400
11	Pulse Width	[μs]	50, 100, 150
12	Samples per Frequency		16, 32, 64, 128, 256
13	Azimuth Resolution	[°]	30, 60, 90, 120, 180, none
14	Wave Polarization		ordinary, extraordinary, ordinary and extraordinary
15	Range Start	[km]	7.5, 37.5, 60.0, 82.5, 112.5, 172.5, 232.5, 352.5, 832.5, 712.5
16	Range Window	[Pulse Period]	-4, -3, -2, -1, no ident., +1, +2, +3, +4, +5
17	Receiver Gain Adj.	[dB]	0, 6, 12, 18, 24, 30, 36, 42
18	Ionogram Rate	[hr^{-1}]	1 to 120 (see Table 2)

*Divide by number of used antenna configurations.

PROGRAMMABLE IONOGRAM PARAMETERS

TABLE 3

No.	1	2	3	4	5	6	7	8	9	10	11	12	13	14	15	16	17	18	19	20	21	22	23	24	25	26	27	28	29	30	31	32
Spectral Lines	2	2	4	4	8	2	4	4	4	8	8	8	16	16	1	1	1	2	2	2	4	2	2	4	1	2	2	2	4	4	8	4
Range Windows	1	2	1	1	1	2	1	2	2	1	2	1	1	1	2	2	1	2	1	1	1	1	1	1	2	1	2	2	2	1	1	1
Polarizations	2	1	2	1	1	2	2	1	2	1	1	2	1	1	2	1	2	1	1	2	1	1	2	1	2	2	1	2	1	2	1	1
Incidence Angles	6	6	3	6	3	2	2	2	1	2	1	1	1	1	3	6	6	3	6	3	3	6	3	3	2	2	2	1	1	1	1	2
Channels	24	24	24	24	24	16	16	16	16	16	16	16	16	16	12	12	12	12	12	12	12	12	12	12	8	8	8	8	8	8	8	8

IONOGRAM PARAMETER COMBINATIONS

TABLE 4

PARAMETER	DRIFT OBSERVATION						AURORA OBSERVATION				
Digitizing Rate [Hz]	100			200			400				
Sample Spacing [sec]	1/4			1/8			1/16			1/32	
Channels	24			24			24			12	
Antennas/FRB's	4/6; 6/4; 8/3*; 12/2$^{\Delta}$; 24/1			4/6; 6/4; 8/3; 12/2; 24/1			4/6; 6/4; 8/3; 12/2; 24/1			4/3; 6/2; 12/1	
Time Samples	256	128	64	256	128	64	256	128	64	256	64
Time Window [sec]	64	32	16	32	16	8	16	8	4	8	2
Spectral Lines	128	128	64	128	128	64	128	64	64	128	64
Spectral Resol. [mHz]	31	31	62	62	62	125	125	250	250	125	500
Spectral Range [Hz]	4	4	4	8	8	8	16	16	16	32	32
Min. Window Spacing [sec]	65	33	17	33	17	9	17	9	5	9	3

* 8 switch positions used for seven antennas with overrange capability (two repetition rates).

Δ 12 switch positions used for 10 antennas with overrange capability (three repetition rates).

DRIFT PROGRAM

TABLE 5

A P P E N D I X B

IONOSPHERIC MONTHLY MEDIAN CURVES

FOR GOOSE BAY, MARCH 1975 - FEBRUARY 1976

MEDIAN VALUES OF h' AND f_0 AT GOOSEBAY, LABRADOR FOR MARCH 1975

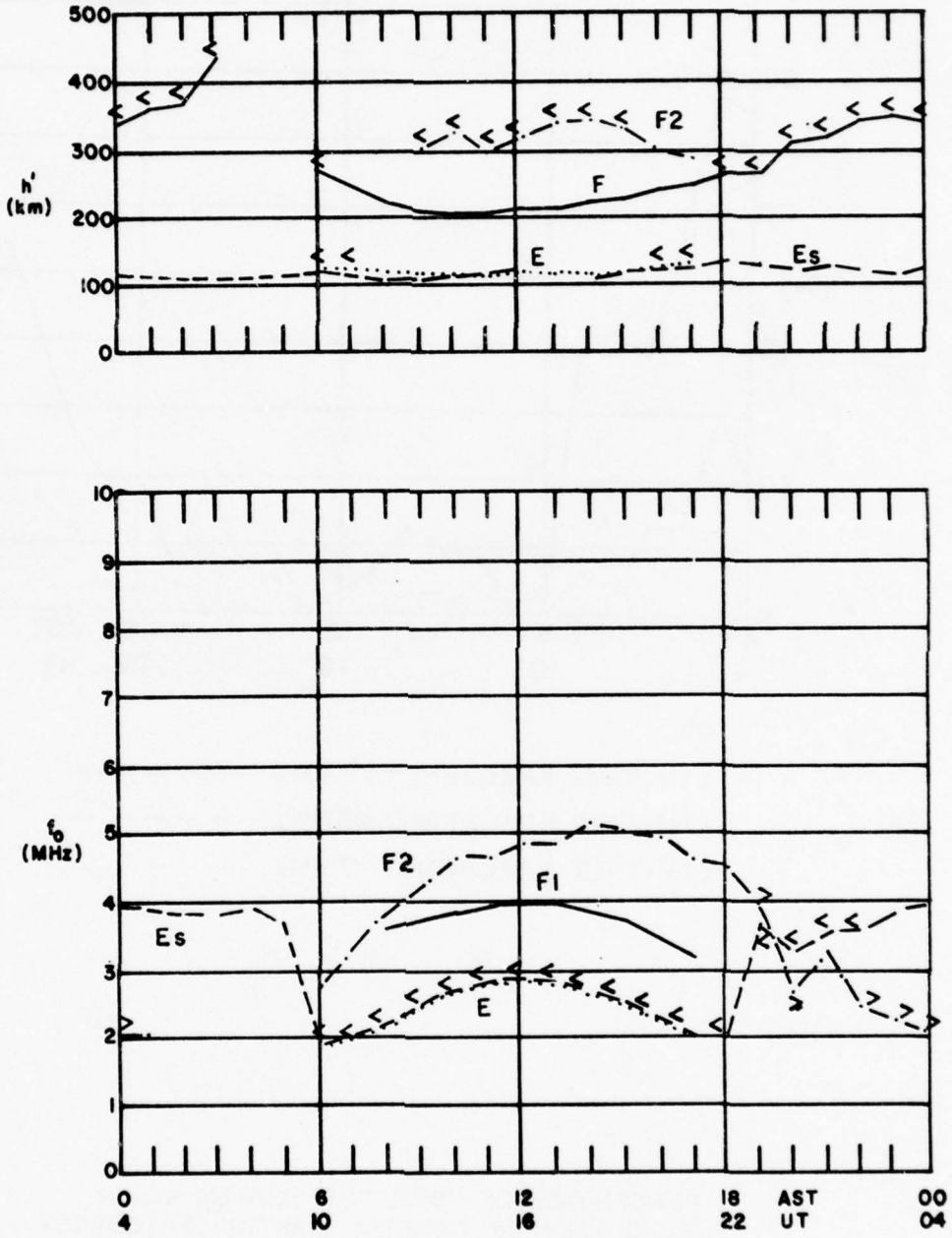

FIGURE 1

MARCH 1975
GOOSE BAY, LABRADOR

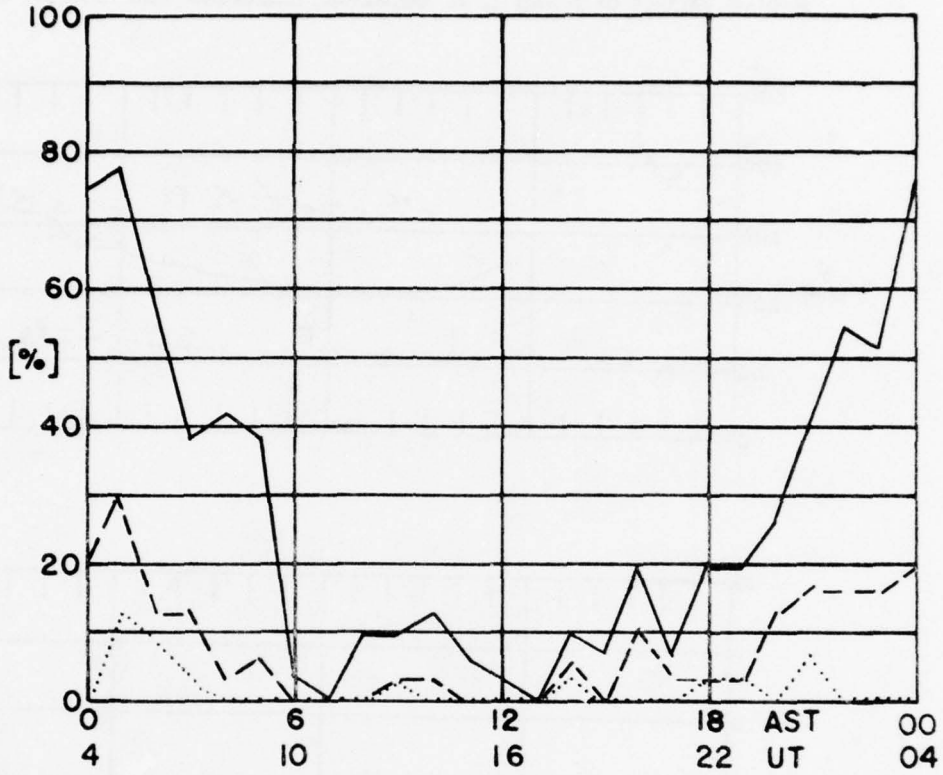

LIMITING FREQUENCY = 3MHz ——————
LIMITING FREQUENCY = 5MHz — — — — —
LIMITING FREQUENCY = 7MHz .....

PERCENTAGE OF TOTAL TIME DURING WHICH
$f_0 E_s$ IS GREATER THAN THE LIMITING FREQUENCY

FIGURE 2

MEDIAN VALUES OF h' AND f_0 AT GOOSEBAY, LABRADOR FOR APRIL 1975

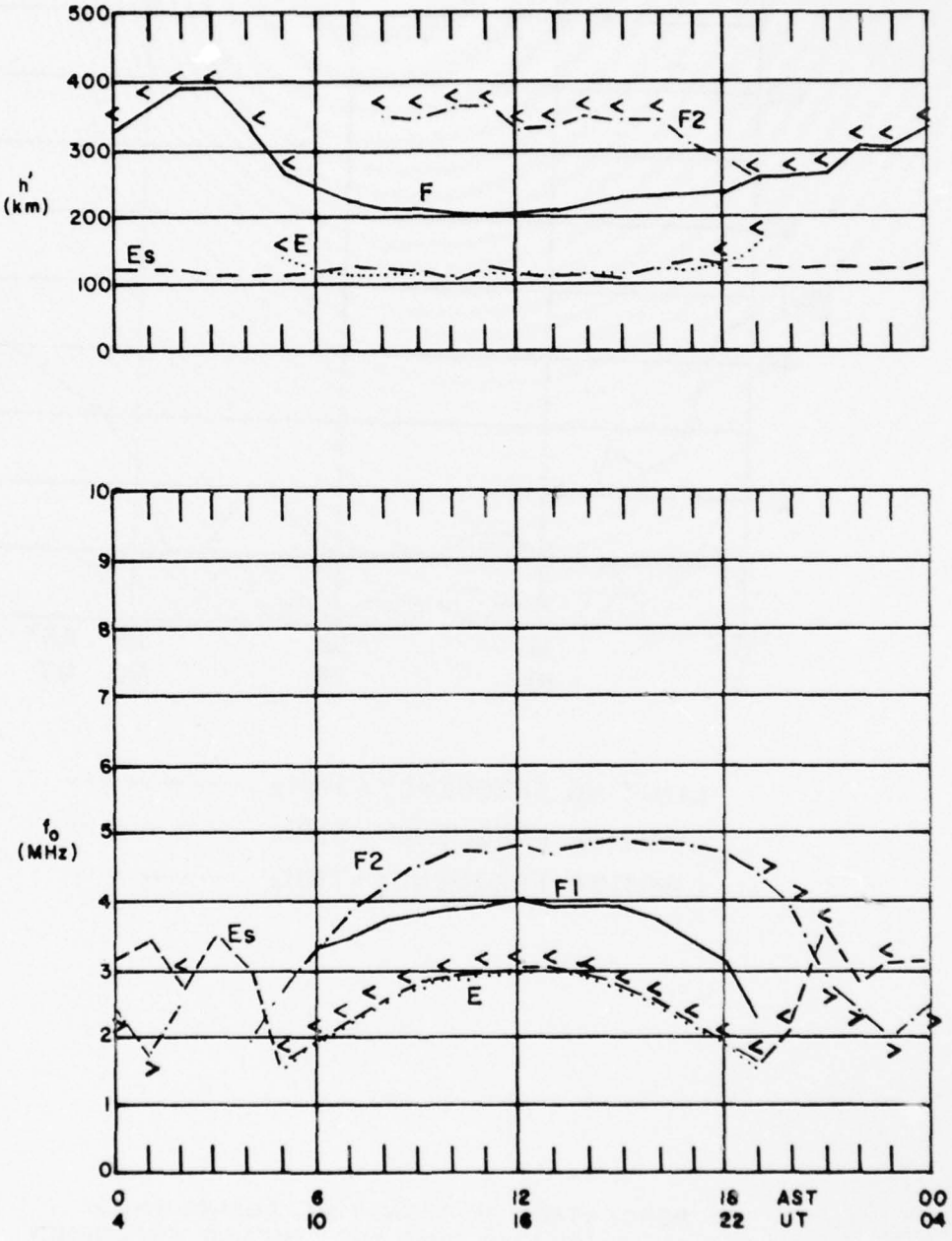

FIGURE 3

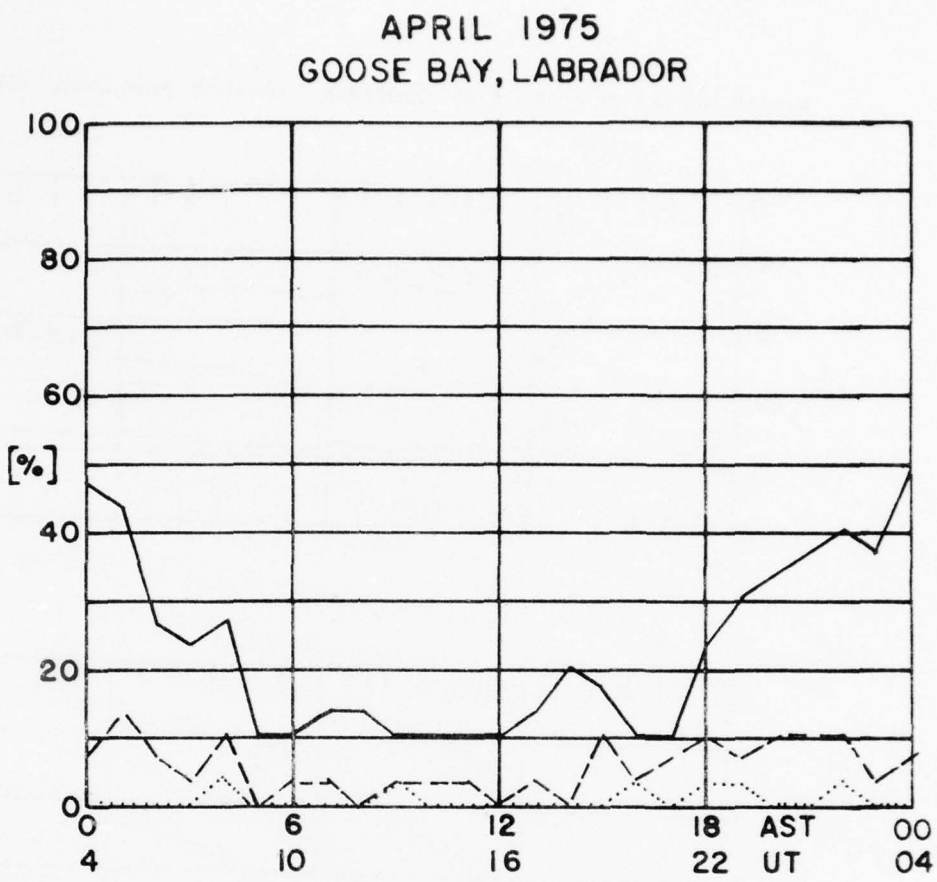

PERCENTAGE OF TOTAL TIME DURING WHICH
$f_0 E_s$ IS GREATER THAN THE LIMITING FREQUENCY

FIGURE 4

MEDIAN VALUES OF h' AND f_0 AT GOOSEBAY, LABRADOR FOR MAY 1975

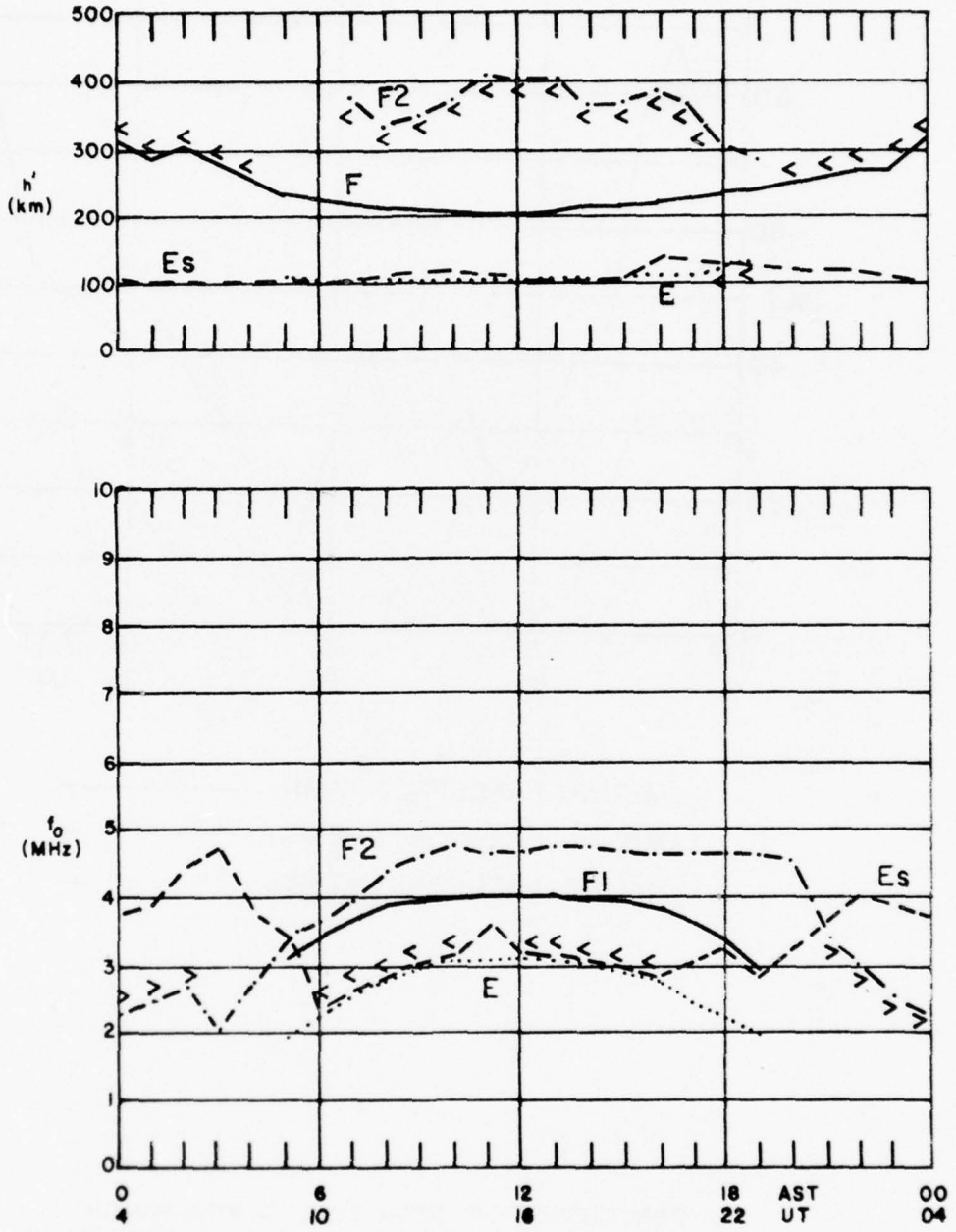

FIGURE 5

MAY 1975

GOOSE BAY, LABRADOR

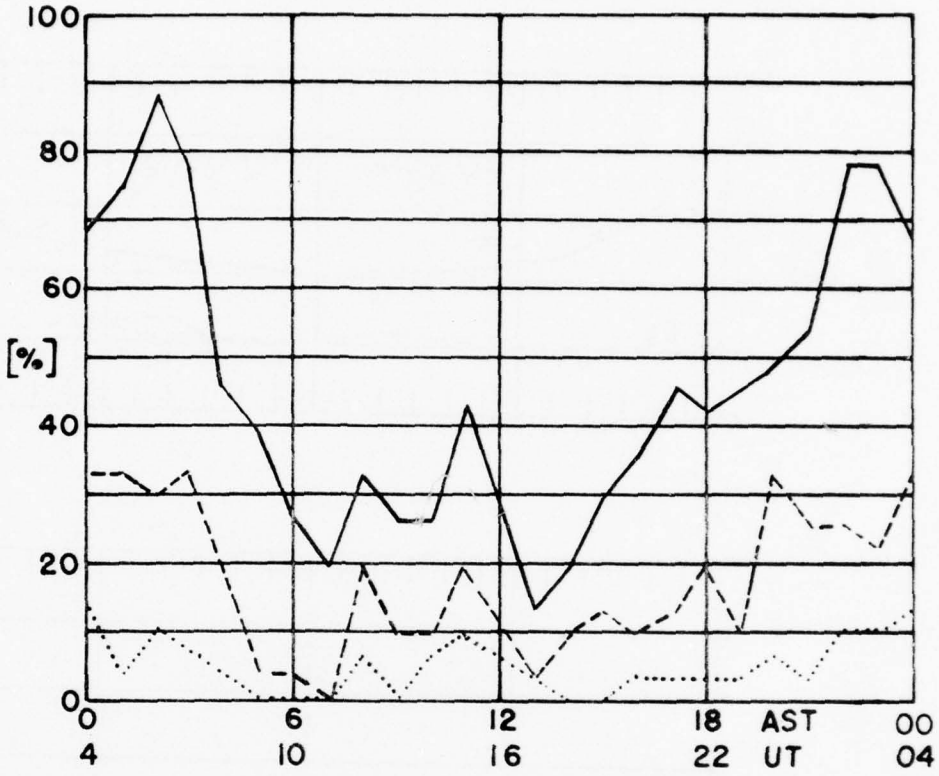

LIMITING FREQUENCY = 3MHz ————————

LIMITING FREQUENCY = 5MHz — — — — — —

LIMITING FREQUENCY = 7MHz .....

PERCENTAGE OF TOTAL TIME DURING WHICH
$f_0 E_s$ IS GREATER THAN THE LIMITING FREQUENCY

FIGURE 6

MEDIAN VALUES OF h' AND f_0 AT GOOSEBAY, LABRADOR FOR JUNE 1975

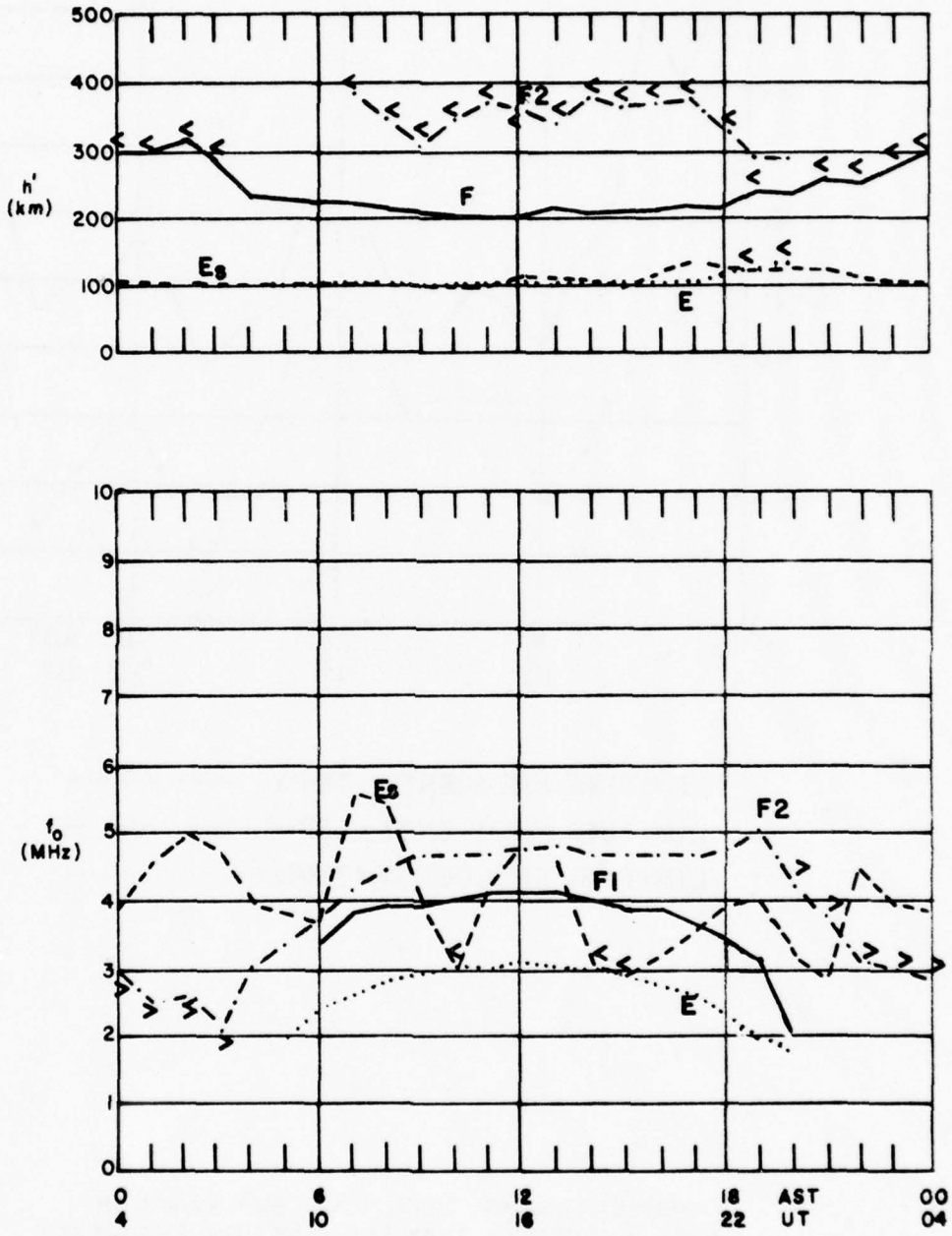

FIGURE 7

JUNE 1975

GOOSE BAY, LABRADOR

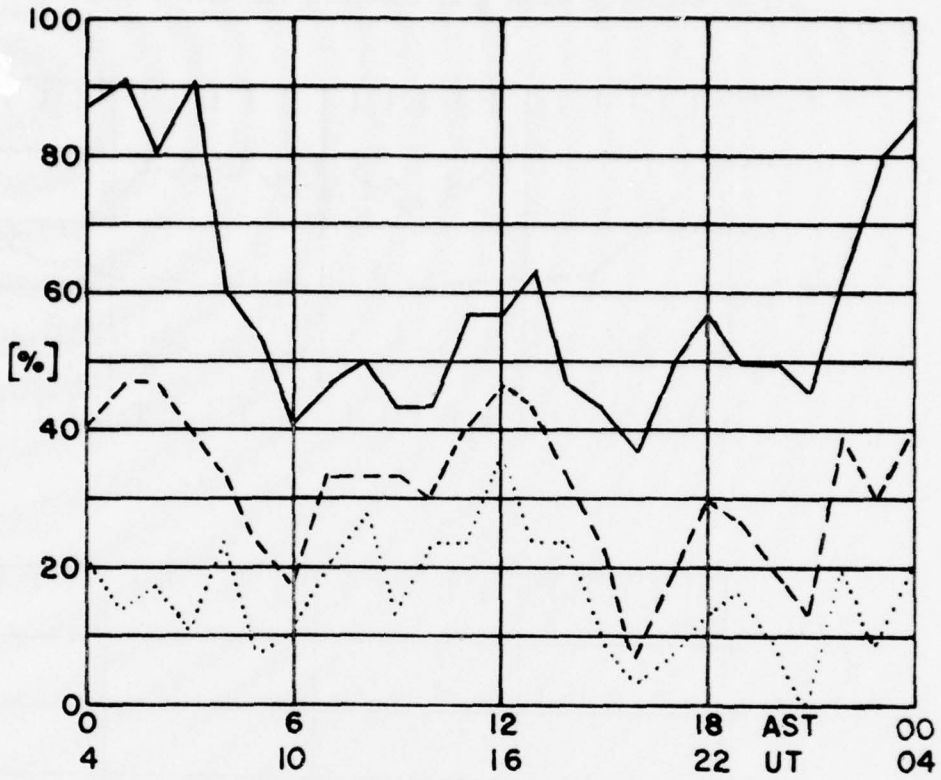

LIMITING FREQUENCY = 3MHz ————————

LIMITING FREQUENCY = 5MHz — — — — —

LIMITING FREQUENCY = 7MHz .....

PERCENTAGE OF TOTAL TIME DURING WHICH
$f_0 E_s$ IS GREATER THAN THE LIMITING FREQUENCY

FIGURE 8

MEDIAN VALUES OF h' AND f_0 AT GOOSEBAY, LABRADOR FOR July 1975

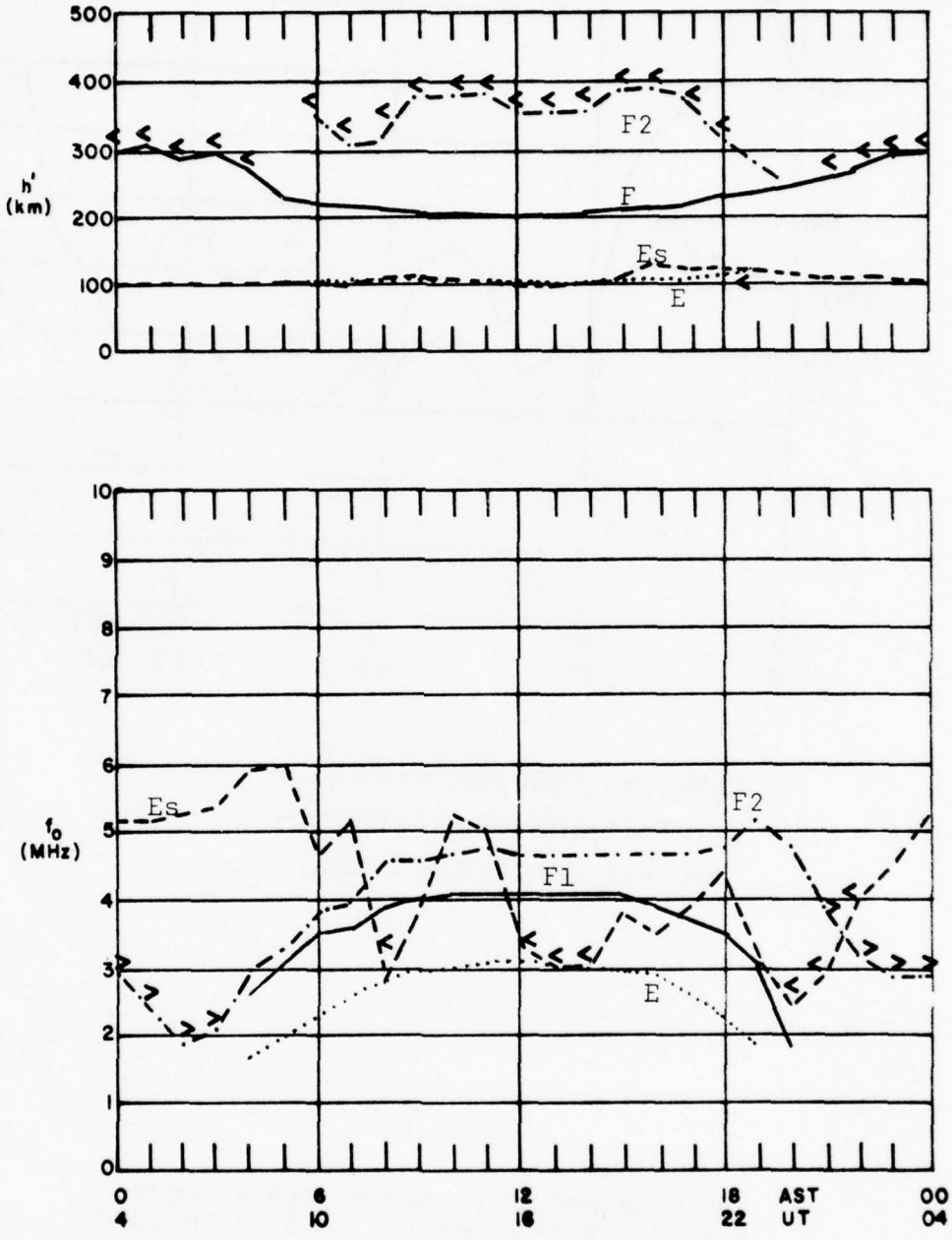

FIGURE 9

JULY 1975

GOOSE BAY, LABRADOR

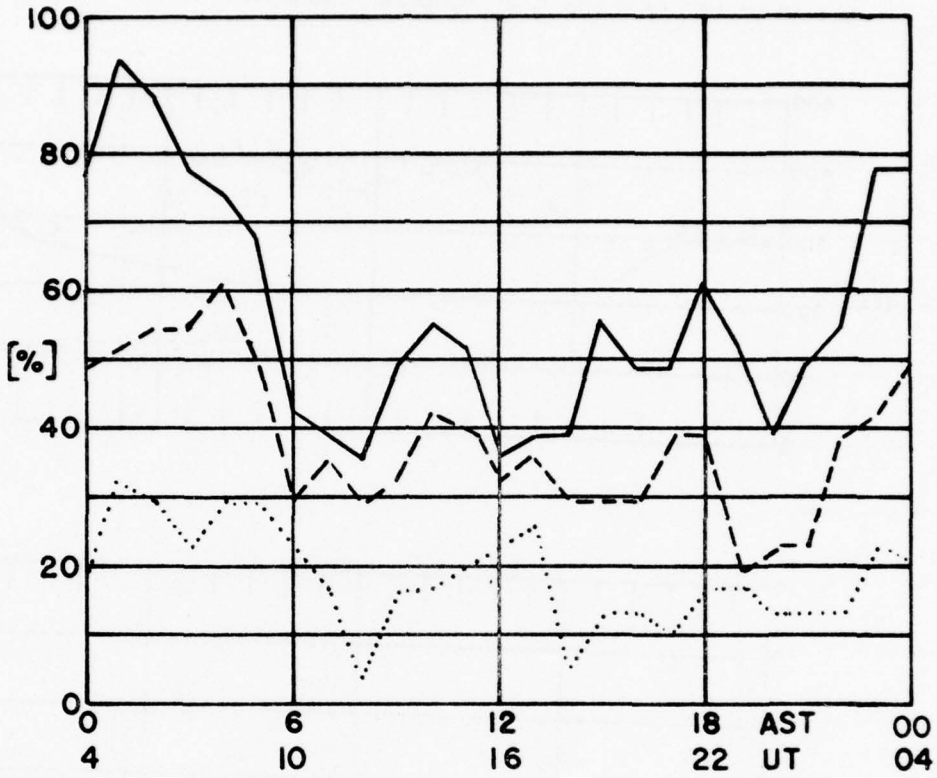

LIMITING FREQUENCY = 3MHz ——————

LIMITING FREQUENCY = 5MHz – – – – – –

LIMITING FREQUENCY = 7MHz .....

PERCENTAGE OF TOTAL TIME DURING WHICH
$f_0 E_s$ IS GREATER THAN THE LIMITING FREQUENCY

FIGURE 10

MEDIAN VALUES OF h' AND f_0 AT GOOSEBAY, LABRADOR FOR AUGUST 1975

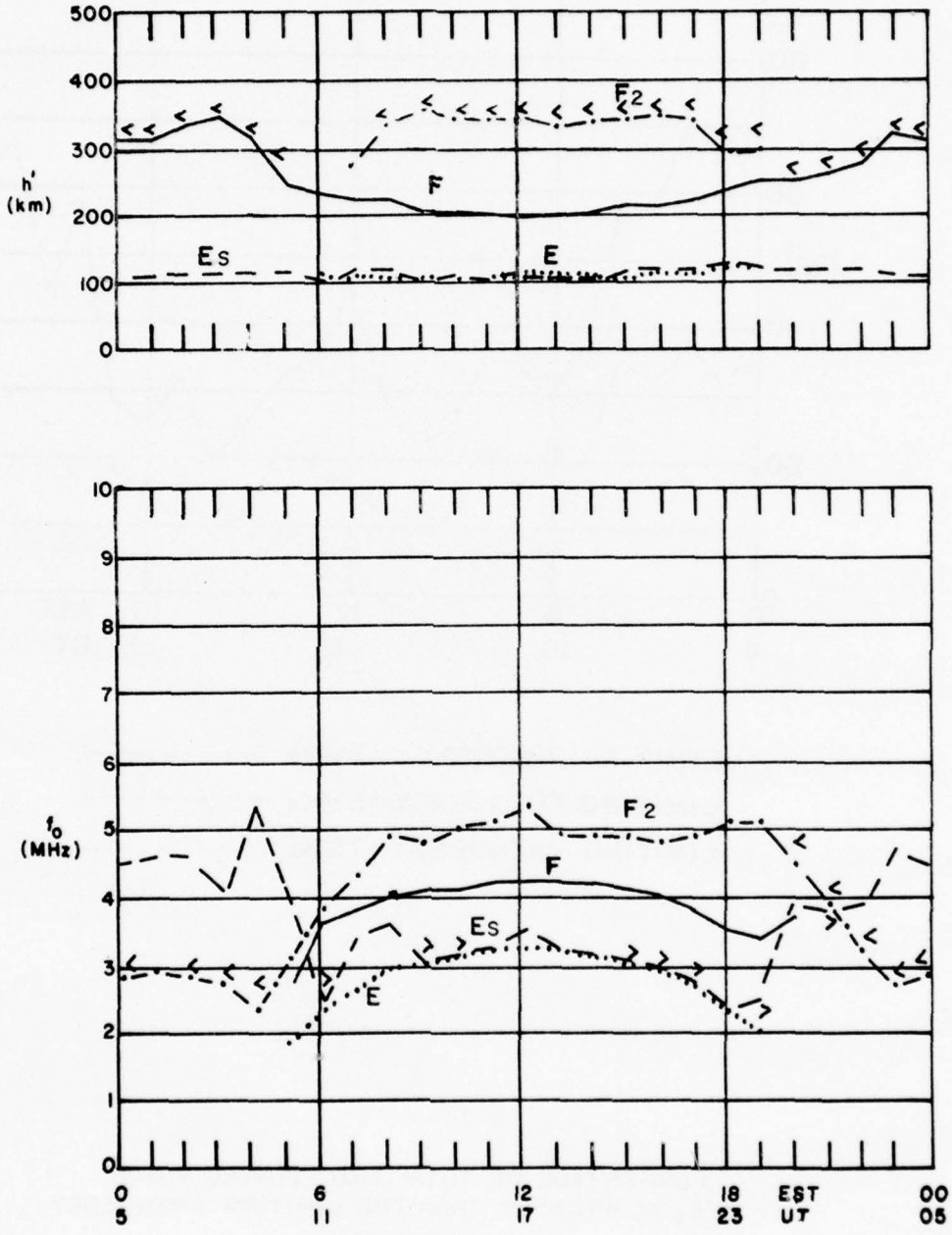

FIGURE 11

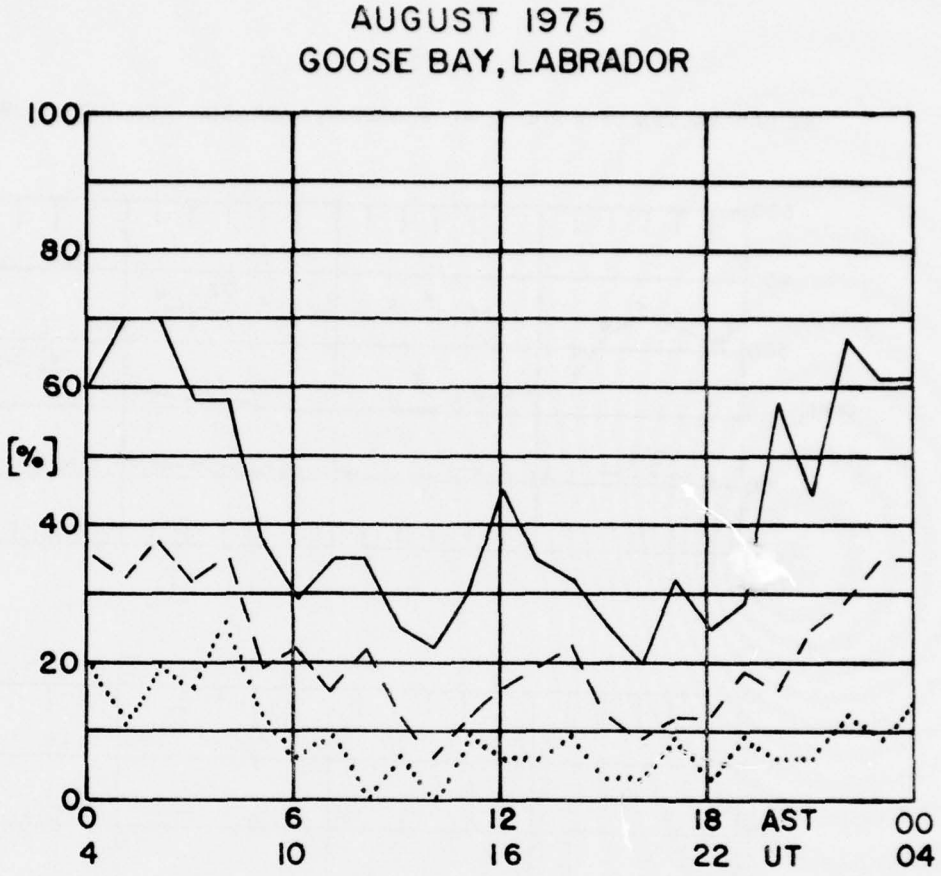

PERCENTAGE OF TOTAL TIME DURING WHICH
$f_0 E_s$ IS GREATER THAN THE LIMITING FREQUENCY

FIGURE 12

MEDIAN VALUES OF h' AND f_0 AT GOOSEBAY, LABRADOR FOR SEPTEMBER 1975

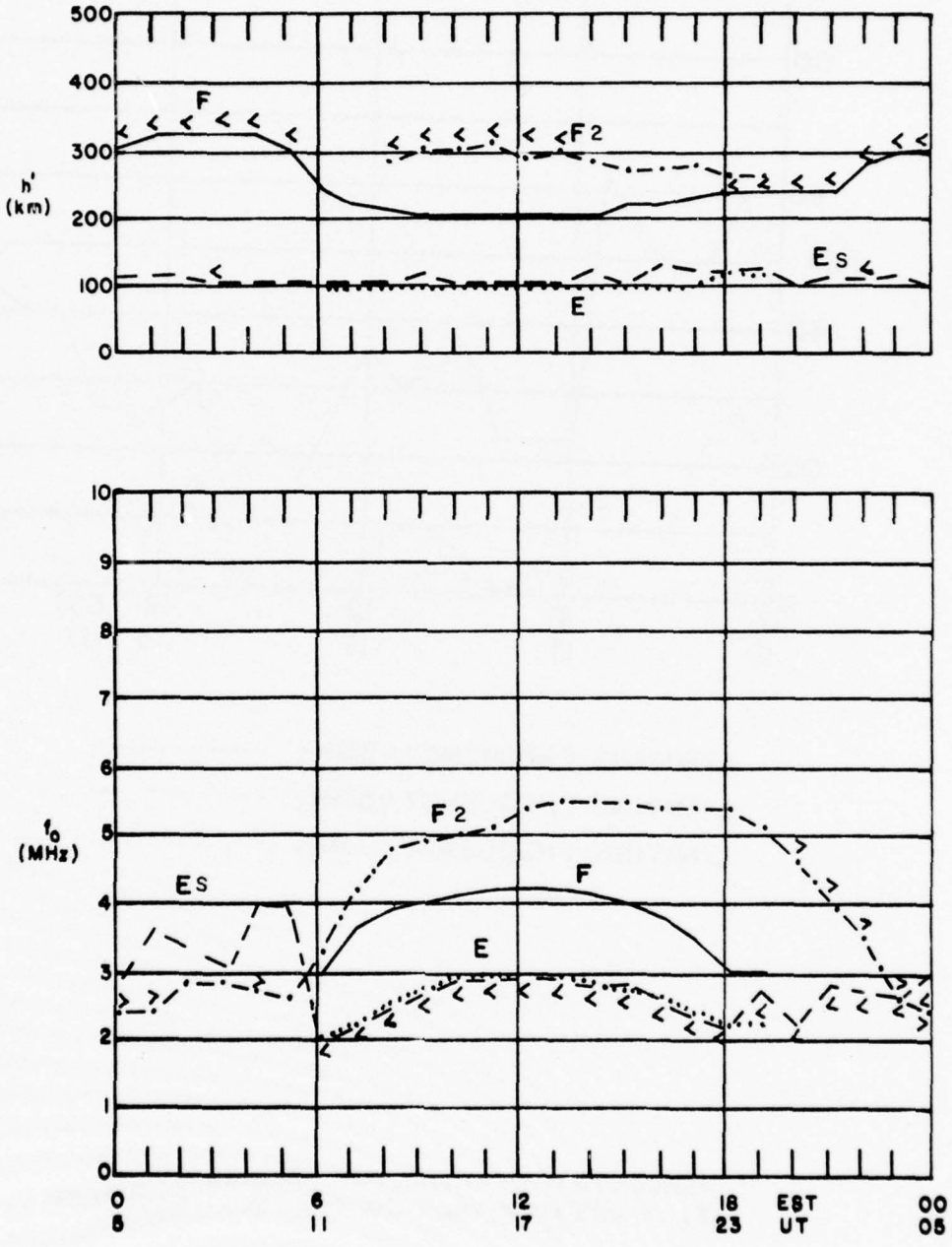

FIGURE 13

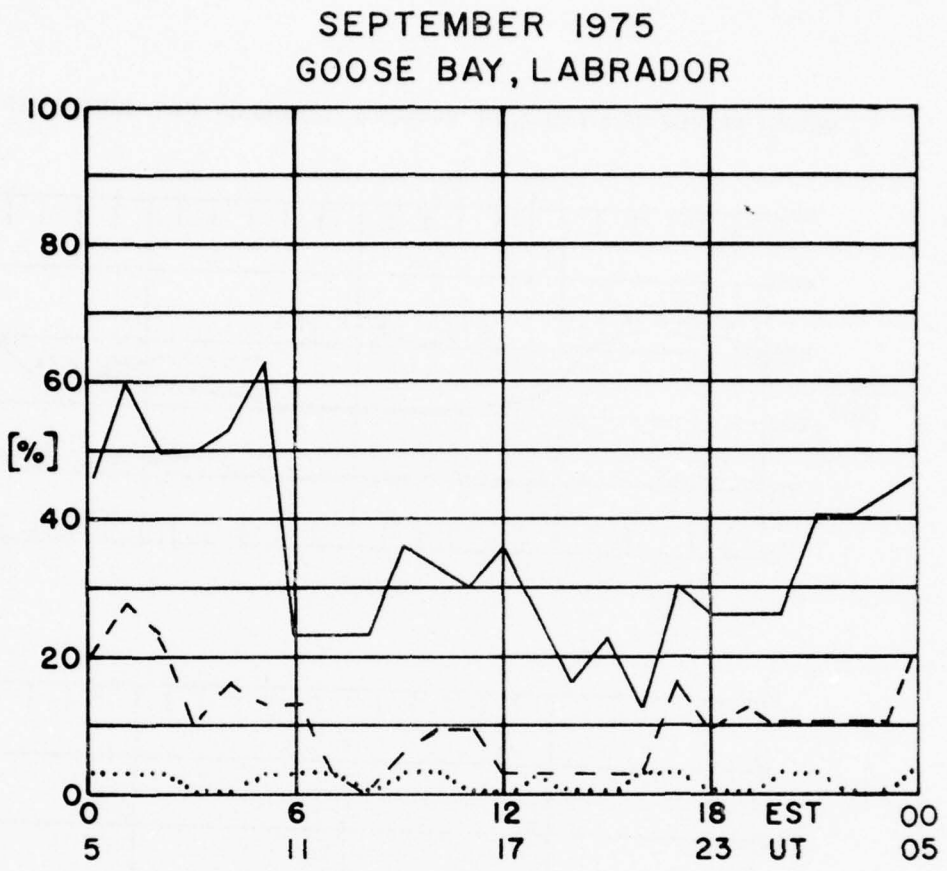

PERCENTAGE OF TOTAL TIME DURING WHICH
$f_0 E_s$ IS GREATER THAN THE LIMITING FREQUENCY

FIGURE 14

MEDIAN VALUES OF h' AND f_0 AT GOOSEBAY, LABRADOR FOR OCTOBER 1975

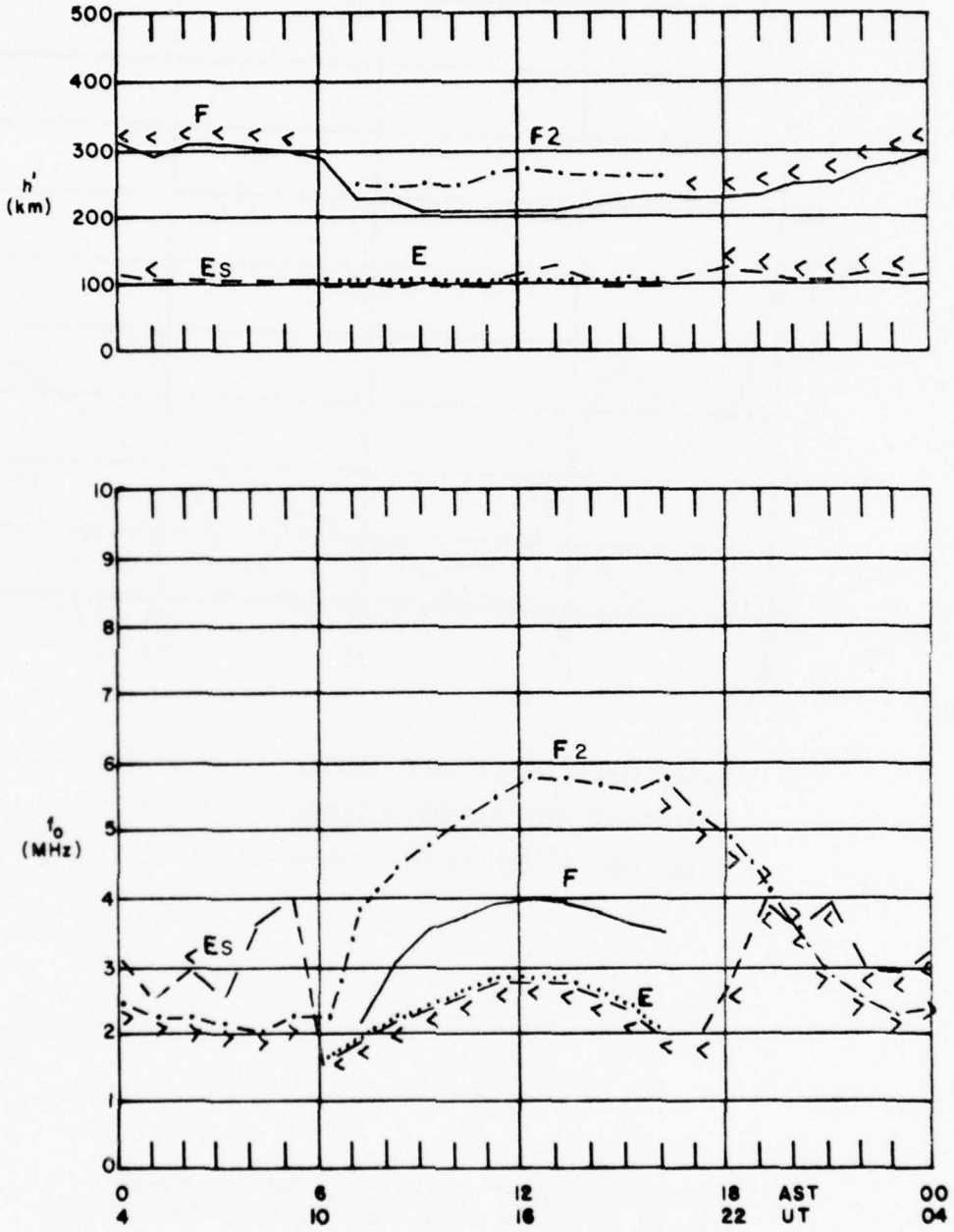

FIGURE 15

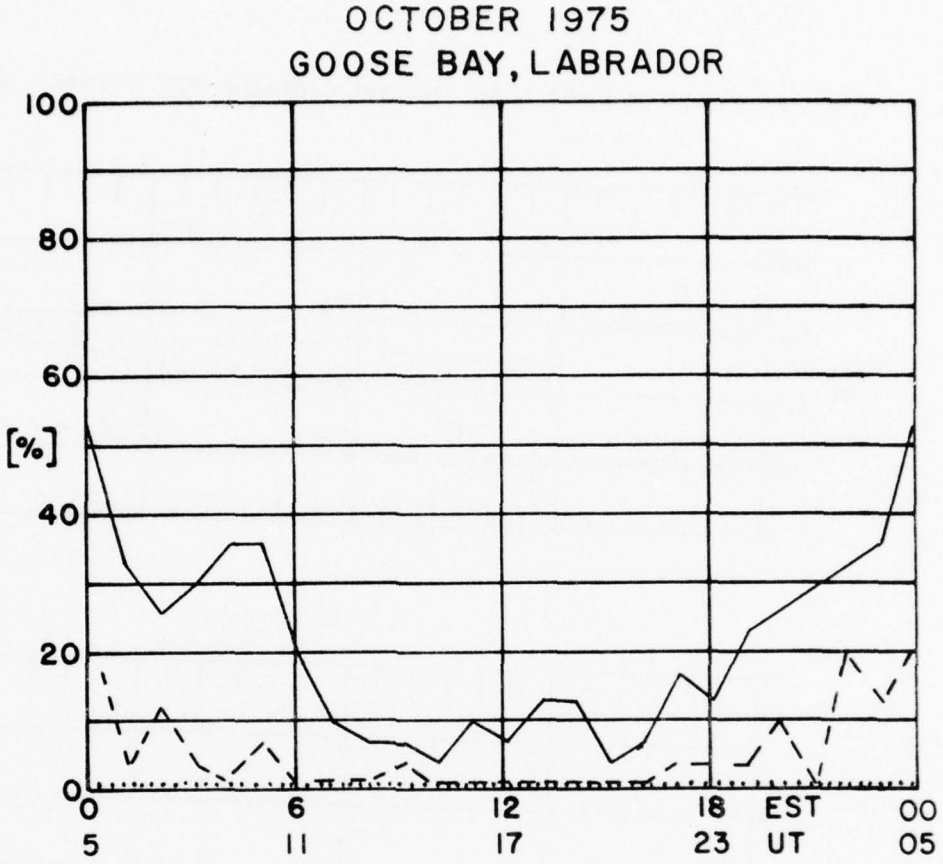

PERCENTAGE OF TOTAL TIME DURING WHICH
$f_o E_s$ IS GREATER THAN THE LIMITING FREQUENCY

FIGURE 16

MEDIAN VALUES OF h' AND f_0 AT GOOSEBAY, LABRADOR FOR NOVEMBER 1975

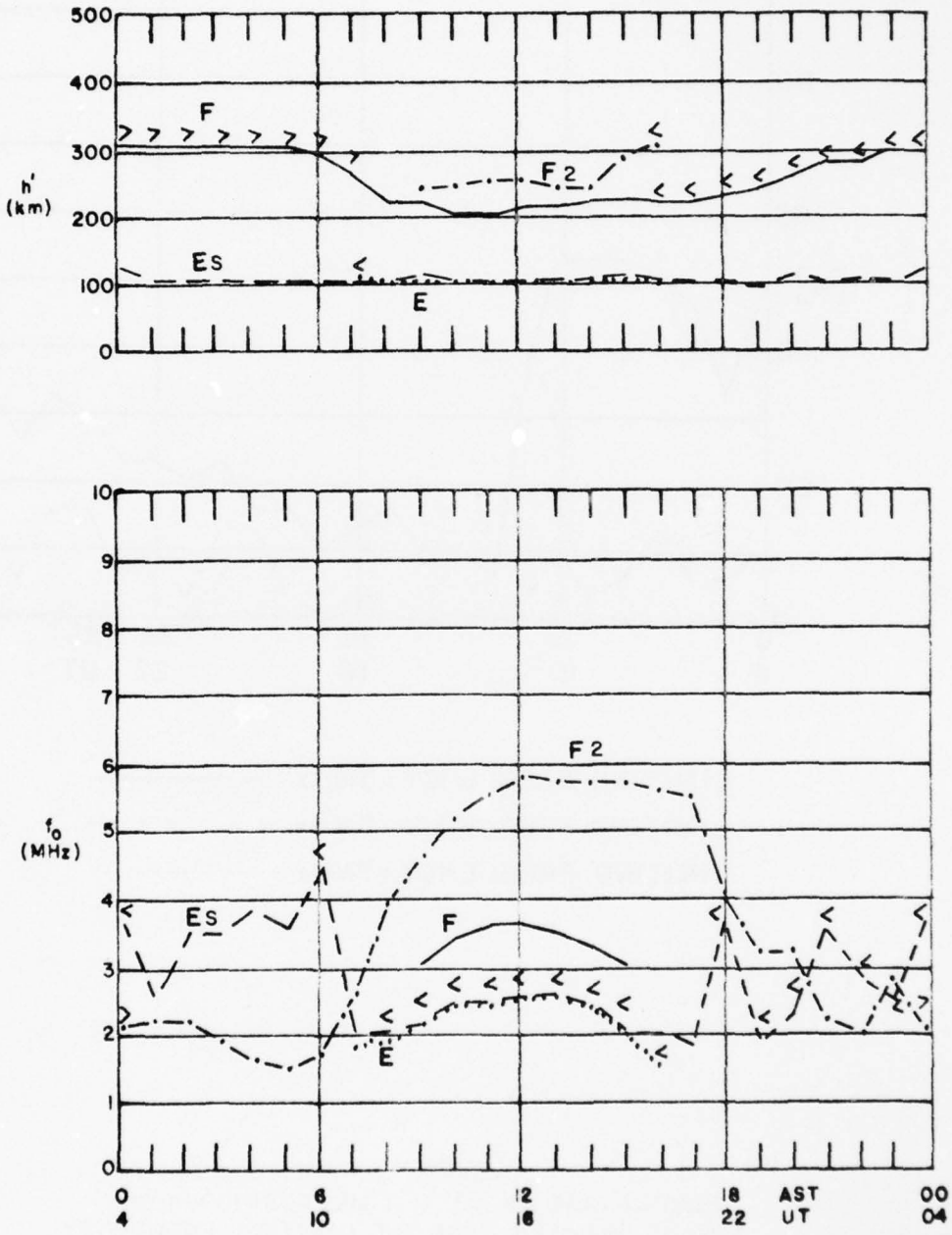

FIGURE 17

NOVEMBER 1975
GOOSE BAY, LABRADOR

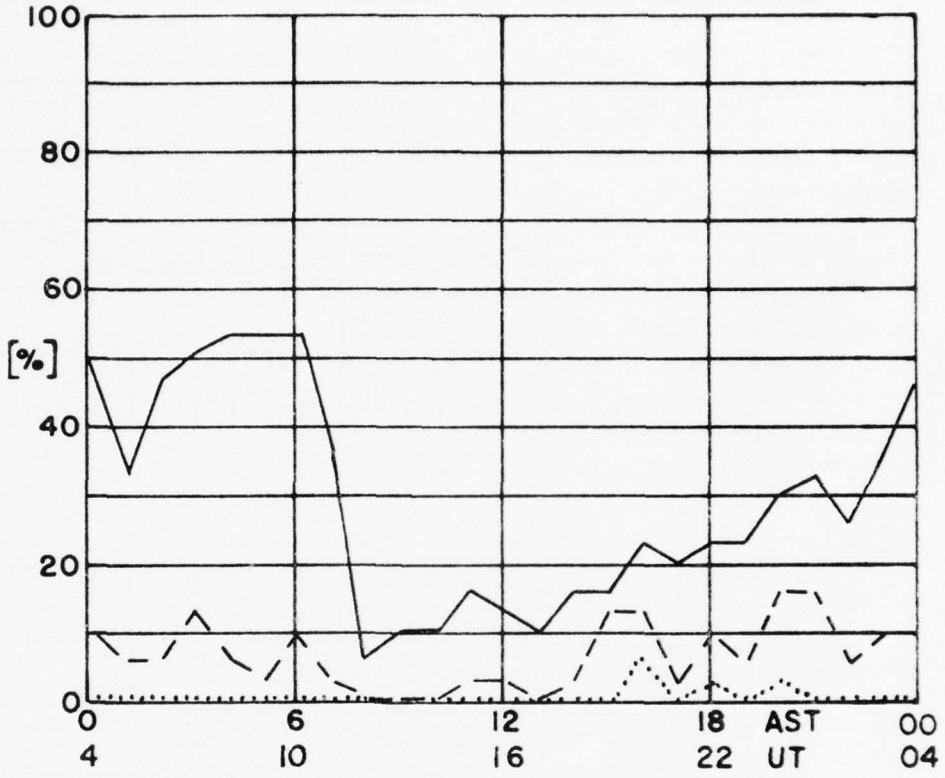

LIMITING FREQUENCY = 3MHz ——————
LIMITING FREQUENCY = 5MHz — — — — — —
LIMITING FREQUENCY = 7MHz .....

PERCENTAGE OF TOTAL TIME DURING WHICH
$f_0 E_s$ IS GREATER THAN THE LIMITING FREQUENCY

FIGURE 18

MEDIAN VALUES OF h' AND f_0 AT GOOSEBAY, LABRADOR FOR DECEMBER 1975

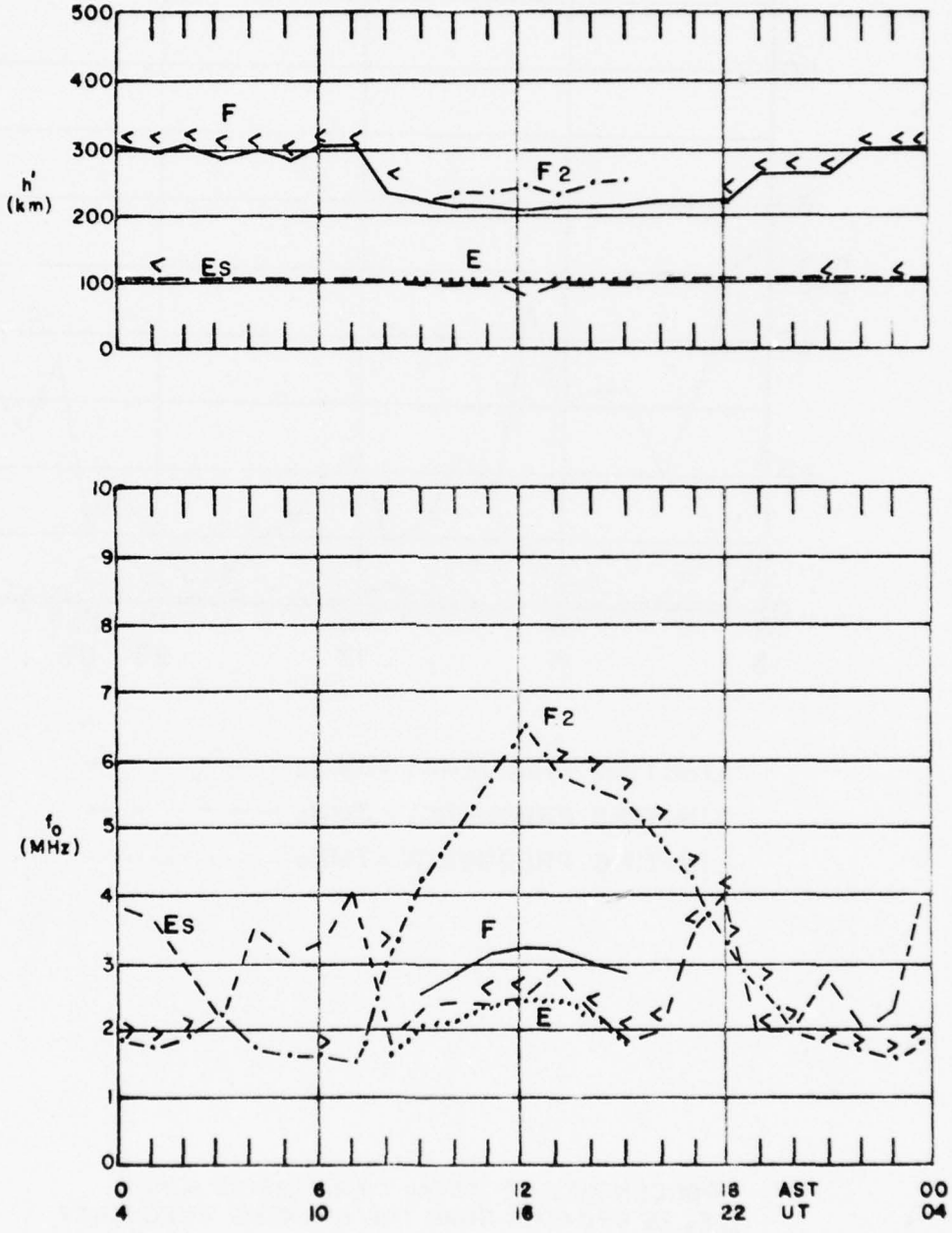

FIGURE 19

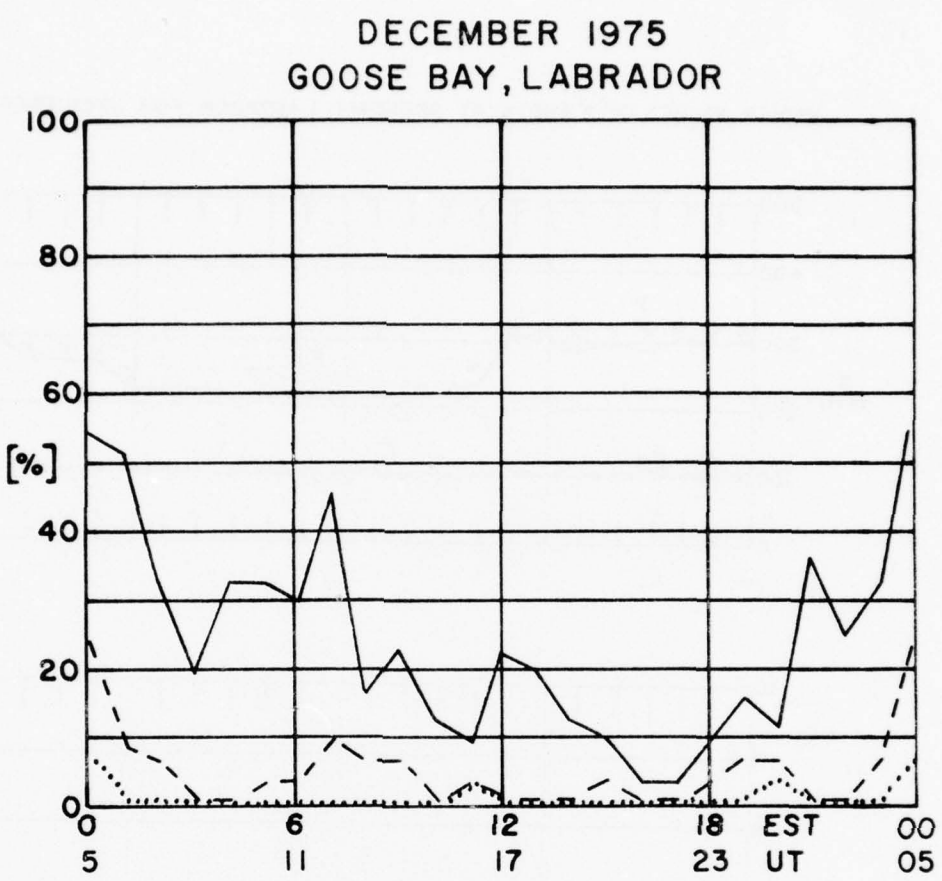

PERCENTAGE OF TOTAL TIME DURING WHICH
$f_0 E_s$ IS GREATER THAN THE LIMITING FREQUENCY

FIGURE 20

MEDIAN VALUES OF h' AND f_0 AT GOOSEBAY, LABRADOR FOR JANUARY 1976

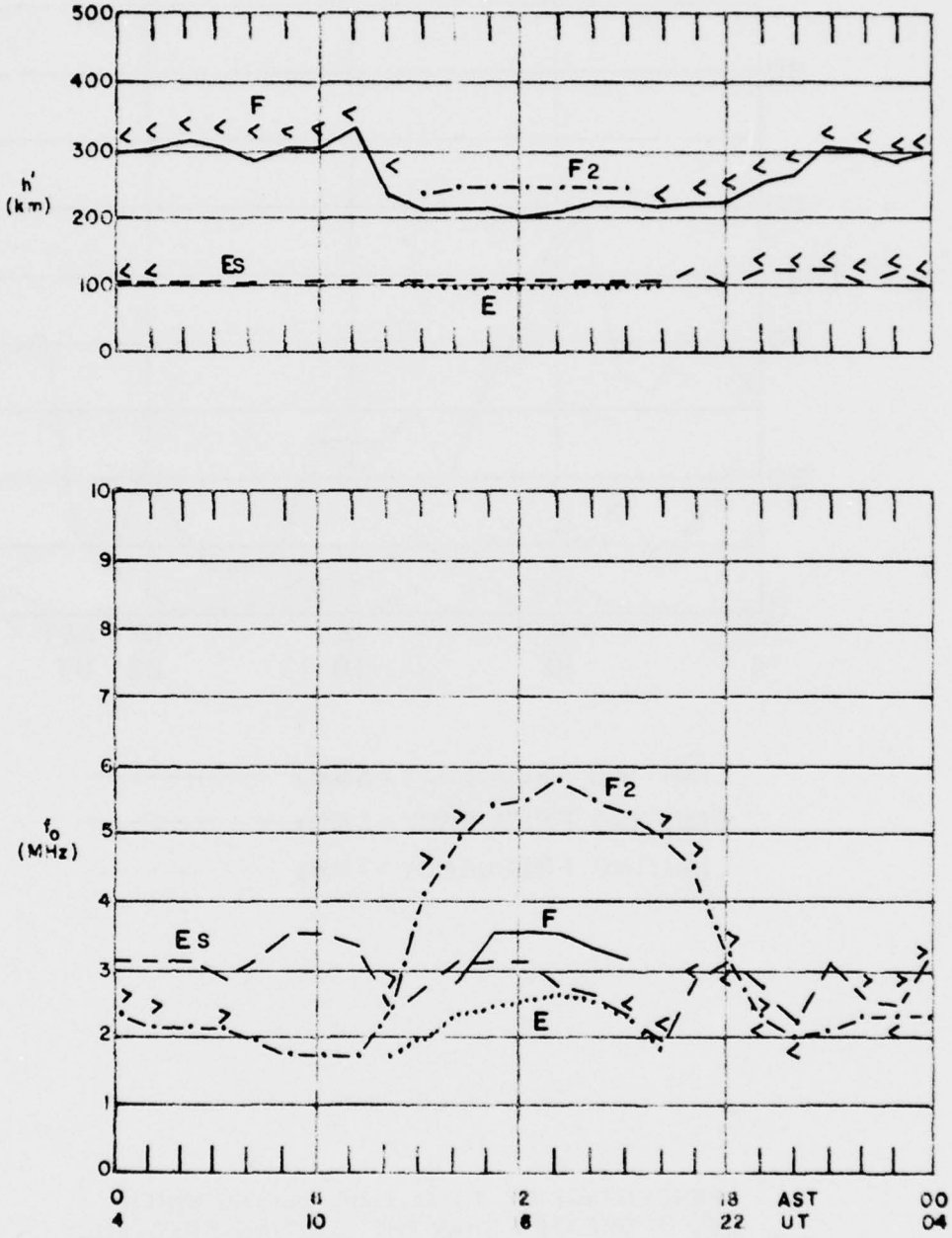

FIGURE 21

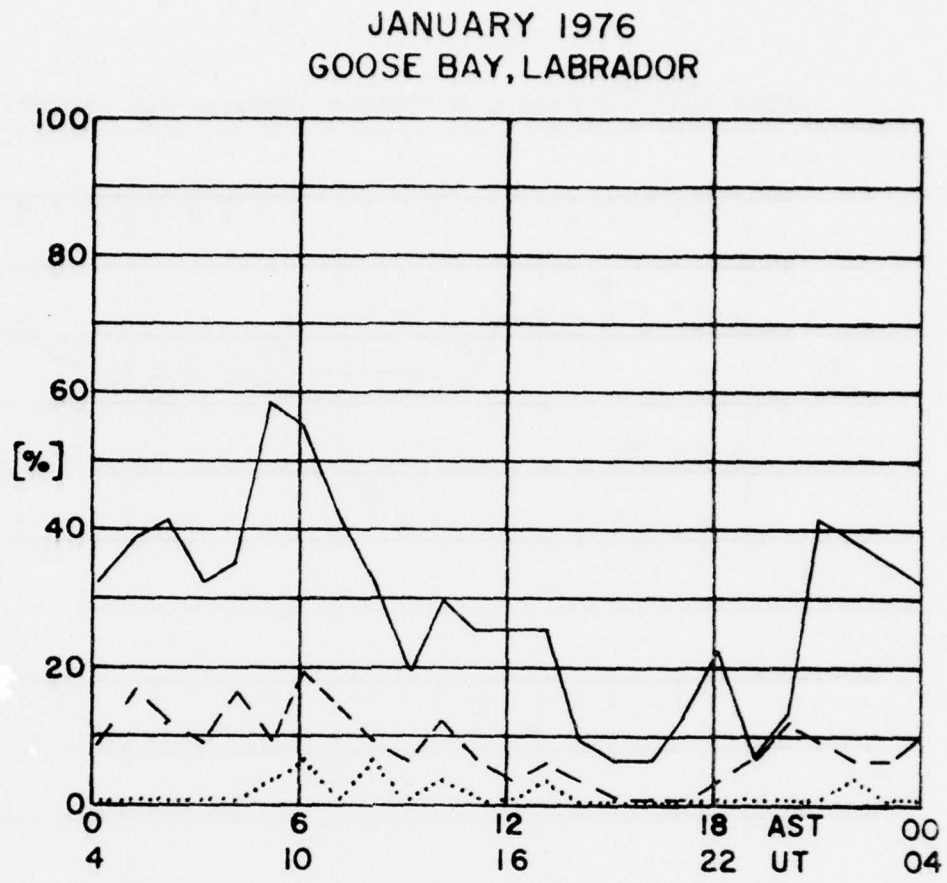

PERCENTAGE OF TOTAL TIME DURING WHICH
$f_0 E_s$ IS GREATER THAN THE LIMITING FREQUENCY

FIGURE 22

MEDIAN VALUES OF h' AND f_0 AT GOOSEBAY, LABRADOR FOR FEBRUARY, 1976

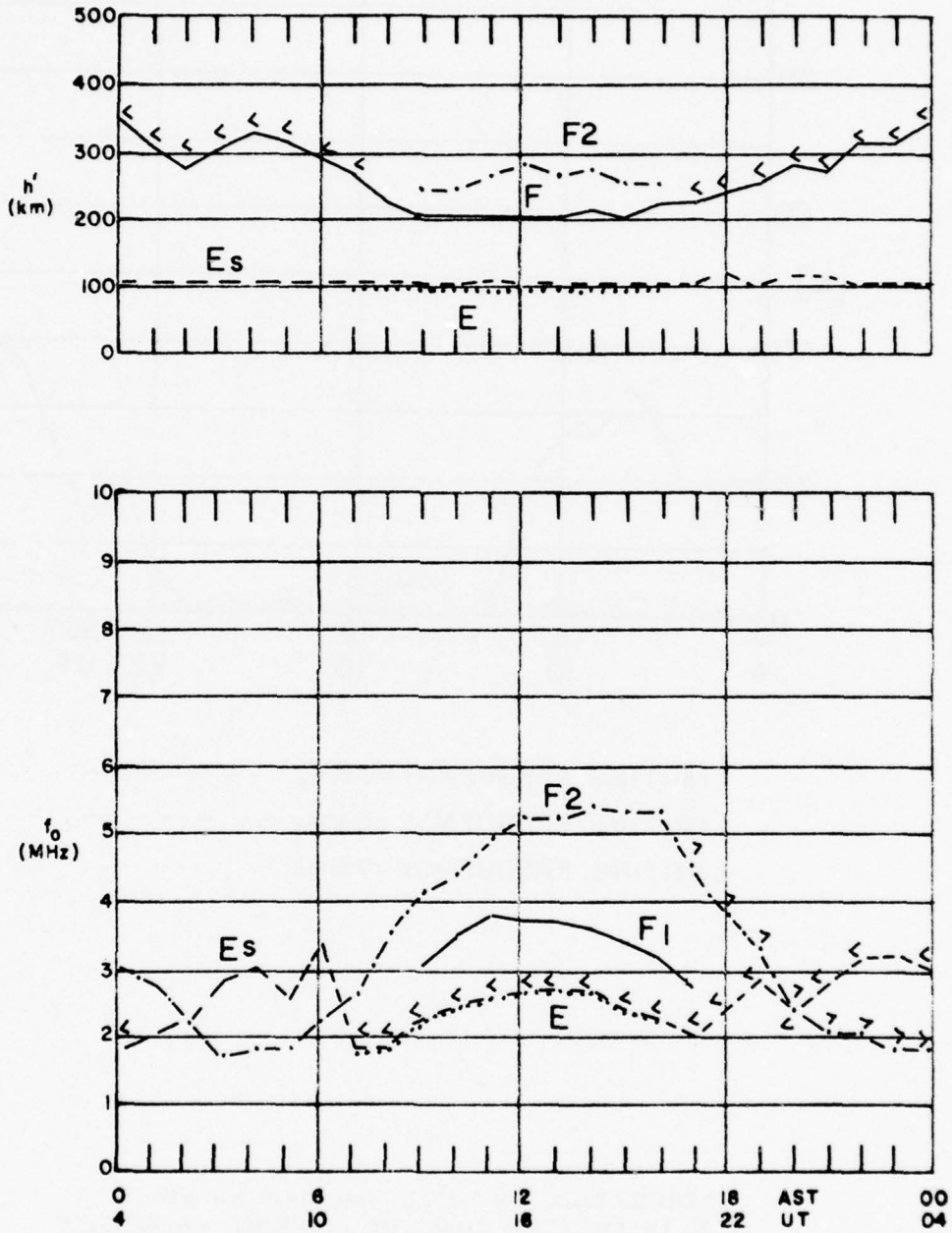

FIGURE 23

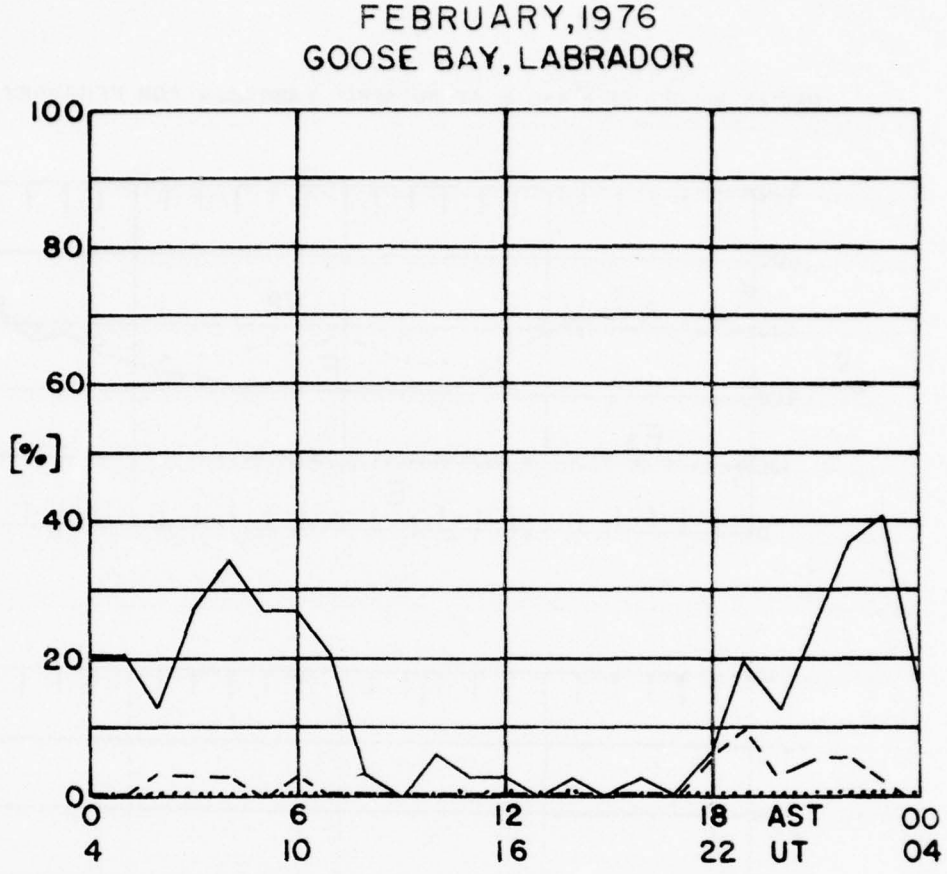

PERCENTAGE OF TOTAL TIME DURING WHICH
$f_0 E_s$ IS GREATER THAN THE LIMITING FREQUENCY

FIGURE 24

A P P E N D I X C

SUCCINCT GUIDE TO THE REDUCTION OF DIGITAL IONOGRAMS

UNIVERSITY OF LOWELL RESEARCH FOUNDATION
Lowell, Massachusetts

SUCCINCT GUIDE TO REDUCTION OF DIGITAL IONOGRAMS

by

Sheryl Smith

October 1975

TABLE OF CONTENTS

I. INTRODUCTION

This manual is primarily a users' guide to digital ionograms. It is not meant to be sufficient unto itself; it must be read with the U.R.S.I. Handbook of Ionogram Interpretation and Reduction. Users of evaluated data as well as raw and processed digital ionograms may find additional information furnished in this guide.

II. IDENTIFICATION OF TRACES

We are concerned with two regions:

E Region	90-150 km
F Region	150-750 km

E-Region

Normal E - A normal layer whose maximum frequency increases with cos χ (solar zenith angle). This layer is thick and shows significant retardation (cusp) near the layer's maximum ionization density (Figure 1).

Sporadic E - An abnormal, and mostly thin, layer caused by localized ionization; this layer can have a very short lifetime. The Es layer is classified into many types dependent on its shape and locality.

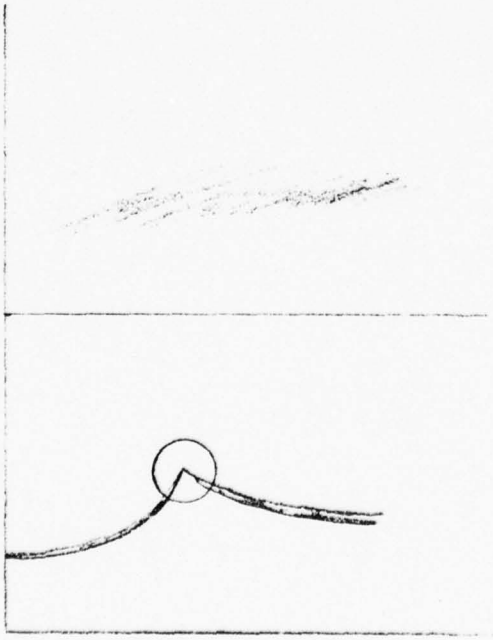

Auroral - diffuse; usually nonblanketing; flat or slowly increasing height with frequency with stratified traces in it which vary rapidly with time; most common Es type in Goose Bay. (See also URSI Handbook, Fig. 4.29.)

Cusp - Es-ionization located near the height of maximum E layer ionization; usually decreasing delay with increasing frequency.

FIGURE 1

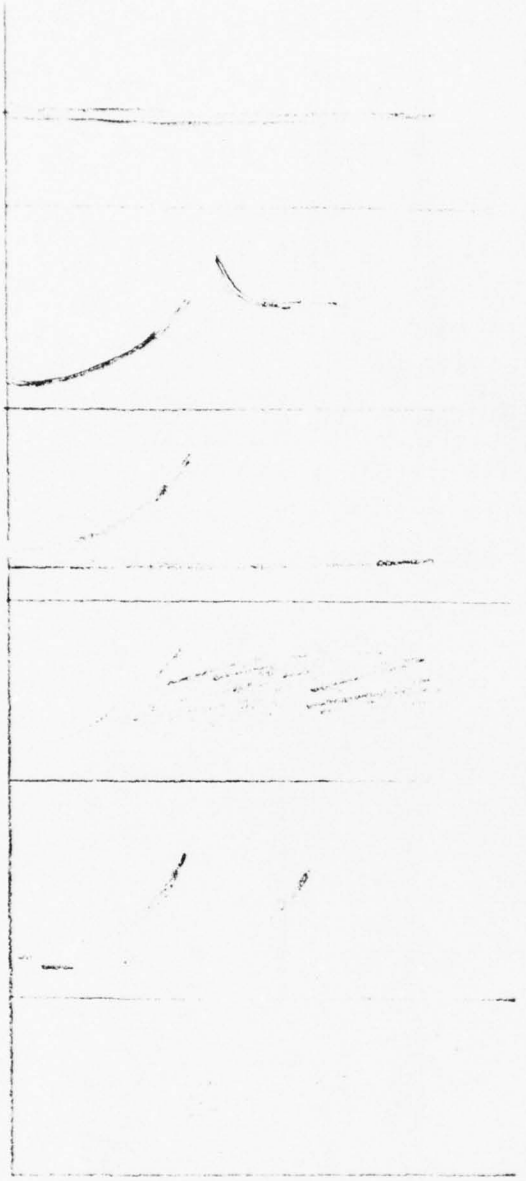

Flat - classification used only at night, when a thick E-layer is not usually observable. At other times this Es will be classified as low.

High - ionization located above maximum height of E.

Low - flat Es; ionization usually located below minimum height of E; similar in appearance to F type Es.

eQuatorial - similar in appearance to Auroral Es, yet caused by different processes.

Retardation - thick Es layer similar in appearance to E. Retardation in high frequency end.

Slant - similar to Auroral, the S type usually develops from another Es.

The most often used type classifications for Goose Bay are A, C, F and L. The H and S types may be labeled as A because they often have the same characteristics.

Night E - A thick layer which shows the same retardation trends as a normal E yet has no relation to χ. The night E is very special in that it is recorded as both an E and Es simultaneously. Night E is usually found to resemble one of the four configurations described in Figures 2 through 5. Note: Frequently foE is more correctly determined by fminF (minimum frequency of F layer) than by the inside cusp of the E trace.

F-Region

Normal F - Some F region ionization is always present. During the daytime (when χ can affect the ionization structure) we have a separation into two layers, F1 and F2 (shown in Figure 1). The F1 layer shows a frequency predictability similar to the normal E. The maximum frequency of the F1 follows the relation

$$foF1 \simeq foE \times 1.5 \ .$$

Transitoria or Intermediate Layers - Fast moving stratifications which are embedded in the F ionization or exist as a layer between the E and F region. Intermediate layers are often referred to as E2 layers.

Oblique F (Figure 6) - In regards to vertical incidence data U.R.S.I. neglects all oblique readings; however, for our arctic studies these values are important. Oblique F echoes always have a longer delay than normal F; during a certain time period the oblique trace can move in and become an overhead echo. Since oblique traces are often only fragments, it is not always possible to differentiate between oblique F and long range oblique Es.

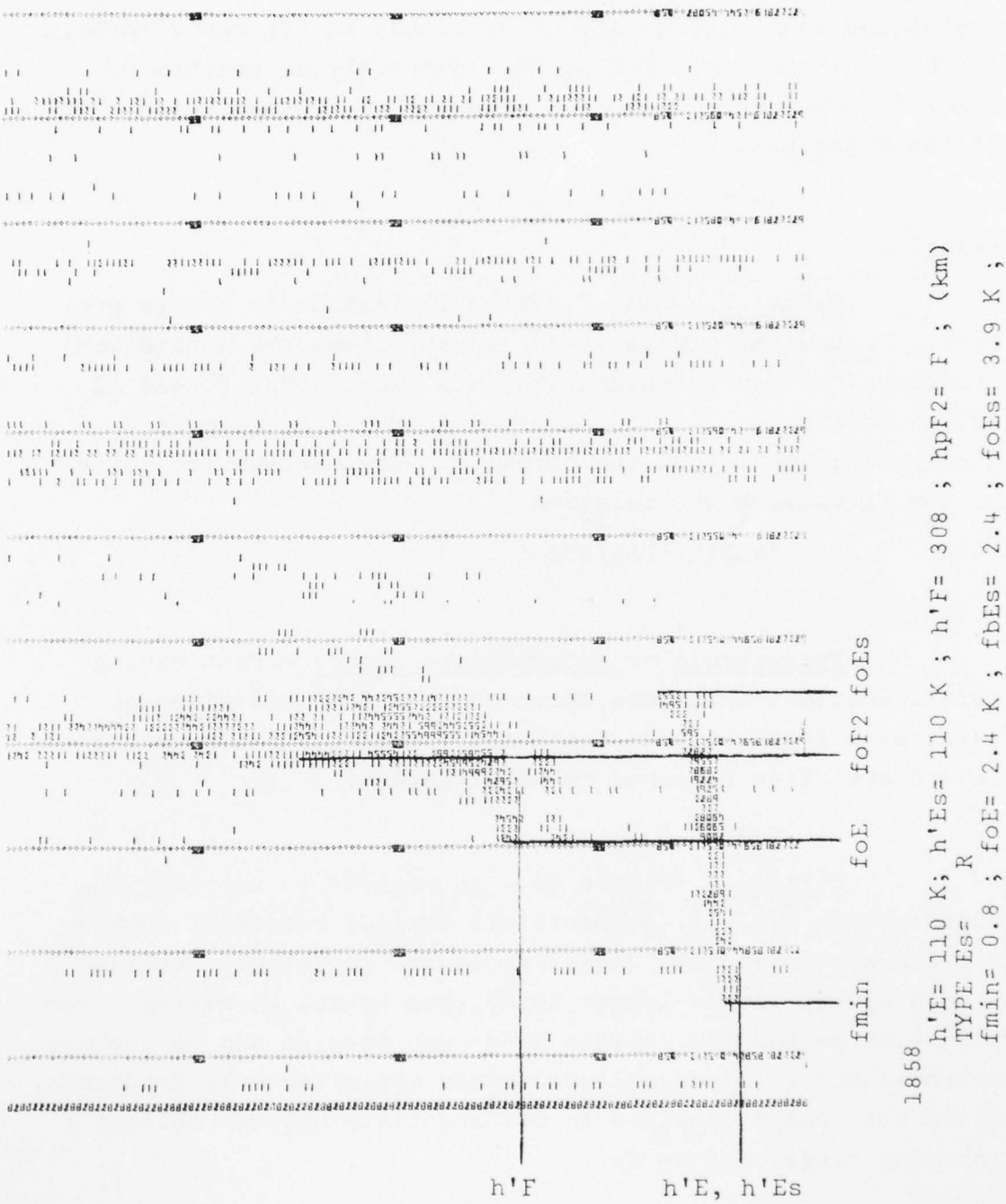
1858
h'E= 110 K; h'Es= 110 K ; h'F= 308 ; hpF2= F ; (km)
TYPE Es= R
fmin= 0.8 ; foE= 2.4 K ; fbEs= 2.4 ; foEs= 3.9 K ;
foF2= 3.3DF
foF2 foEs
foE
fmin
h'F
h'E, h'Es

FIGURE 2

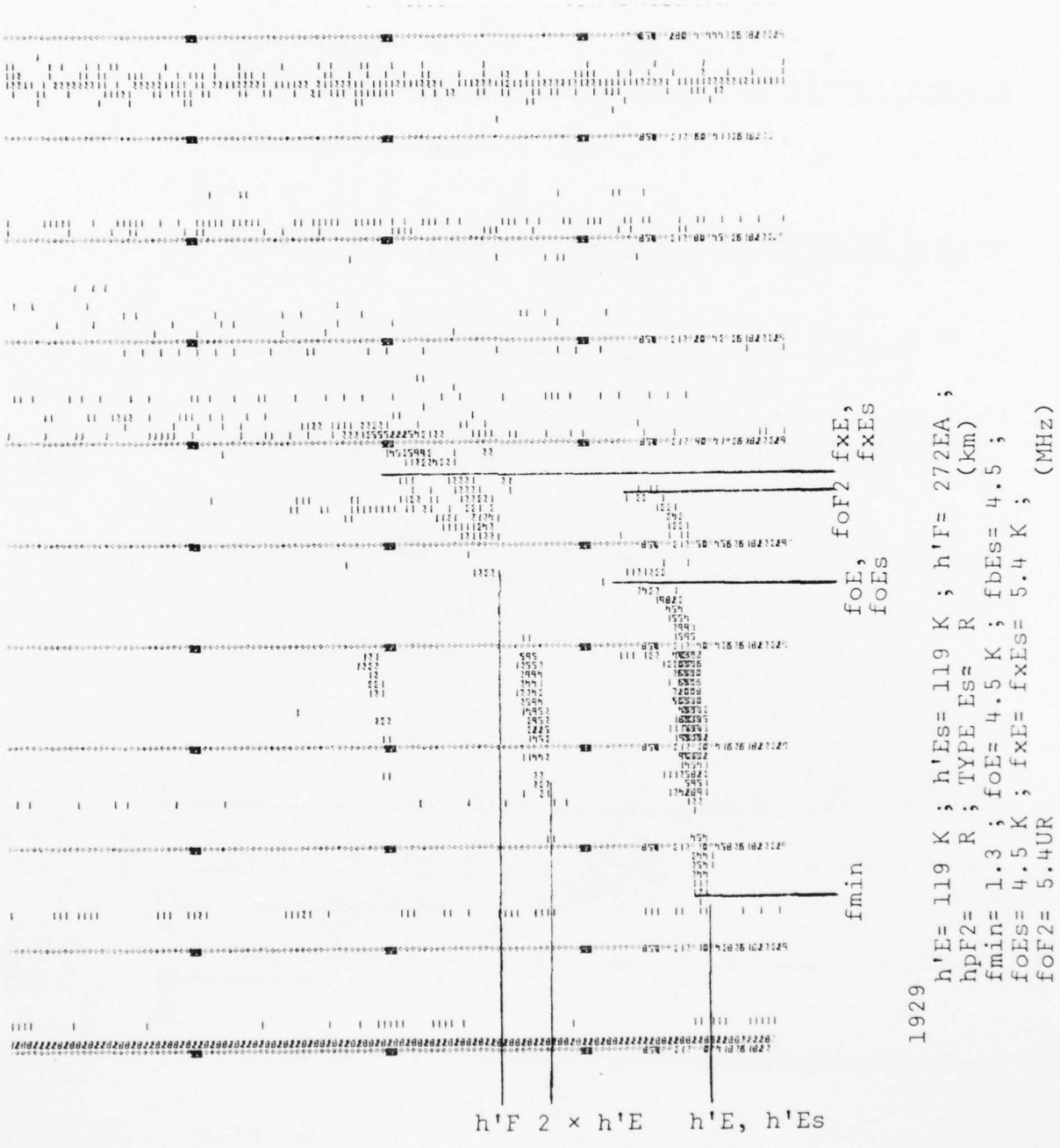
foF2
fxE,
fxEs
foE,
foEs
fmin
h'F 2 × h'E
h'E, h'Es
1929
h'E= 119 K ; h'Es= 119 K ; h'F= 272EA ;
hpF2= R ; TYPE Es= R (km)
fmin= 1.3 ; foE= 4.5 K ; fbEs= 4.5 ;
foEs= 4.5 K ; fxE= fxEs= 5.4 K ; (MHz)
foF2= 5.4UR

FIGURE 3

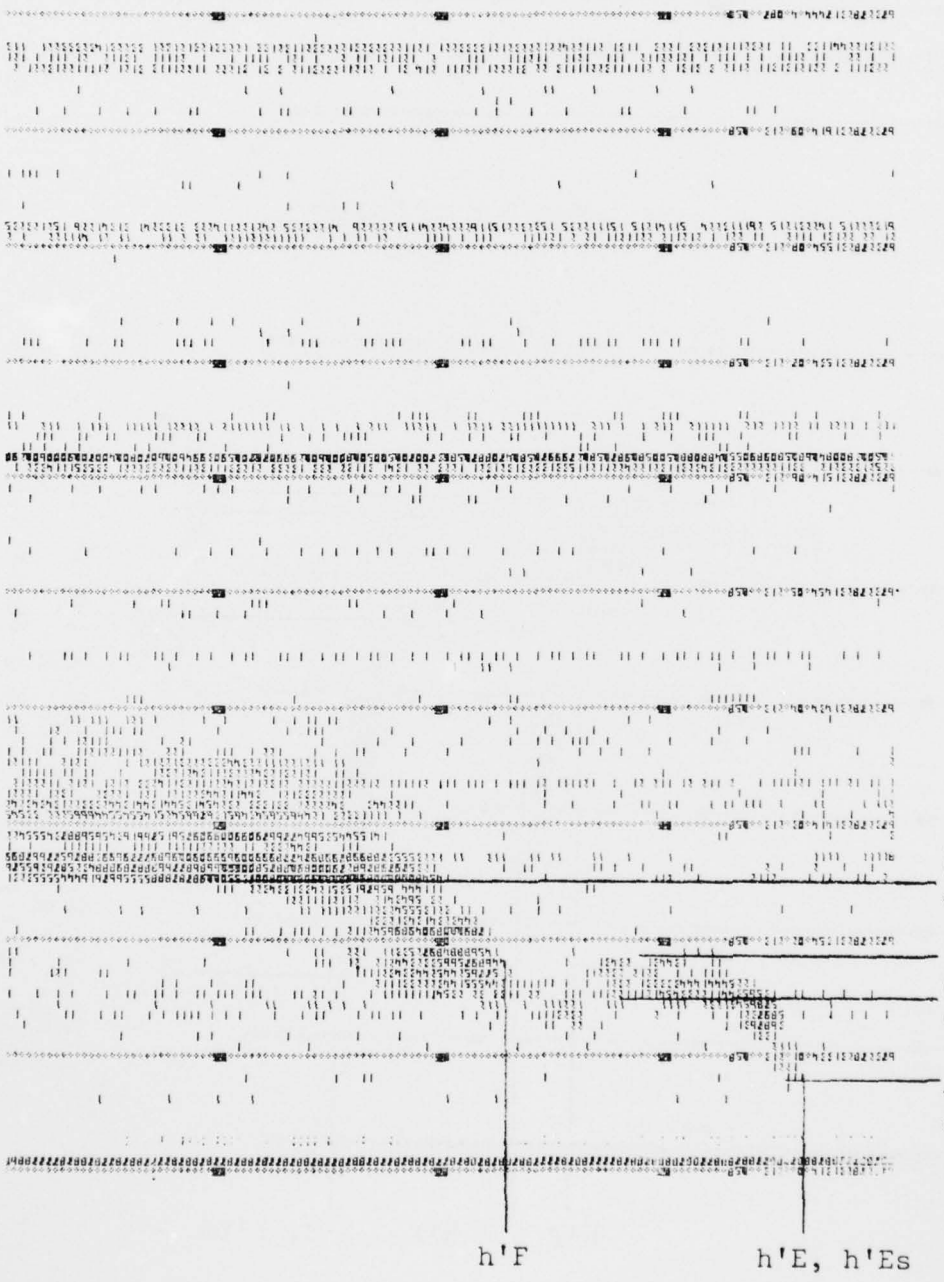

2313
h'E= 119 K ; h'Es= 119 K ; h'F= 308 ;
hpF2= F ; TYPE Es= R (km)
fmin= 0.7 ; foE= 1.5 K ; fbEs= 1.5 ;
foEs= 1.8 K ; foF2= A (MHz)

FIGURE 4

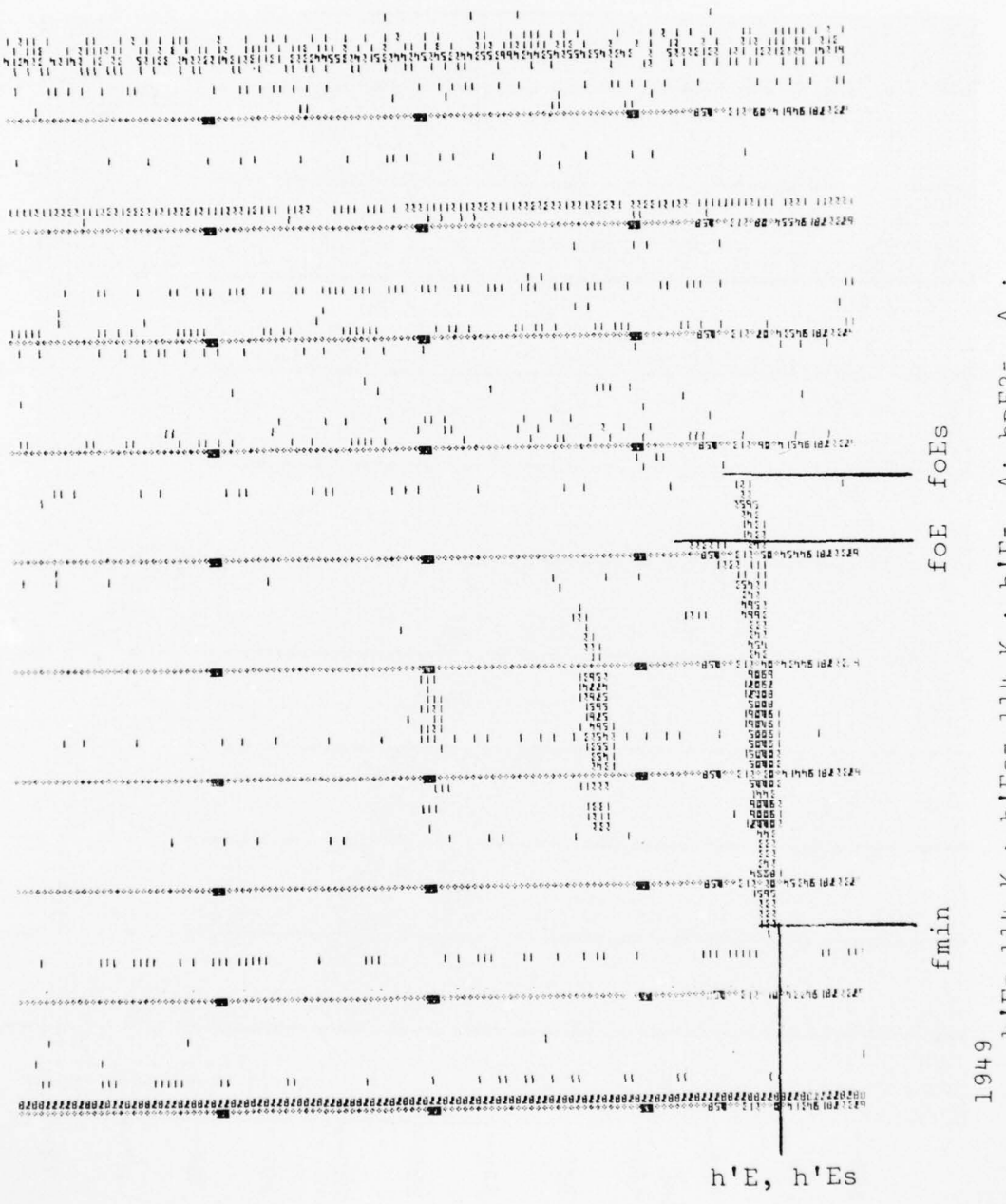
foE foEs
fmin
h'E, h'Es
1949
h'E= 114 K ; h'Es= 114 K ; h'F= A; hpF2= A ;
TYPE Es= R
fmin= 1.6 ; foE= 5.2 K ; foEs= 5.9 K ; foF2= A

FIGURE 5

OBLIQUE F-LAYER
2013 LMT
3 APR 72
GOOSEBAY, LABRADOR

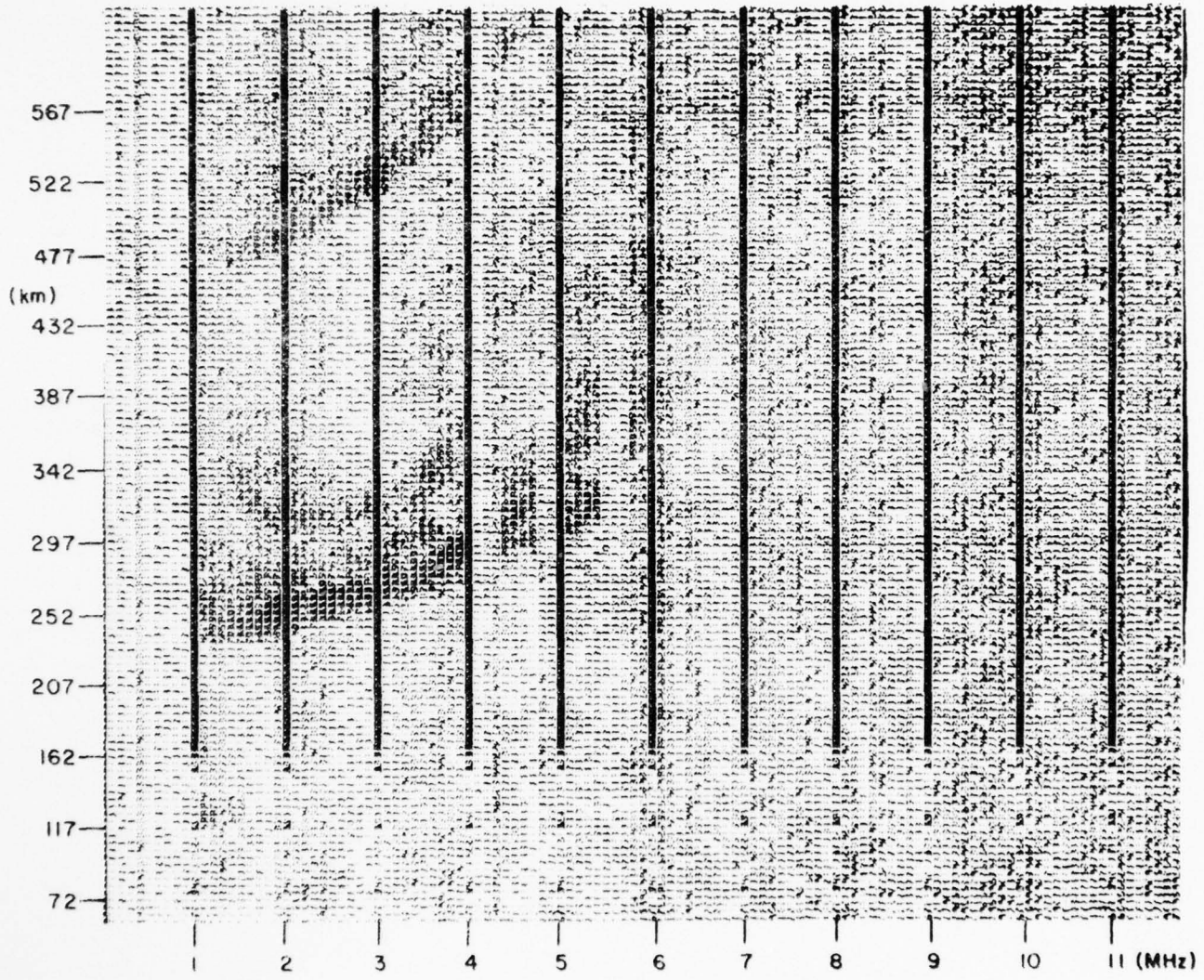

FIGURE 6
C.10

III. TAKING OF READINGS

Each trace has up to three magneto-ionic components (Figure 7) which may be visible simultaneously: the ordinary (O), extraordinary (X), and Z mode (Z). The frequency separation between Z and X is equal to fH (gyrofrequency). For Goose Bay the gyrofrequency is approximately 1.52 MHz at 100 km. Therefore the equation for frequency mode is

$$fo - fz = 1/2\ fH$$

$$fx - fo = 1/2\ fH$$

thus,

$$fx - fz = fH$$

The normal E and F layers are considered monotonic; this means that the curve of ionization density vs range is a continuous trace, therefore foE $\leq$ fminF; foF1 $\leq$ fminF2.

For Digisonde ionograms there are three criterion for a trace:

1) the amplitude must be at least 6 dB greater than background noise (Note: be very sure what you see is not merely a spike on a noisy frequency line);

2) the trace has a finite thickness - in K = 3 (vertical ionograms) the pulse width is 4 height bins, in K = 7 (backscatter) the pulse width is 2 height bins;

3) the virtual height of the echo is the highest range bin where the amplitude is 20 dB (five units) below the average maximum amplitude.

F-LAYER Z TRACE
1259 LMT
20 SEP 71
MAYNARD, MASS.

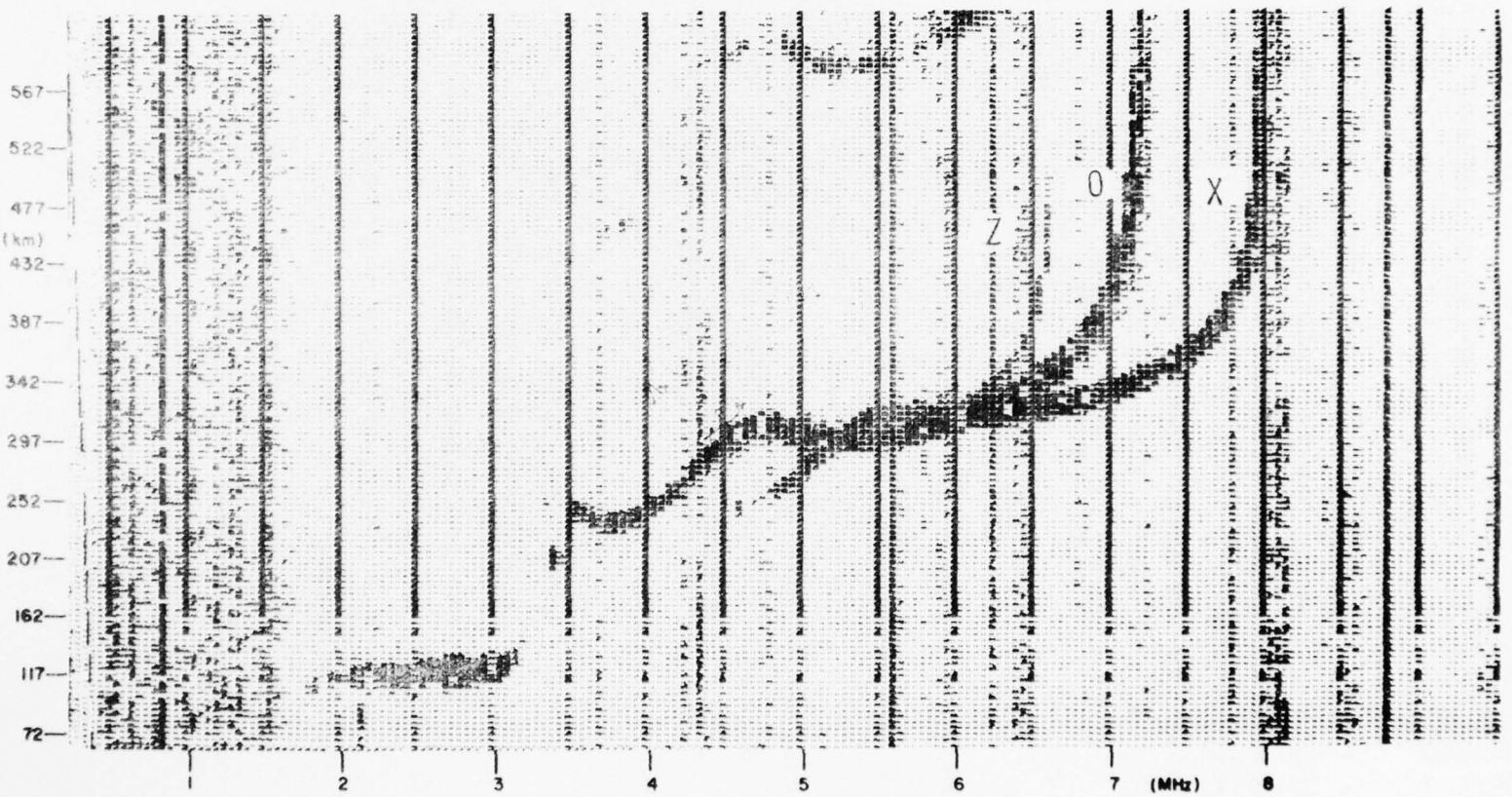

FIGURE 7

The most significant readings are:

h' - minimum virtual height
h'E; h'Es; h'F; h'F2
When there is only one F layer its height is taken as h'F.

fo - maximum frequency of ordinary trace
foE; foEs; foF1; foF2
When there is only one F layer, its maximum critical frequency is foF2 except in G-effect cases when the ordinary trace is not easily discernible as in the case of spread E or spread F conditions; foE or foF2 has to be read from the inner edge of the spread E or spread F pattern. (See URSI Handbook, page 41, and Fig. 2.11, and Fig. 12, this report. For determination of M(3000) under spread F conditions see URSI Handbook Fig. 3.14.)

ftEs - top frequency of Es - when O and X modes are not distinguishable.

fmin - the minimum frequency at which we first see continuous echoes.

fbEs - the frequency at which the Es becomes transparent or nonblanketing.

hpF2 - parabolic height F2. The height of the F2 layer when the frequency is .834 × foF2.

frEs - retardation frequency of Es, as shown in Figure 11.

Type Es - classification of Es according to its appearance.

IV. QUALIFYING OF READINGS

If there is any doubt or further explanation is needed to clarify a reading, qualifying and descriptive letters are added to the numerical value. Qualifying letters cannot exist without descriptive letters, yet the descriptive letters may be used alone. In the case of a probable error > 15% just a descriptive letter is used with no numerical reading.

Qualifying Letters

With respect to the actual reading the real value would be:

D - greater than 5% < error < 10%
E - less than 5% < error < 10%
I - interpolated
J - derived from X component
U - approximately 2% < error < 5%

If the error is < 2% no qualifier is necessary.

Descriptive Letters

Measurements influenced or impossible because of:

A - blanketing (Figures 8 to 10)
B - absorption (Figure 10)
C - technical difficulties
D - upper frequency limit
E - lower frequency limit
F - spread (Figure 8, Figures 11 and 12)
G - low ionization density (Figure 10)
H - stratification
K - night E (Figures 2 to 5, Figure 12)

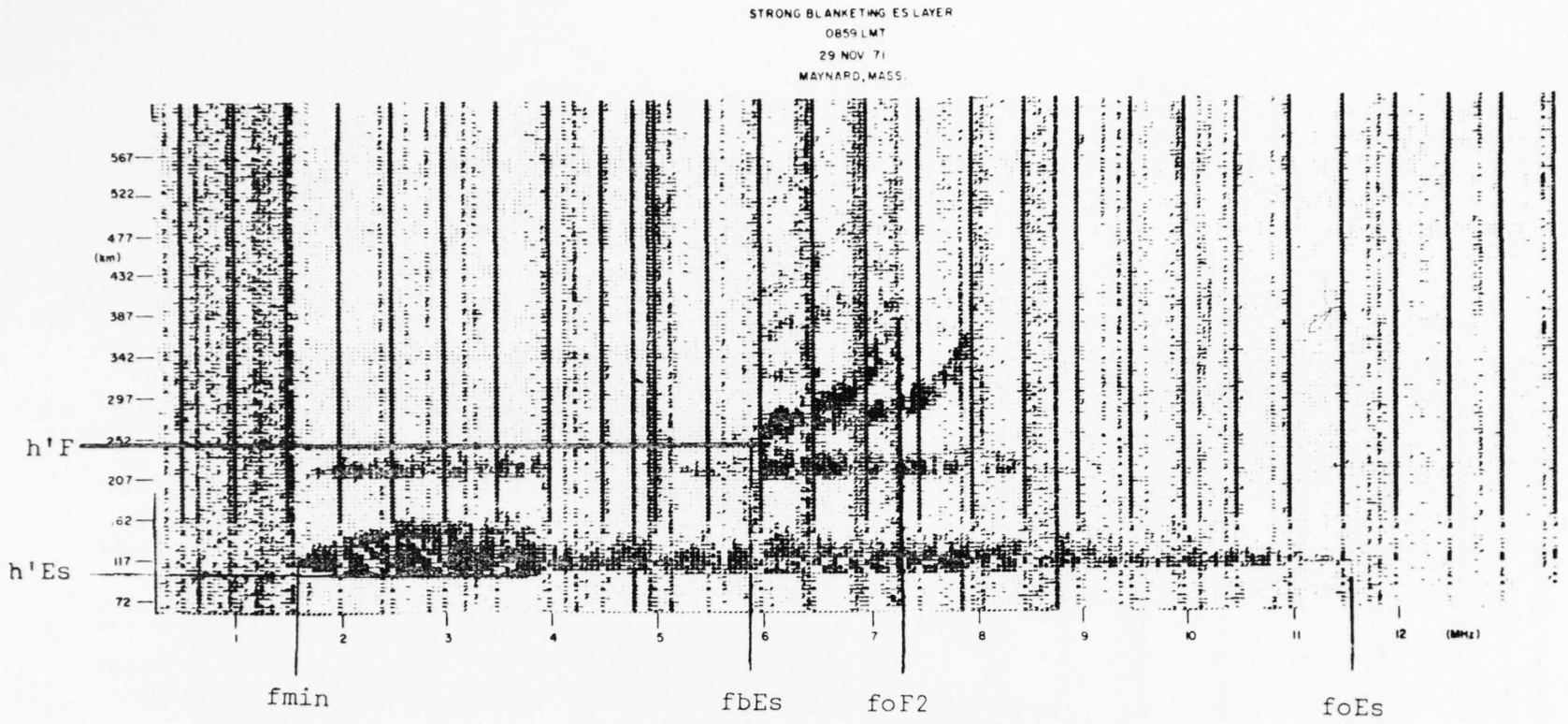

FIGURE 8
C.15

0859
h'Es= 104 ; h'F= 248EA (km)
fmin= 1.55 ; fbEs= 5.9 ; foEs= 11.5 ; foF2=7.3 UF (MHz)

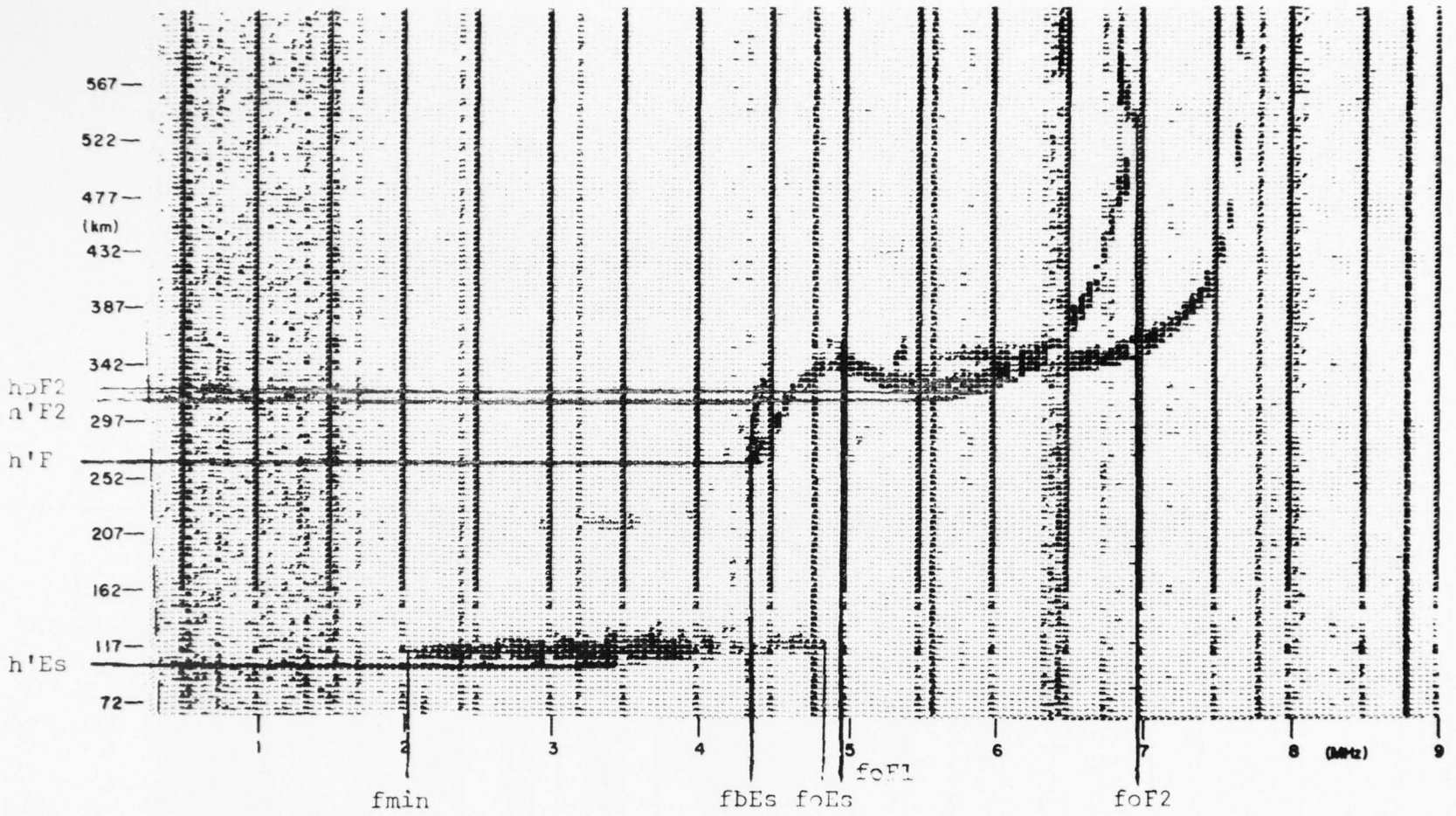

FIGURE 9

C.16

1259

h'E= A ; h'Es= 104 ; h'F= 266EA ; h'F2= 315 ; hpF2= 320 ;
(km)

TYPE Es= L

fmin= 2.0 ; foE= A ; fbEs= 4.40 ; foEs= 4.8 ; foF1= 4.95 ;
(MHz)

foF2= 6.95

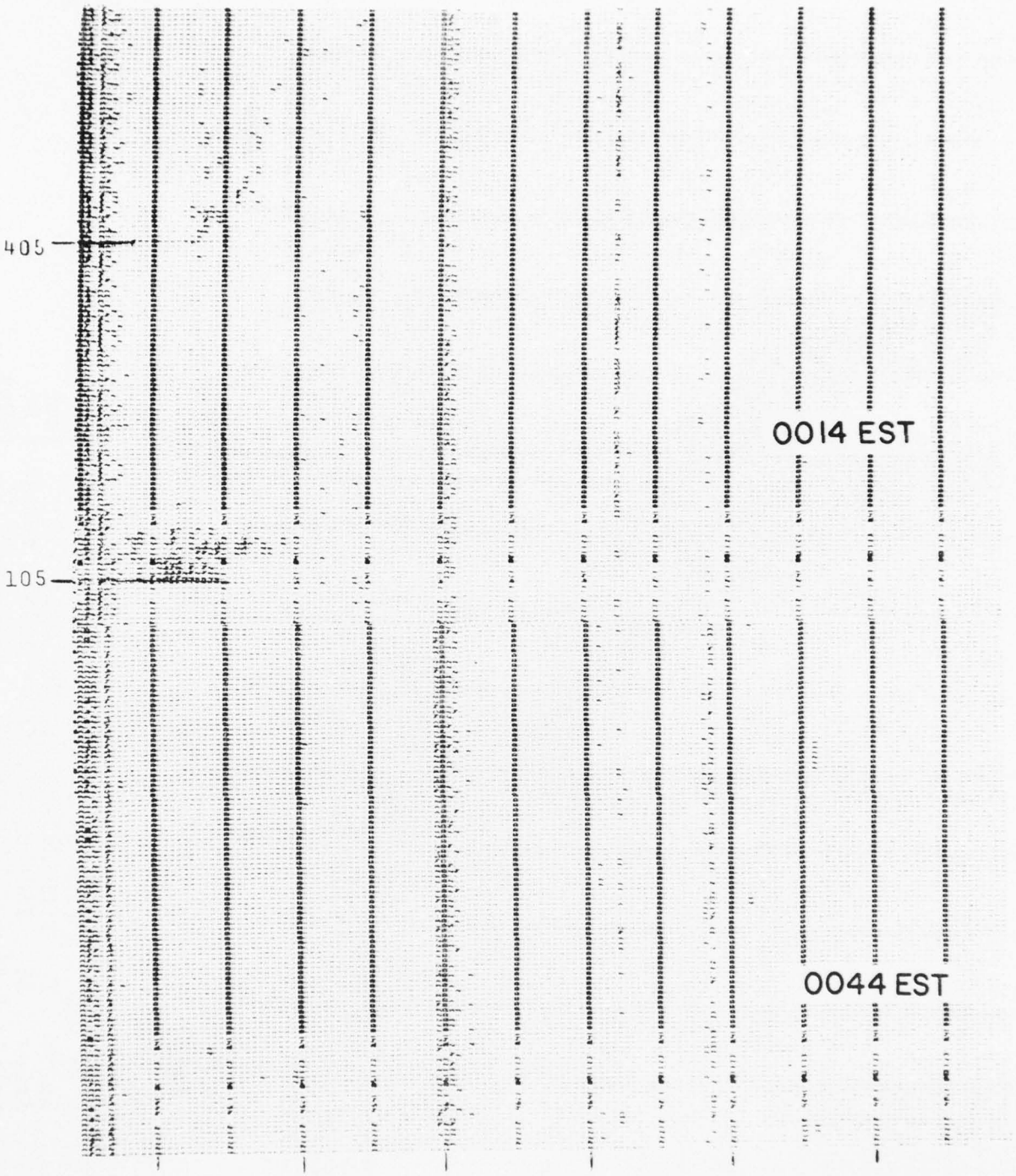

0014
h'Es= 105 ; h'F= 405 EA ; hpF2= G (km)
fmin= 1.7 ; foEs= 3.8 ; fbEs= 2.4 ; foF2= G (MHz)

0044
h'Es= B ; h'F= B ; hpF2= B (km)
fmin= B ; foEs= B ; foF2= B (MHz)

FIGURE 10

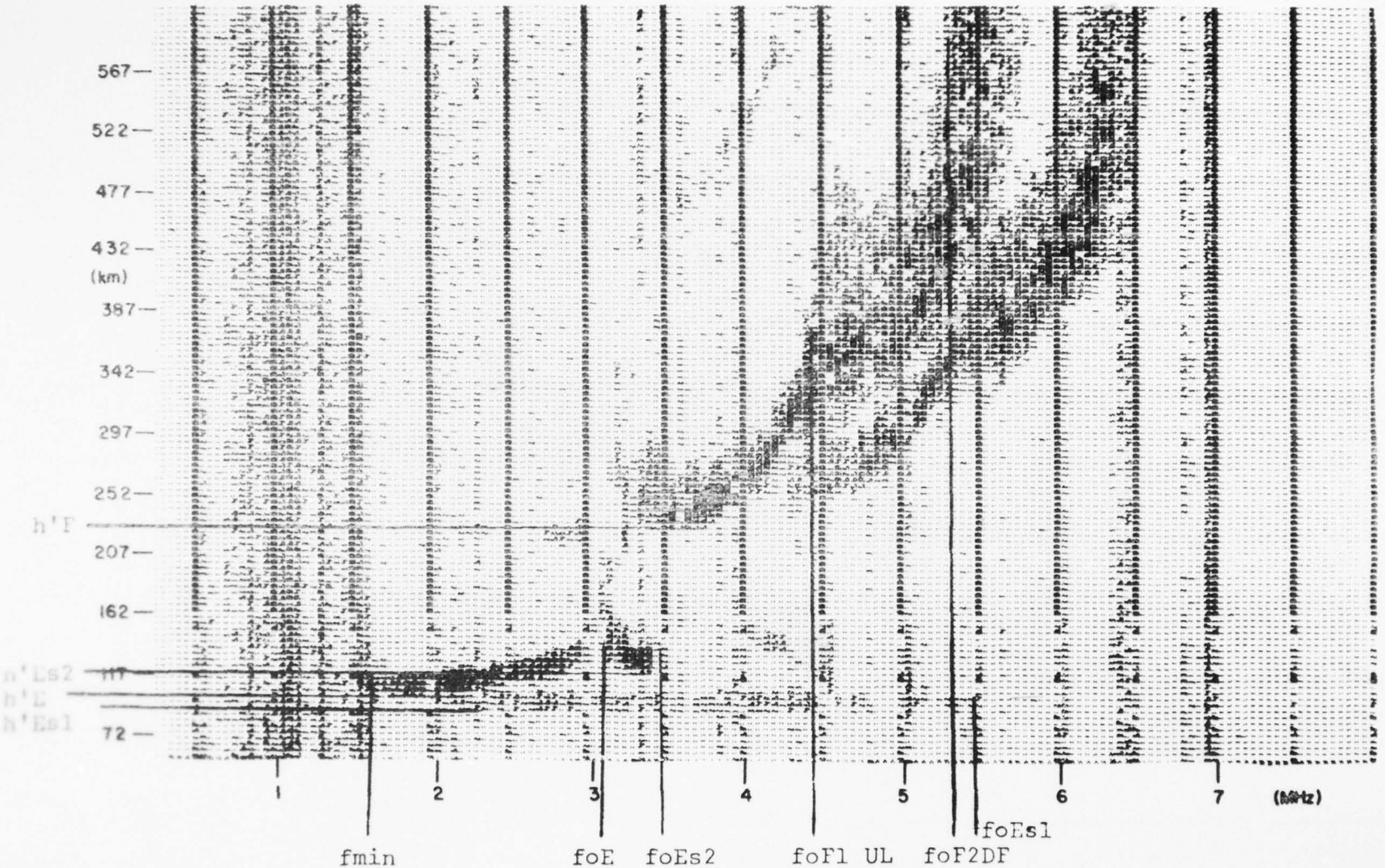

FIGURE 11
C.11a

0659
h'E= 110 ; h'Es1= 96 ; h'Es2= 117 ; h'F= 225 ; h'F2= L ;
hpF2= F ; TYPE Es1= L ; TYPE Es2= C (km)
fmin= 1.55 ; foE= 3.05 ; frEs= 3.05 ; foEs1= 5.45 ;
foEs2= 3.45 ; foF1= 4.45 UL ; foF2= 5.30 DF (MHz)

AD-A051 428 LOWELL UNIV RESEARCH FOUNDATION MASS F/G 4/1
DIGITAL IONOSPHERIC SOUNDING IN THE ARCTIC.(U)
JUL 77 K BIBL, B W REINISCH, S SMITH F19628-76-C-0012
UNCLASSIFIED ULRF-387/CAR AFGL-TR-77-0152 NL

2 OF 2
AD
A051 428

END
DATE FILMED
4-78
DDC

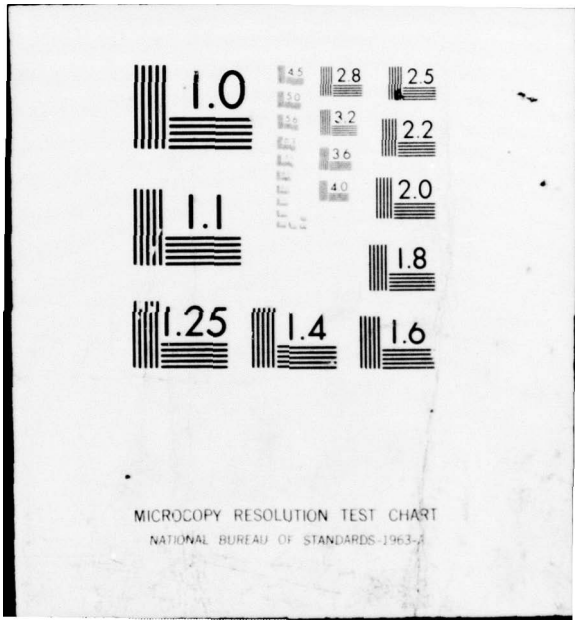
1.0
1.1
1.25
1.4
1.6
1.8
2.0
2.2
2.5
2.8
3.2
3.6
4.0
4.5
5.0
MICROCOPY RESOLUTION TEST CHART
NATIONAL BUREAU OF STANDARDS-1963-A

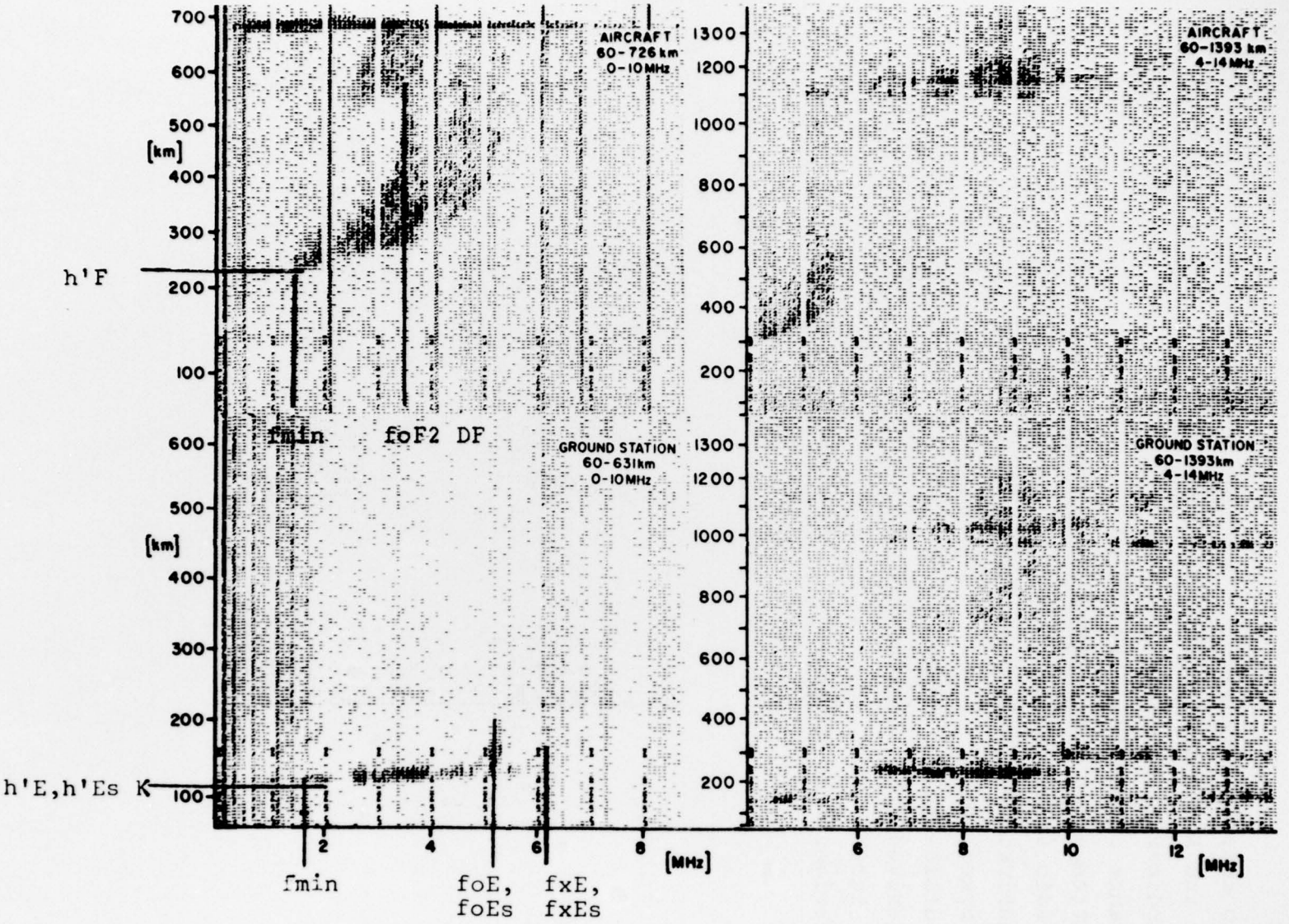

1949 AIRCRAFT
h'F= 230 EB ; hpF2= F
fmin= 1.3 ; foF2=3.4 DF

1949 GROUND STATION
h'E= 109 K ; h'Es= 109 K ; h'F= A ;
hpF2= A ; TYPE Es= R
fmin= 1.5 ; foE= 5.0 K ; fxE= 6.0 K ; foF2= A
foEs= 5.0 K ; fxEs= 6.0 K

FIGURE 12

L - no cusp (Figure 11)
M - O and X not distinguishable
O - ordinary component
Q - range spread (usually use F)
R - attenuation near maximum frequency (Figure 13)
S - radio interference
T - derived from other readings
V - forked trace
W - outside height range
X - derived from X trace
Y - F lacuna
Z - derived from Z trace

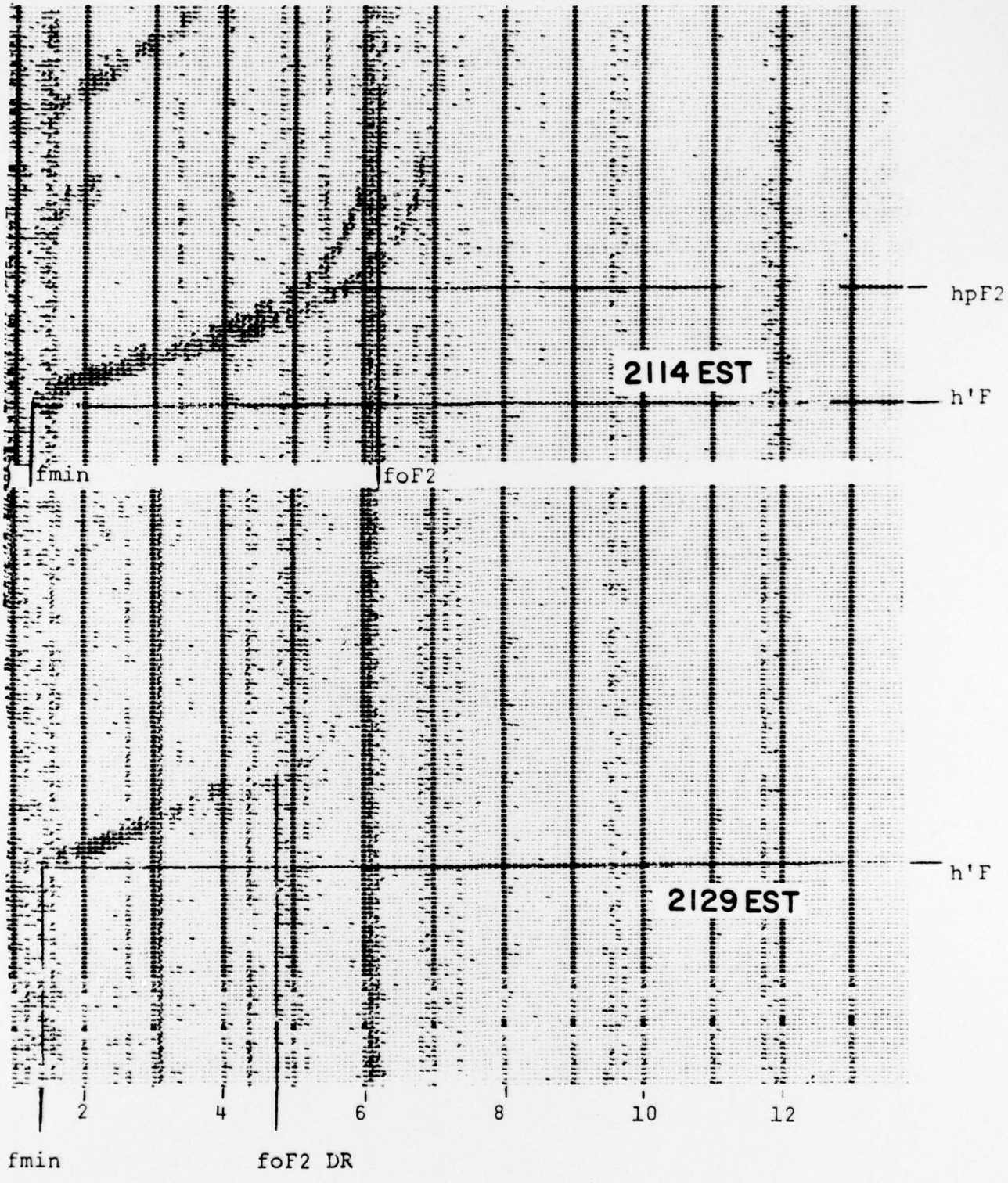

2114
fmin= 1.1 ; foF2= 6.1 (MHz)
2129
fmin= 1.3 ; foF2= 4.7DR (MHz)

FIGURE 13

V. SPECIAL EXAMPLES

If a trace is discontinuous then there are only four choices for descriptive letters: B, G, R and C. The letter C indicates technical difficulties; in Goose Bay C usually refers to suppressed frequencies. Examples of B, G, and R follow.

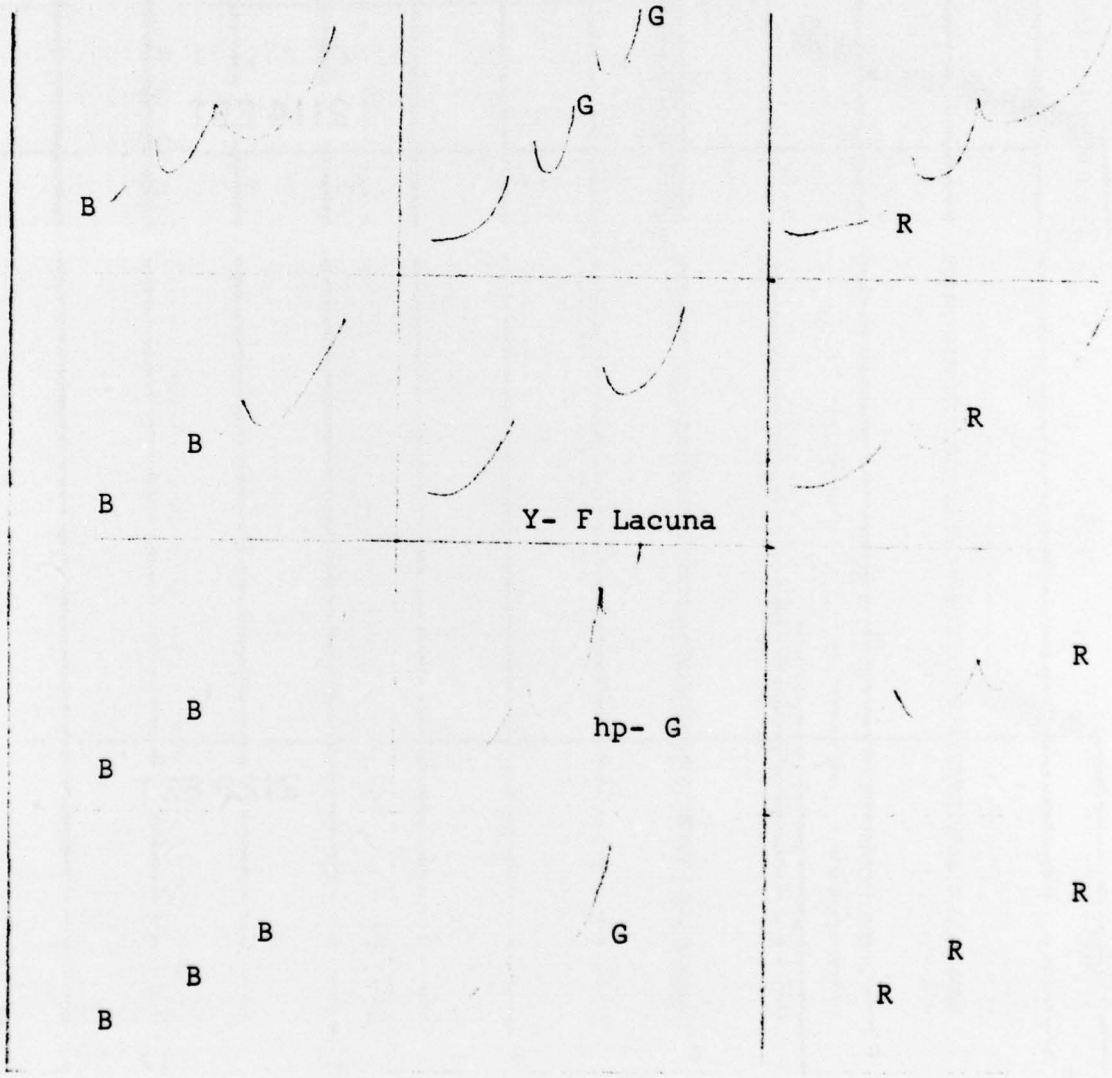

VI. PROCESSING

There are several modes of processing which have been used to present the Digisonde ionograms in diurnal displays.

A. Compressed Data (Figure 14)

h'(t) - each height bin was summed along all frequencies of one ionogram and the array of 128 summed height bins was then normalized to 63 using the relation

$$Anew = \left(\frac{63}{A_{max}-A_{min}}\right) \cdot (A_i-A_{min})$$

ftF(t) - maximum amplitude of height bins > 156 km for each frequency was saved and a display of frequency vs amplitude was made.

ftE(t) - maximum amplitude of height bins < 156 km is saved and displayed.

B. Reconstituted Ionograms (Figure 15)

Using a process of matching a pulse filter along each height bin of a certain frequency, six significant traces are extracted from each ionogram. These traces may then be displayed as the reconstituted ionogram which has the information of amplitude, height and spread of the original ionogram.

C. AIR6

The method which can create the reconstituted ionograms also produces the many displays shown in Figures 16 and 17.

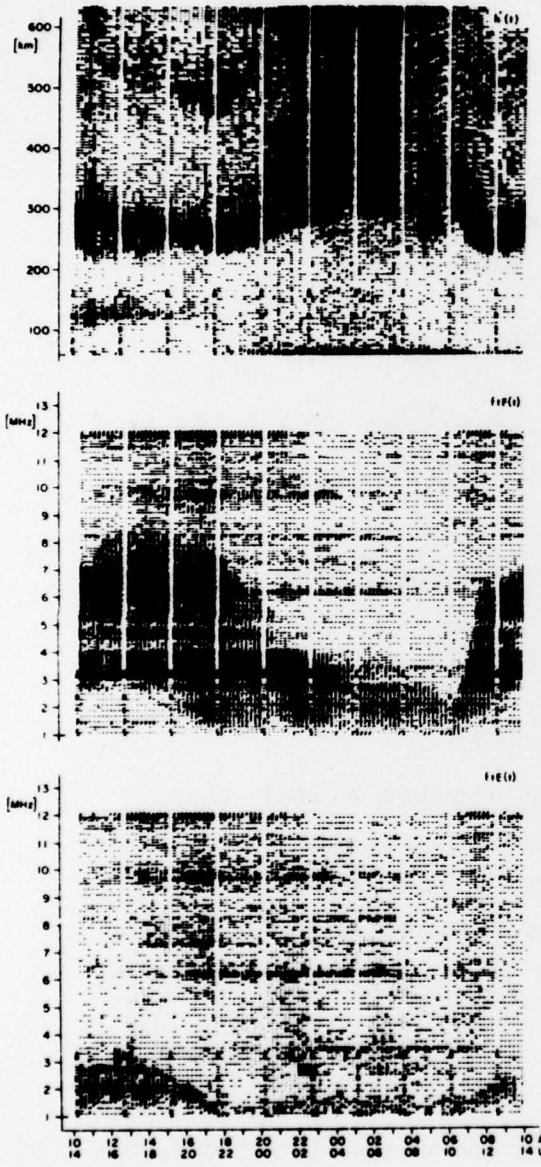

VERTICAL IONOGRAMS

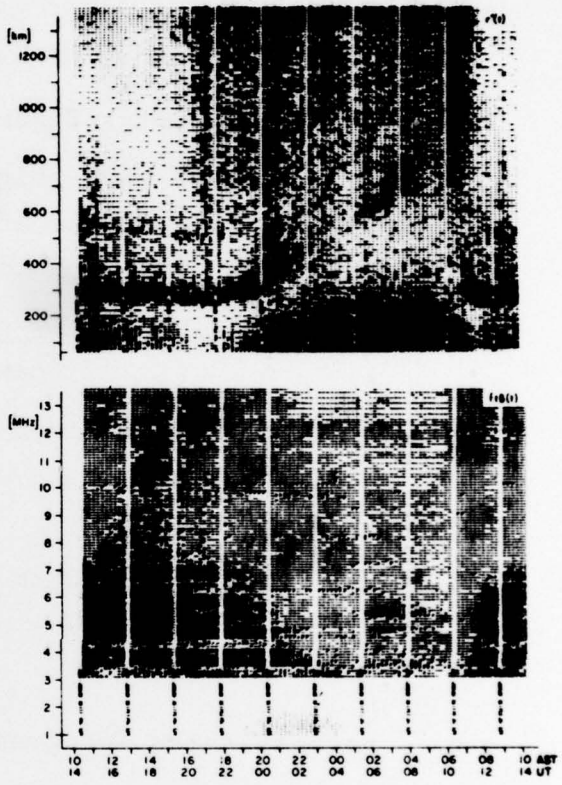

BACKSCATTER-OBLIQUE IONOGRAMS

COMPRESSED DATA
17 FEB 1973
GOOSE BAY, LABRADOR

FIGURE 14

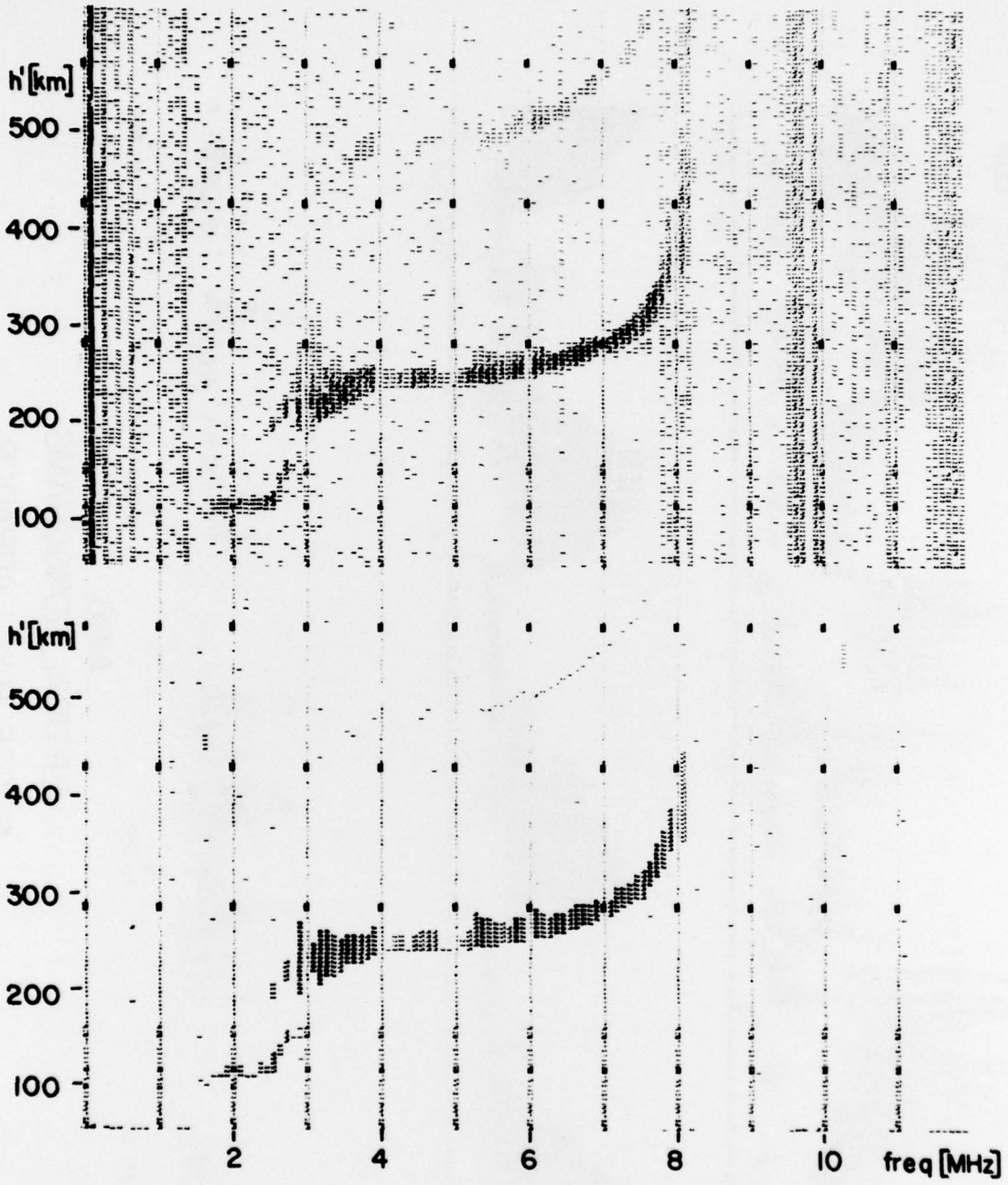

AIR6

FILTERED VERTICAL IONOGRAM

13 FEB 1973, GOOSE BAY, LAB.

FIGURE 15

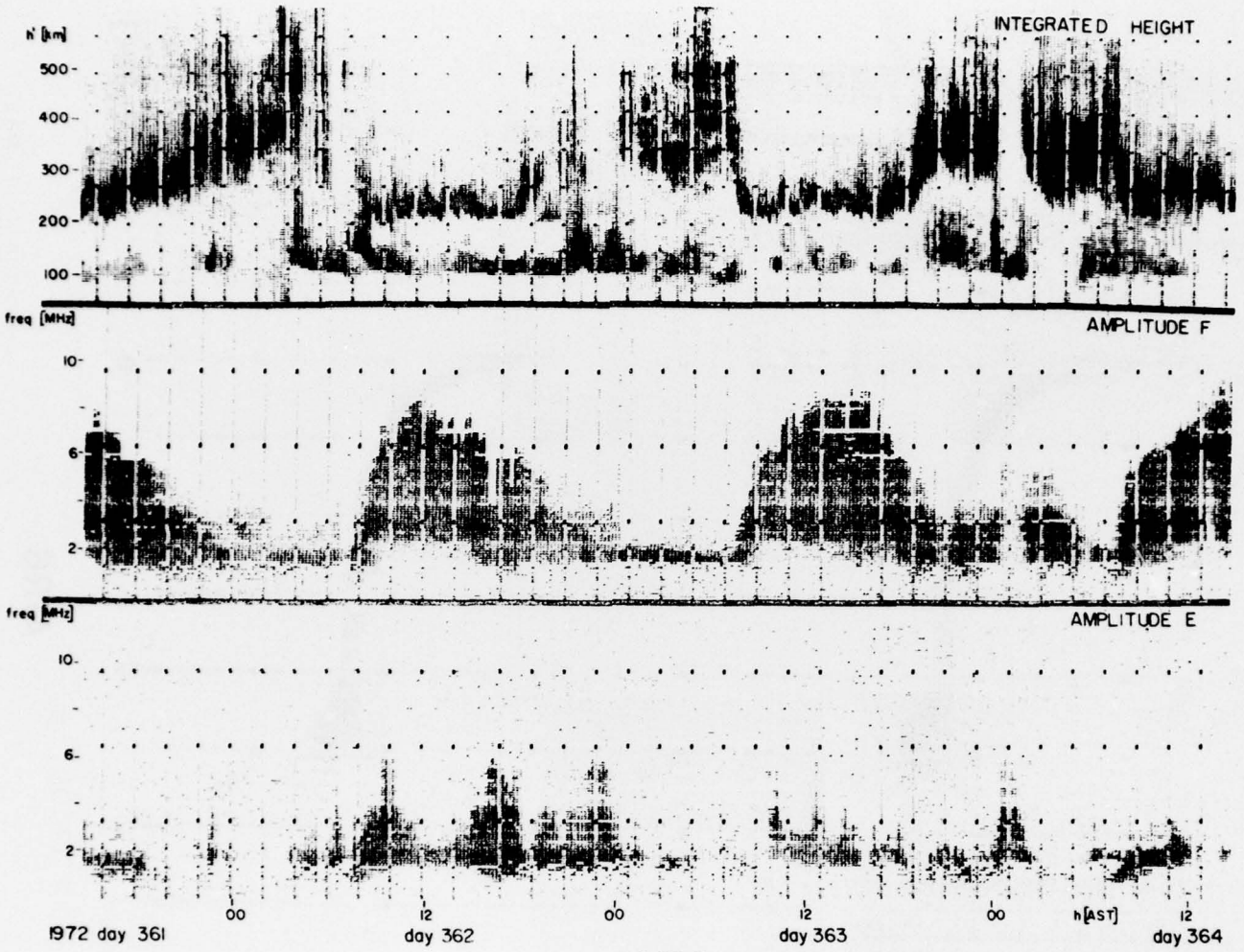

FIGURE 16

AIR6
VERTICAL IONOGRAMS
GOOSE BAY, LABRADOR

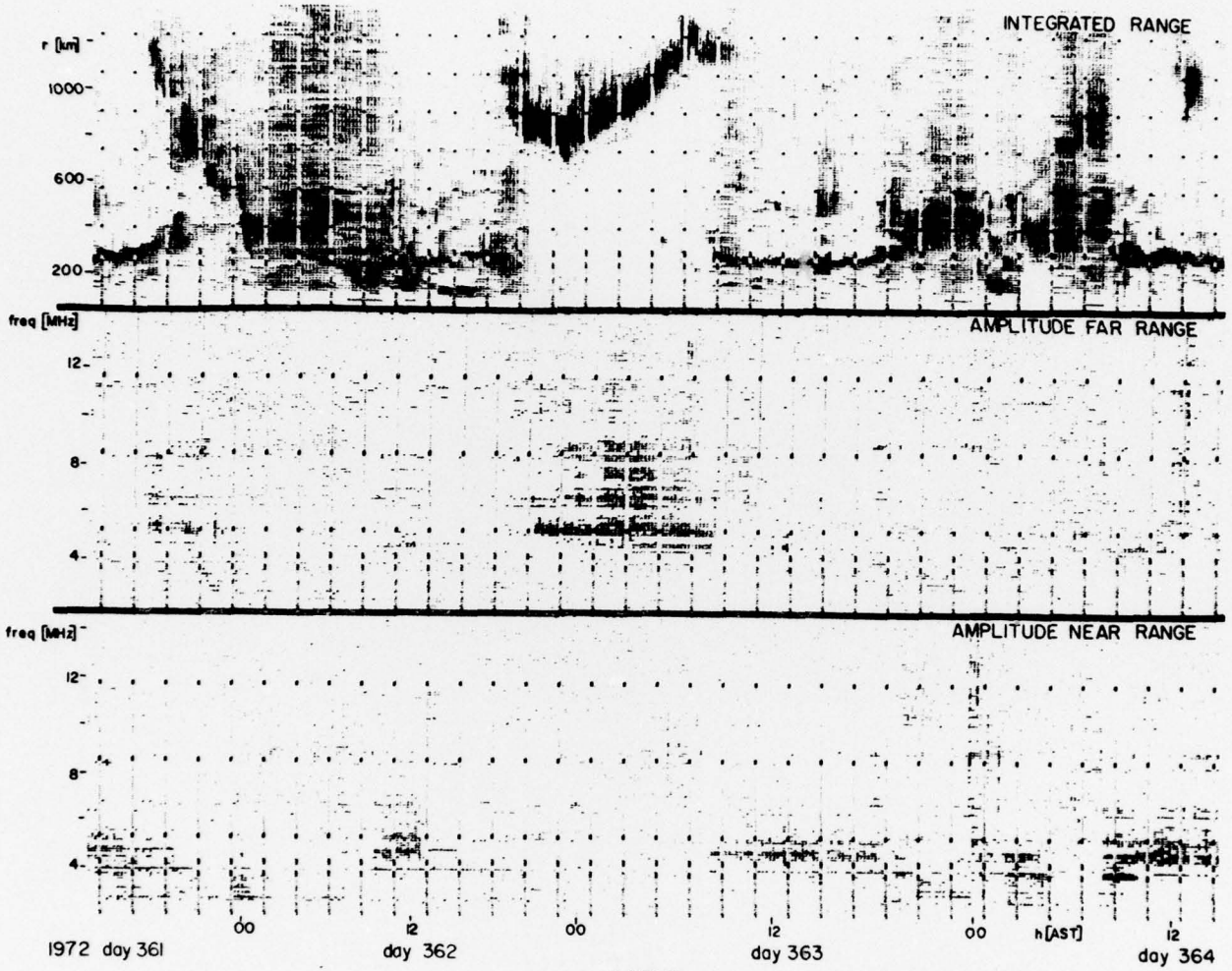

AIR6
OBLIQUE IONOGRAMS
GOOSE BAY, LABRADOR

FIGURE 17